ANALYSIS OF RETINAL GANGLION CELL DEVELOPMENT: FROM STEM CELLS TO SYNAPSES

A Dissertation

Submitted to the Faculty

of

Purdue University

by

Sarah K. Ohlemacher

In Partial Fulfillment of the

Requirements for the Degree

of

Doctor of Philosophy

August 2018

Purdue University

Indianapolis, Indiana

THE PURDUE UNIVERSITY GRADUATE SCHOOL
STATEMENT OF COMMITTEE APPROVAL

Dr. Jason S. Meyer, Chair

Purdue University- Indianapolis: Department of Biology

Dr. Anthony J. Baucum II

Purdue University- Indianapolis: Department of Biology

Dr. Henry Chang

Purdue University: Department of Biological Sciences

Dr. Theodore R. Cummins

Purdue University- Indianapolis: Chair, Department of Biology

Dr. Maria B. Grant

University of Alabama: Department of Ophthalmology and Visual Sciences

Approved by:

Dr. Theodore R. Cummins

Head of the Graduate Program

ACKNOWLEDGMENTS

I would like to express my sincere gratitude to my mentor, Dr. Jason Meyer, for your patience, motivation, encouragement, and immense knowledge. Your guidance helped me construct this body of research and your support was imperative in my development as a scientist. I quite simply cannot imagine a better advisor and mentor.

I would also like to thank my committee members including Dr. AJ Baucum II, Dr. Henry Chang, Dr. Ted Cummins, and Dr. Maria Grant for their time, invaluable input, and insightful questions that have helped guide the development of this dissertation.

To my first mentor, Dr. Denise Boots, thank you for motivating me to go pursue my graduate education. I am thankful for the excellent example you have provided as a successful woman, leader, and scientist.

To my lab mates, Dr. Akshayalakshmi Sridhar, Kirstin Langer, Clarisse Fligor, Dr. Ridhima Vij and Dr. Jessica Cooke- thank you for always being willing to take care of my cells during holidays, conferences, and weekends. Stem cell research is truly a team effort and I couldn't ask for a better group of people to work with day in and day out. I am grateful to all of those with whom I have had the pleasure to work during this and other related projects, including members of Dr. William Guido's lab as well other members of the Meyer lab including Sailee Levekar, Elyse Feder, Priya Shields, and all the other undergraduate students who have helped keep the lab running smoothly.

I am also grateful to Sue Merrell for her invaluable assistance and advocacy on behalf of all students in the Biology department.

I was honored to receive fellowships to support my research including a 2nd year Fellowship from IUPUI, a CTSI Predoctoral Fellowship from Indiana CTSI (Grant #ULTL1TR001107), and a Predoctoral Fellowship from Stark Neurosciences Re-

search Institute and Eli Lilly (Grant #UL1TR001108) to support my research through the majority of my PhD. I gratefully acknowledge additional grants from the National Eye Institute (R01 EY024984), the Indiana Department of Health Brain and Spinal Cord Injury Fund, an IU Collaborative Research Grant from the Office of the Vice President for Research, an IU Signature Center for Brain and Spinal Cord Injury grant, a BrightFocus foundation grant (Grant #G201027), and a Project Development Team award within the ICTSI NIH/NCRR (Grant #UL1TR001108).

I would like to thank my family and friends for their unwavering encouragement and support over the years including Charlette Lee, Maddie Cooper, the Kershners, Liz Moehler and Levi Boaz, Jennifer Robison, Akshayalakshmi Sridhar, Esther Ng, Therri Usher, Ralph Ohlemacher, Ellen Greenwald, Jason Katte, Jessica Barrera and Dr. Michael Edler.

To my mom, thank you for your steadfast belief I must be saving the world, despite not knowing exactly what I do all day. You have set an extraordinary example for me as a compassionate, generous, and strong woman.

To Laura Brockway, thank you for instilling in me a love of science at a young age, for being my voice of reason, and my strongest supporter. I am truly grateful for your unwavering encouragement. I would not be where I am today without you.

TABLE OF CONTENTS

Page

Page

Page

LIST OF TABLES

LIST OF FIGURES

Figure Page

ABBREVIATIONS

ACM	astrocyte conditioned media
AMD	age-related macular degeneration
AP	action potential
BDNF	brain-derived neurotrophic factor
CAG	closed angle glaucoma
CNS	central nervous system
CNTF	ciliary neurotrophic factor
CRISPR	clustered regularly interspaced short palindromic repeats
dCAMP	dibutyryl-cAMP
DIC	differential interference contrast
DLK	dual-leucine zipper kinase
DMEM	Dulbecco's modified eagle medium
DMEMF/12	Dulbecco's modified eagle medium: nutrient mixture F-12
EB	embryoid body
EGF	epidermal growth factor
EPSP	excitatory postsynaptic potential
FBS	fetal bovine serum
FGF2	fibroblast growth factor 2
GDNF	glial cell-derived neurotrophic factor
hESC	human embryonic stem cell
hiPSC	human induced pluripotent stem cell
hPSC	human pluripotent stem cell
ipRGC	intrinsically photosensitive retinal ganglion cell
LGN	lateral geniculate nucleus

LZK	leucine zipper kinase
MACS	magnetic activated cell sorting
MEM NEAA	minimum essential medium non-essential amino acids
NGF	nerve growth factor
NIM	neural induction medium
NT4/5	neurotrophin-4/5
OPC	oligodendrocyte progenitor cell
OPTN	optineurin
OV	optic vesicle
PBS	phosphate buffered saline
PEDF	pigment epithelium-derived factor
POAG	primary open angle glaucoma
qRT-PCR	quantitative reverse transcription polymerase chain reaction
RDM	retinal differentiation medium
RGC	retinal ganglion cell
RPE	retinal pigment epithelium
RMP	resting membrane potential
SC	superior colliculus
RT-PCR	reverse transcription polymerase chain reaction
TBS	tris buffered saline
TEA	tetraethylammonium
TTX	tetrodotoxin
ZFN	zinc finger nuclease

ABSTRACT

Ohlemacher, Sarah K. Ph.D., Purdue University, August 2018. Analysis of Retinal Ganglion Cell Development: From Stem Cells to Synapses. Major Professor: Jason S. Meyer.

Human pluripotent stem cells (hPSCs) have the ability to self renew indefinitely while maintaining their pluripotency, allowing for the study of virtually any human cell type in a dish. The focus of the current study was the differentiation of hPSCs to retinal ganglion cells (RGCs), the primary cell type affected in optic neuropathies. hPSCs were induced to become retinal cells using a stepwise differentiation protocol that allowed for formation of optic vesicle (OV)-like structures. Enrichment of OV-like structures allowed for the definitive identification of RGCs. RGCs displayed the proper temporal, spatial, and phenotypic characteristics of RGCs developing in vivo. To test the ability of hPSC-RGCs to serve as a disease model, lines were generated from a patient with an E50K mutation in the Optineurin gene, causative for normal-tension primary open angle glaucoma. E50K RGCs displayed significantly higher levels of apoptosis compared to a control lines. Apoptosis was reduced with exposure to neuroprotective factors. Lastly, hPSC-derived RGCs were studied for their ability to develop functional features possessed by mature in vivo RGCs. hPSC-derived RGCs displayed a few immature functional features and as such, strategies in which to expedite synaptogenesis using hPSC-derived astrocytes were explored. Astrocyte and RGG co-cultures displayed expedited synaptic and functional maturation, more closely resembling mature in vivo RGCs. Taken together, the results of this study have important implications for the study of RGC development and by extension, the advancement of translational therapies for optic neuropathies.

1. INTRODUCTION

Retinal ganglion cells (RGCs) play an essential role in transmitting visual information from the eye to the brain. When this transduction pathway is perturbed, light information gathered from the eye cannot reach the appropriate processing centers in the brain, resulting in blindness. Degeneration of RGCs can occur in common disease states called optic neuropathies or can undergo damage in response to certain instances of traumatic brain injuries [1, 2]. Irrespective of the cause of degeneration, all of these conditions are associated with the impairment and eventual loss of RGCs, which do not possess the capacity for regeneration into adulthood. To date, no therapies exist to delay or halt progression of RGC degeneration. Furthermore, by the time a patient observes vision abnormalities, upwards of 50% of their retinal ganglion cells have irreversibly degenerated [3,4]. This necessitates the development of strategies to study the etiology of degeneration and develop translational therapeutic approaches.

Human pluripotent stem cells (hPSCs) encompass both human embryonic stem cells (hESCs) and human induced pluripotent stem cells (hiPSCs). Both populations have the remarkable ability to self renew and can be differentiated into virtually any cell type of the body [5, 6]. Human embryonic stem cells were first generated in 1998 by isolating the inner cell mass of a human blastocyst [5]. Soon after, researchers began elucidating mechanisms conferring pluripotency, which led to the generation of hiPSCs less than a decade later [6]. Unlike hESCs, hiPSCs can be generated from adult somatic cells by genetic reprogramming to force expression of pluripotency genes, making them analogous to hESCs. Reprogramming allows for the unprecedented ability to modify somatic cells whose fates were traditionally considered to be determined. Moreover, because hiPSCs can be created from patients, they have important implications for generation of personalized medicine. Both hESCs and hiPSCs have revolutionized our understanding of human development, can serve

as a complement to existing animal models, and help narrow the gap in generating translational therapies.

1.1 RGC differentiation from hPSCs

In order to efficiently derive RGCs from hPSCs, a clear understanding of retinal development is essential because many of the same principles are translated from in vivo development to inform in vitro systems. For instance, retinal ganglion cells are the earliest born neural cell type in the retina, followed closely by amacrine cells, cones and horizontal cells [7]. At later stages of retinal development, rods are generated, followed by bipolar cells and eventually Muller glia. Similarly, when hPSCs are directed to differentiate toward a retinal lineage, this same birth order is recapitulated, wherein RGCs are the first cell type specified, sequentially followed by other retinal cell types as predicted from in vivo studies [8–13].

RGCs serve as the final output of the retina by sending light information to brain regions such as the lateral geniculate nucleus (LGN) or superior colliculus (SC) [14,15]. As such, RGCs tend to have much larger cell bodies and thicker axons compared to other retinal neurons, both of which are needed for long distance propagation of action potentials [16–19]. RGC axons fasciculate in the nerve fiber layer to form the optic nerve, which relays information to multiple brain regions. hPSC-derived RGCs have displayed similar distinct morphologies (Figure 1.1), with long neurites and fasciculated axons [13, 20–26]. In addition, the RGC layer occupies a distinct position in the retinal architecture, residing in the innermost retinal layer [27–29]. Remarkably, hPSCs have shown the ability to self-organize into organoid structures that recapitulate in vivo retinal structure. RGCs reside within the inner portion of these retinal organoids, while photoreceptors develop near the outer layers [9, 11, 13, 30].

hPSC-derived RGCs respond to neurotransmitters such as glutamate, recapitulating what is observed in vivo [21]. These cells have also exhibited excitatory postsy-

naptic potentials (EPSPs) [20], action potentials (APs) [13,20–22,25,26], spontaneous calcium transients [26] and are sensitive to the voltage gated potassium and sodium channel blockers TEA and TTX, respectively [13, 20, 22, 25, 26]. While these features do not necessarily distinguish RGCs from other neuronal cell types, RGCs are the predominant cell type within the retina that possess these features [31].

In order to distinguish RGCs from other cell types in differentiating cultures of hPSCs, a variety of protein markers are often used to confirm the identity of these cells (Figure 1.1). Early studies utilized TUJ1 as a common marker of RGC-like cells [8, 32]. TUJ1 is expressed by RGCs but does not confer any specificity, as many neuronal subtypes throughout the central nervous system (CNS) also express this marker [33, 34]. Thus, more specific markers were needed to identify RGCs from a pluripotent source.

Perhaps the most common transcription factor used to identity RGCs has been BRN3. BRN3 is expressed specifically by RGCs within the retina, is expressed by a large majority of RGCs beginning shortly after RGC specification, and its expression persists into adulthood [35–38]. However, BRN3 expression itself is not specific to RGCs, as it is also present in subsets of somatosensory and auditory neurons [36, 37, 39, 40]. Thus, when culturing a population of hPSCs that can differentiate into any cell type of the body, caution must be taken not to rely solely on one marker as confirmation of identity.

A variety of additional markers can be used to identify RGCs, including Islet1, HuC/D, and SNCG. Within the retina, these markers show some degree of specificity for RGCs, but they are less reliable in identifying hPSC-derived RGCs because they are expressed in other retinal cell types [41–46]. More recently, a protein called RNA Binding Protein With Multiple Splicing (RBMPS) has been shown to specifically label RGCs. However, the expression of RBPMS occurs later in development, complicating efforts to identify RGCs early in hPSC differentiation [13, 21, 47].

To further complicate matters, ongoing research involving the identification of RGC subtypes has shown that some subtypes do not express common markers. For in-

stance, many intrinsically photosensitive RGCs (ipRGCs) preferentially express Brn3 alongside the photopigment Melanopsin. However, certain populations of the M1 ipRGC subtype lack expression of any BRN3 isoform [13, 48–50]. Therefore, the combinatorial expression of genetic markers, morphological features and functional characteristics must be used to identify a presumptive RGC.

1.2 Translational applications of hPSC-derived RGCs

Human pluripotent stem cells have revolutionized the field of human biology. Large populations of individual cells can be differentiated and isolated to study the cellular mechanisms that contribute to a disease state, for high throughput drug screening, and for development of cell replacement therapies (Figure 1.2) [51,52]. Differentiation protocols used to generate retinal cells are numerous and provide many different methods to derive retinal neurons [8,9,12,13,20–23,26,30,53,54]. Additionally, the advent of retinal organoids allows for the retina to be studied in its native structure, more closely resembling an in vivo tissue [9,11,30].

hPSCs serve as an effective developmental model because they allow access to some of the earliest time points of development that would otherwise be inaccessible to investigation. Before the advent of pluripotent stem cells, our understanding of human retinal development was largely informed by animal models. The only option for studying retinogenesis in humans was through the use of human fetal or post-mortem tissue [55]. Such samples were only accessible at limited developmental time points and could be difficult to obtain due to legal and ethical issues. Following the emergence of hPSC technology, studies have effectively demonstrated the ability to recapitulate all of the major stages of human retinogenesis. This includes the primitive eye field stage, which gives rise to the evaginating optic vesicle, eventually developing into retinal organoids [9–11, 13, 30]. These hPSC-derived retinal organoids contain many distinct populations of neurons which remarkably recapitulate the cellular mo-

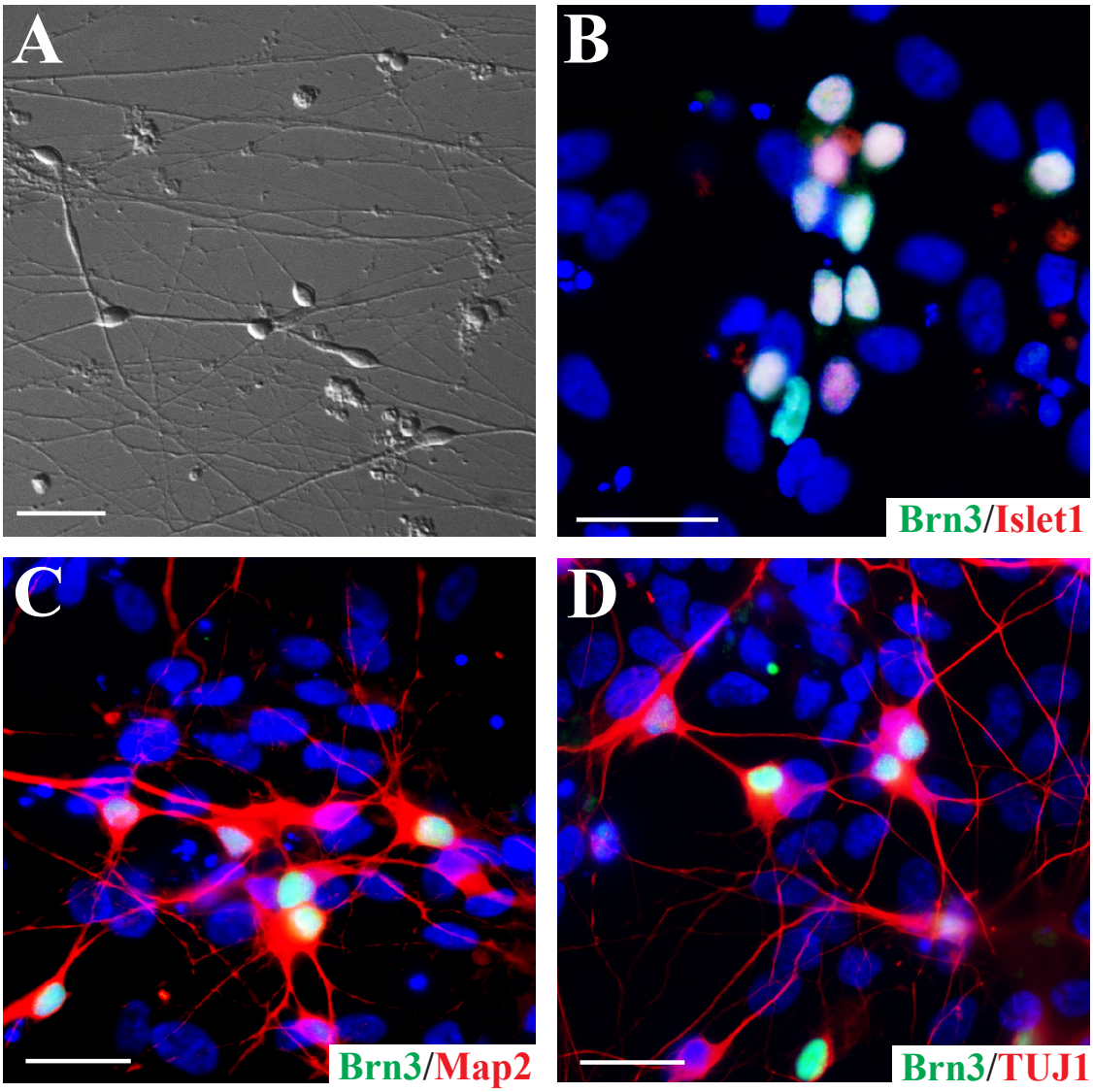

Fig. 1.1. Common markers of hPSC-derived retinal ganglion cells.

hPSC-derived RGCs exhibit transcriptional and morphological features associated with in vivo RGCs. DIC imaging of retinal cultures demonstrated RGC-like morphology with large, three-dimensional somas and long neurite projections (A). hPSC-derived RGCs can be identified by the expression of RGC-associated transcription factors such as ISLET1 and BRN3 (B). Immunocytochemistry displayed unique morphological features of RGCs with BRN3-positive cells extending lengthy MAP2- and TUJ1-positive neurites (C-D).

saicism of an in vivo retina, paving the way for a more comprehensive understanding of human retinal development.

hPSCs can be used to generate models to elucidate mechanisms of RGC disease. Glaucoma is the most prevalent of these disorders and it is estimated that by 2020, 79.9 million people will be diagnosed with primary open angle glaucoma (POAG) [56]. Like many forms of neurodegeneration, a majority of glaucoma cases are sporadic in nature, while a small percentage are caused by specific gene mutations. Although it is not known what mechanisms underlie glaucomatous degeneration, elevated intraocular pressure (IOP) has been commonly associated with onset of the disorder. However, in up to 50% of POAG cases, no elevated IOP is observed [3, 57, 58]. Thus, work is currently ongoing to determine the precise etiology of glaucomatous degeneration using hPSC disease modeling.

IntroFig2.pdf

RGC degeneration in optic neuropathies may share common features, even if the initial causes of the disorders are different. For instance, glaucomatous degeneration involves a targeted loss of RGCs by apoptosis [4, 59, 60]. Recapitulating this mechanism in a dish may provide a useful platform to study all forms of glaucoma and complement existing animal models to help narrow the gap in generating translational therapies. Inherited disorders are of particular interest as a disease model and offer many advantages as a model system. Genetic forms of glaucoma are caused by known mutations within a patients genome, allowing for more straightforward connections to be made between cellular changes and particular genotypes [51, 61]. Genetic models are more likely to display a phenotype in a consistent and reliable manner, allowing for more straightforward experimental design and analysis. hPSC-derived retinal neurons can be studied and clearly assayed for changes at the cellular level, such as cell death, changes in intracellular trafficking, or disturbances of the autophagy pathway, which might inform mechanisms of degeneration in sporadic cases [13, 26, 54, 62]. Furthermore, when modeling forms of glaucoma involving elevated intraocular pressure, the complexity of modeling diurnal changes in eye pressure in a cell culture

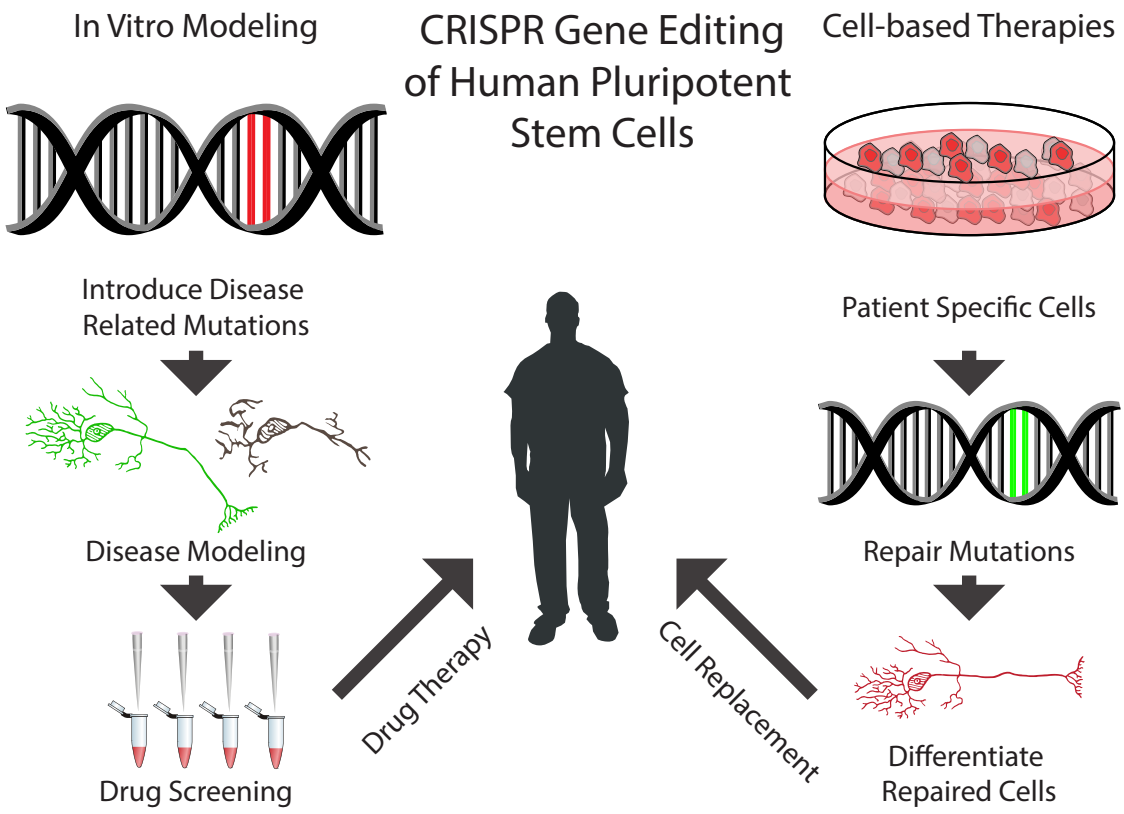

Fig. 1.2. Translational applications for hPSC-derived RGCs

hPSC-derived RGCs can be used for disease modeling purposes. Mutations can be introduced using CRISPR/Cas9 and isogenic controls created to control for cell line variability. These populations can be further used for high throughput drug screening to identify potential therapeutic compounds. hPSC-derived RGCs can also be used for developing cell replacement therapies by correcting mutations and inserting healthy RGCs into patients.

system can prove challenging [63–65], underscoring the need for genetic models that do not involve exogenous stressors to induce a phenotype. Disease models allow for development of tests for early detection in a clinical setting [61]. Early detection is imperative because neuroprotective strategies have a greater likelihood of success than cell replacement therapies due to the hurdles that exist when transplanting projection neurons in vivo.

Many genetic models of glaucomatous degeneration have been developed over the past few years [13, 26, 54]. These include mutations in TANK Binding Kinase 1 (TBK1), Optineurin (OPTN) and SIX6, all of which have been associated with forms of POAG. These models have recapitulated the RGC specific cell death observed across all forms of glaucoma and have helped uncover the role of autophagy dysregulation as a potential mechanisms of degeneration. These papers represent the first demonstration of disease modeling using hPSC-derived RGCs and are an important step forward in understanding disease mechanisms and identifying potential therapeutic interventions.

hPSCs also allow for the generation of large populations of patient specific cells for high throughput drug screening [51, 52]. This ability has many advantages, namely that the affected human cell type can be generated for screening instead of relying on animal models. Although animal models provide insight as to how a drug will impact an entire organism, many therapeutics that initially show promise in animals fail when translated to humans in a clinical setting [66, 67]. hPSCs allow for the screening of thousands of compounds at once, which provide critical safety and toxicity information to inform drug development in human cells that can complement existing animal models and help narrow the gap in generating translational therapies.

In addition, the ability to derive patient specific cells is a groundbreaking advancement in personalized medicine [51, 68]. It is well established that a patients genetic background is a contributing factor to drug efficacy. The ability to screen compounds on a patient's own cells could greatly optimize the process of discovering the most

effective therapy for a particular patient. Patient-derived RGCs can also be used to uncover neuroprotective agents that slow or even halt the progression of degeneration.

Recent work has described the ability to elucidate potential therapeutic pathways involved in RGC degeneration and discover suitable compounds to intervene within pathways of interest [69]. In particular, the dual leucine zipper kinase (DLK) pathway and its downstream partner, leucine zipper kinase (LZK) pathway, were discovered as prospective mediators of RGC cell death and were proposed as possible targets for intervention to increase cell survival. Treatment of RGCs with Sunitinib, a FDA-approved drug known to interfere with the DLK and LZK pathways was shown to enhance survival of injured hPSC-RGCs in a dose dependent manner. This study provided integral insights into RGC degeneration, particularity the role of the DLK and LZK pathway in RGC injury and demonstrated the first use of hPSC-derived RGCs for drug screening applications.

However, it must be noted that limitations of hPSC in vitro systems exist. Namely, human cells differentiated in vitro lack the inherent structure of an in vivo tissue. Moreover, even in retinal differentiation protocols which have the ability to derive organoids that recapitulate the three dimensional organization of an in vivo retina, other important organ systems such as the kidneys are not present. The lack of these organs certainly plays a role in discerning the actual pharmacokinetics of drugs of interest. As such, hPSCs should serve as a compliment to existing animal models to fully explore drug screening in humans.

hPSCs can also be utilized for the development of cell replacement therapies. Cell replacement approaches will be most effective in later stages of a disease where a majority of the RGC population has already degenerated and cellular rescue is no longer an option. Ideal replacement strategies necessitate a clearly defined and easily differentiated cell type which have unique and specific features to identify them in living culture. However, as replacement neurons will have to navigate an already unhealthy environment to connect with their proper synaptic targets in vivo, hPSC replacement strategies will most likely be successful for those cell types with relatively short

distance synaptic targets. As such, the effective replacement of projection neurons such as RGCs faces numerous potential obstacles before these cellular replacement approaches can be implemented.

Transplanted RGCs must first integrate into the inner plexiform layer and connect with their pre-synaptic targets, primarily amacrine and bipolar cells. After integration, RGCs must be able to navigate through a likely unhealthy environment and navigate up to 110mm to reach the proper synaptic targets [19]. Once this feat has been accomplished, RGCs must make functional connections with their postsynaptic targets in order to propagate information from the eye to the brain.

To date, many groups have explored various aspects of this puzzle. hPSC-derived neurons have displayed some capacity to integrate into the retina [70–74]. hPSC-derived RGCs grown in a dish exhibit some capacity to respond to environmental growth cues and generate lengthy neurites [13, 21, 25]. In fact, hPSC-derived RGCs plated in close proximity to ex vivo mouse tissue can preferentially target the superior colliculus, a main RGC synaptic target in the brain, over non-preferred synaptic target such as the olfactory bulb [25].

Lastly, work is currently underway exploring the electrophysiological capabilities of these cells [13, 20–22, 25, 26] to determine to what extent they can recapitulate the mature functional characteristics of in vivo RGCs. However, much more work is needed to piece these aspects together to ensure successful cell replacement.

1.3 Conclusion

hPSC technology allows for many different interventions at varying stages of disease. hPSCs provide a window into early human development from which we might better understand and uncover mechanisms of disease progression and neural regeneration. hPSC-derived RGCs allow for personalized drug discovery to rescue degenerating cells early in a disorder. Furthermore, cell replacement therapies at the end stages of disorders can be explored and developed. Although still a nascent field,

hPSC technology holds exciting promise to bring translational therapies from bench to bedside through the unprecedented ability to study human cells in a dish. While many protocols exist to derive retinal cells from hPSCs, the Meyer protocol is explored in depth in the following chapters. The method used to derive RGCs from hPSCs is described, followed by characterization of hPSC-derived RGCs for disease modeling. Finally, the capacity of hPSC-derived RGCs to fully mature and recapitulate features of in vivo, adult RGCs is elucidated.

1.4 Acknowledgements

Sarah K. Ohlemacher: Conception and design, financial support, collection and/or assembly of data, data analysis and interpretation, manuscript writing, final approval of manuscript.

Michael C. Edler: Manuscript writing, final approval of manuscript.

Clarisse M. Fligor: Conception and design, collection and/or assembly of data, data analysis and interpretation, manuscript writing.

Kirstin B. Langer: Conception and design, collection and/or assembly of data, data analysis and interpretation, financial support.

Elyse M. Feder: Collection and/or assembly of data, data analysis and interpretation, manuscript writing.

Jason S. Meyer: Conception and design, financial support, collection and/or assembly of data, data analysis and interpretation, manuscript writing, final approval of manuscript.

2. GENERATION OF HIGHLY ENRICHED POPULATIONS OF OPTIC VESICLE-LIKE RETINAL CELLS FROM HUMAN PLURIPOTENT STEM CELLS

2.1 Introduction

In recent years, several groups have described the ability to direct hPSCs to a retinal fate [8, 11, 32, 75–78]. In order to serve as an effective in vitro model for human retinogenesis, as well as provide a foundation for translational applications of these cells, the stepwise differentiation of hPSCs through all of the major stages of retinogenesis helps to ensure the proper differentiation and prospective identification of hPSC-derived retinal progeny [10, 53, 79, 80]. The procedure to efficiently and reproducibly differentiate retinal cells from hPSCs is described below (Figure 2.1). Cells are taken through a stepwise protocol to direct them toward a neural fate by treatment with neural induction medium (NIM), then to a retinal fate by exposure to retinal differentiation medium (RDM). Undifferentiated hPSCs are enzymatically lifted from matrigel-coated plates and exposed to NIM in suspension. Differentiation in suspension allows the cells to form three-dimensional aggregates. At 7 days of differentiation, aggregates are plated and attached to 6 well plates, where a neuroepithelial fate is established. Upon 16 days of differentiation, neurospheres are lifted and maintained in RDM to establish a three-dimensional optic vesicle (OV)-like fate. OV structures will give rise to a variety of retinal cell types, including retinal ganglion cells, retinal pigment epithelium (RPE), as well as cone and rod photoreceptors. The use of this protocol to generate a myriad of retinal cell types facilitates in vitro studies of human retinogenesis [10, 30, 53], and retinal dysfunction [10, 81–84], and provides a large population of cells to aid in drug development in addition to patient specific therapies [76, 77, 85, 86].

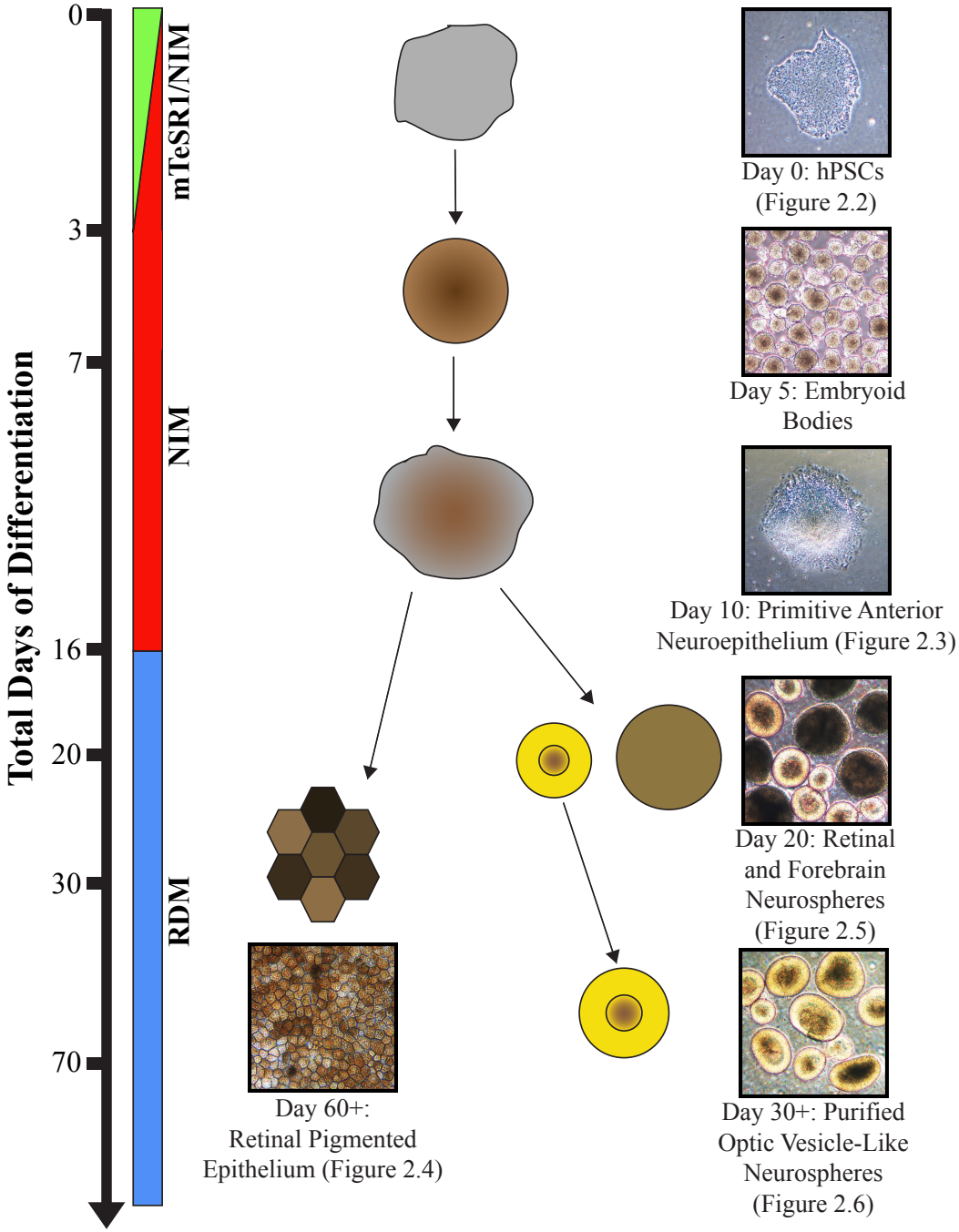

Fig. 2.1. Overview of stepwise retinal differentiation protocol.

hPSCs can be directed to differentiate by the generation of embryoid bodies (EBs). By 7 total days of differentiation, EBs are adhered and maintained for a total of 16 days. Neurospheres are generated and retinal progenitor populations can be enriched by 20 days of differentiation. Retinal neurospheres will yield all of the major cell types of the neural retina within the first 70 days of differentiation. Alternatively, optic vesicle-like cultures at day 16 of differentiation may be utilized to generate retinal pigment epithelium through the maintenance of adherent cultures.

NOTE: All medium and solutions added directly to cells must be warm. It is recommended that reagents be heated in a 37 °C water bath prior to use.

NOTE: All protocols below should be performed in a Class II biological culture hood to prevent contamination of cells.

NOTE: Standard incubation temperature is 37 °C with 5% CO_2.

2.2 Basic protocol 1: Enzymatic passaging of human pluripotent stem cells

The following procedure can be used to maintain and passage hPSCs for long-term use [5, 6, 10, 53, 80, 87, 88]. The protocol detailed below (Figure 2.1) focuses on the use of mTeSR1 medium and matrigel to maintain hPSCs, although previous reports have demonstrated the ability to maintain hPSCs in alternate systems such as fibroblast feeder cells [10, 53, 80]. Cells are maintained on matrigel-coated 6-well culture plates and are split when a confluency of approximately 70% is reached. This will aid in preventing spontaneous differentiation of cells due to overgrowth and subsequently ensures that an abundant amount of cells can be collected for directed differentiation. Typically, hPSCs are expanded at a ratio of 1:6, with a single well of cells capable of seeding an entire six well plate. A starting population of hPSCs should display a tightly clustered and bright morphology as well as exhibit immunoreactivity to pluripotency markers (Figure 2.2).

2.2.1 Materials

- hPSCs plated on matrigel-coated 6 well plates
- Matrigel, hESC-qualified (BD Biosciences, see Reagents and Solutions unit)
- mTeSR1 (StemCell Technologies)
- Neural Induction Medium (NIM, see Reagents and Solutions unit)

- DMEM-F/12, 1:1 (Life Technologies)
- Dispase (Life Technologies, see Reagents and Solutions unit)
- 6-well culture plates (Falcon)
- Inverted light microscope
- T75 Flask (Falcon)

2.2.2 Passaging undifferentiated cells

1. Matrigel coat 6-well plates (1mL/well) and transfer to incubator for a minimum of 1 hour.
2. Aspirate excess matrigel from plates then add 2 ml mTeSR1 medium to each well and set aside until step 13.
3. Prepare two 15 mL conical tubes, one to collect undifferentiated cells to expand and another to collect cells that will be directed to differentiate (see section 2.2.4 regarding the generation of embryoid bodies).
4. Using an inverted light microscope, mark areas of spontaneous differentiation in wells that will be used for expansion.
5. Transfer plate to biological safety cabinet and using a 1ml pipette tip, scrape away any cells from the marked areas of differentiation.
6. Aspirate medium from wells, add 1ml of dispase to each well and transfer to incubator for 10 minutes.
7. Monitor the plates every few minutes thereafter to ensure the dispase is allowing for the start of cell detachment from the culture surface. If dispase is sufficiently warmed to 37 °C, this process should not take more than 15 minutes. Once a

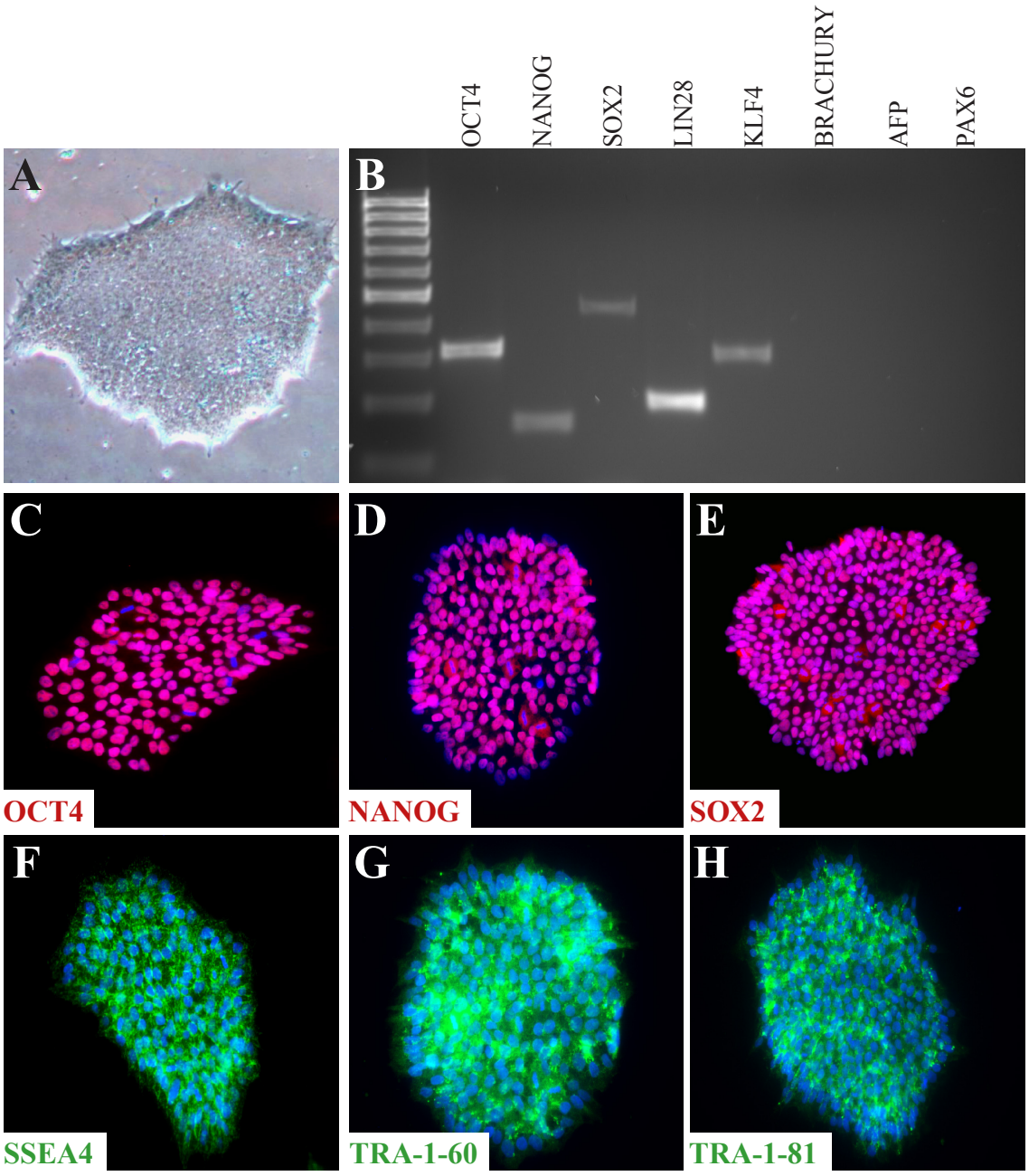

Fig. 2.2. Characterization of undifferentiated hPSCs.

hPSCs displayed a typical undifferentiated morphology, including tightly packed colonies of cells and clearly defined edges (A). RT-PCR analysis demonstrated the expression of characteristic pluripotency makers in hPSCs, while lacking mesodermal, endodermal and ectodermal markers (B). Immunocytochemistry further demonstrated widespread expression of pluripotency-associated transcription factors (C-E) as well as cell surface markers (F-H).

majority of the cell clusters display curled edges, dispase should be removed immediately by aspiration.

8. Wash each well once with 1ml DMEM/F12, ensuring that the medium is added to the side of the well, not directly onto the cells. Doing so will ensure that colonies are not prematurely detached from the culture surface during the wash step.

9. Aspirate DMEM/F12 from wells and add an additional 1ml of DMEM/F12 in each well, this time added with force directly onto the cells to detach colonies from the plate by pipetting. Note that it is better to forcefully dislodge colonies by pipetting 3-4 times than to gently agitate any more than this. Minimizing the amount the cells are broken up is key to ensure maximum survival.

10. Transfer the cells from marked wells that will be expanded in one 15ml conical tube and remaining wells for retinal differentiation to another 15ml conical tube.

2.2.3 Expansion of undifferentiated hPSCs

11. Allow cells to settle to the bottom of 15 ml conical tube (either by gravity or centrifuge for 1 minute at 800 rpm) and aspirate supernatant, taking care to avoid aspirating the cell pellet.

12. Re-suspend cells in mTeSR1 medium so that each new well will receive 500μL of cell suspension per well. For example, if one well of hPSCs is being passaged to six new wells, 3 ml of mTeSR1 should be used. Break up clusters by pipetting forcefully 4-5 times with a 5 mL serological pipette. Note that each cell line can vary in ease of breaking up cell clusters. If cell clusters are not broken up sufficiently, increase pipetting during the next passage. It is better that clusters remain large than to break them up too much.

13. Pipet 500μL of undifferentiated cell suspension at a 90 degree angle into each new well from step 2.

14. Transfer to the incubator and agitate plates in side-to-side followed by front-to-back motions to ensure even distribution of cells. Be sure to pause briefly between each series of agitations to ensure that cells are evenly dispersed across the well rather than accumulated in the middle.

15. Medium should be changed daily (2mL/well) until the next passage, typically within 4-5 days.

2.2.4 Generation of embryoid bodies for differentiation

16. To begin the differentiation process, cells must be slowly transitioned out of mTeSR1 medium into NIM, and maintained in a T75 flask. Day 0 is defined as the day cells are lifted from the Matrigel plate.

17. After cells have settled by gravity in the 15 ml conical tube (from step 10), aspirate the supernatant. Gently resuspend the cell pellet in a 3:1 mixture of mTeSR1:NIM and transfer to a T75 flask, and place flask in the incubator overnight.

18. Over the first few days of differentiation, embryoid bodies should be gradually transitioned from mTeSR1 to NIM. To accomplish this, transition cells with the following ratios of mTeSR1 to NIM. Day 0- 3:1 Day 1- 1:1 Day 2- 1:3 Day 3- Complete NIM

19. After day 3 of differentiation, change NIM every other day until day 7 is reached.

2.3 Basic protocol 2: Induction to a primitive anterior neuroepithelial fate

As retinal cells are derived from a pluripotent source through a stepwise process in vivo [89–92], likewise hPSCs should be differentiated through analogous stages of differentiation, including a primitive anterior neural fate, an optic vesicle stage, and eventually a retinal and/or RPE fate [10, 30, 53, 80]. To initiate this stepwise process, embryoid bodies are kept in suspension to begin differentiation for the first 7 days, at which point they are allowed to adhere to 6-well plates and maintained until day 16. By day 10 of differentiation, cells can be characterized by a larger, more uniform appearance as well as the expression of typical neural and eye field transcription factors (Figure 2.3).

2.3.1 Materials

- hPSC-derived embryoid bodies in T75 flask (from Basic Protocol 1)
- NIM (see Reagents and Solutions unit)
- Fetal Bovine Serum

2.3.2 Plating embryoid bodies

After 7 total days of differentiation, cells should be plated onto 6-well culture plates to allow for further neural differentiation. This can be accomplished by the addition of 10% fetal bovine serum (FBS) for the first 24 hours of the plating process to ensure cells adhere to the wells. In general, EBs derived from 5 wells of undifferentiated cells will plate on 1 six well plate, approximately 30-40 EBs per well.

1. Collect EBs in a 15mL conical tube and allow them to settle by gravity, typically within 5 minutes.
2. Add 2 mL of NIM to each well of a 6 well plate.

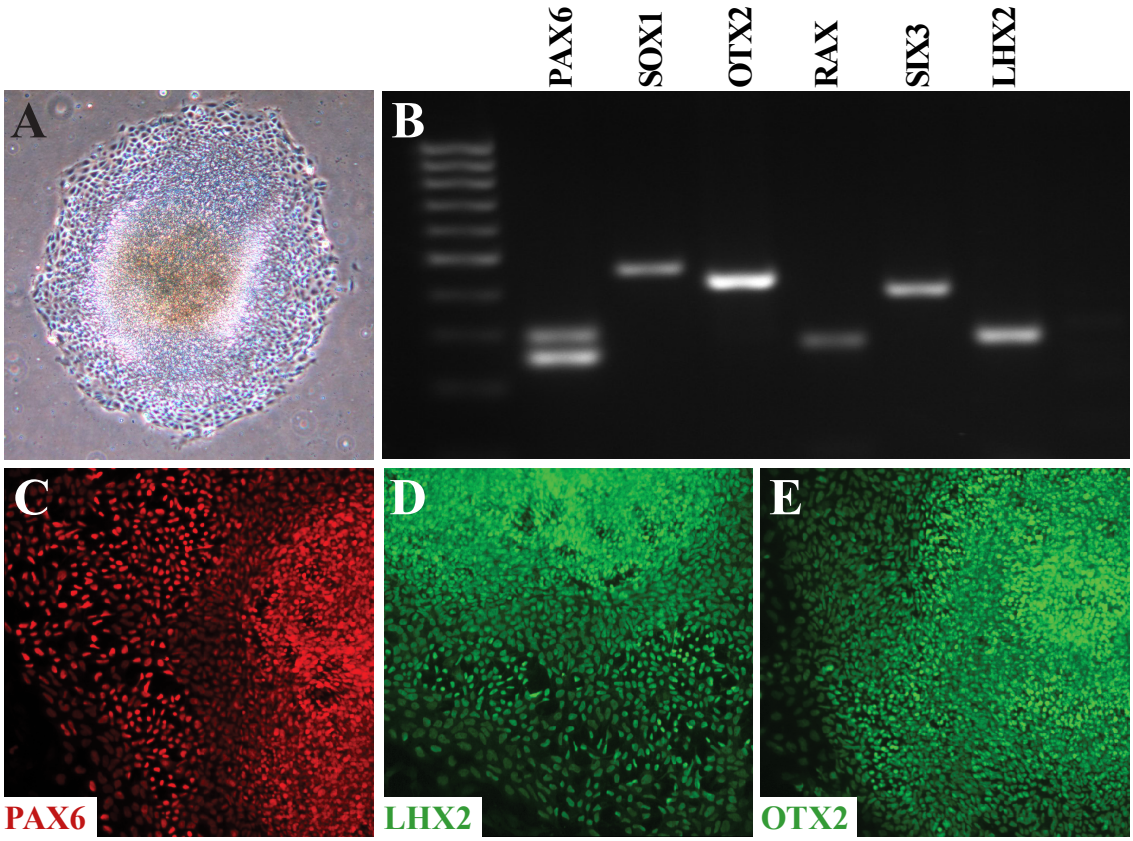

Fig. 2.3. Induction of hPSCs to a neural progenitor fate.

After ten days of differentiation and plating (A), differentiating hPSCs were analyzed by RT-PCR and demonstrated expression of the neural markers PAX6 and SOX1. An anterior neural, eye-field fate was further indicated by the expression of OTX2. RAX, SIX3, and LHX2 (B). Immunocytochemistry demonstrated the widespread expression of many of these transcription factors (C-E).

3. Aspirate the supernatant from the EBs, being careful to avoid removing the cell pellet. Resuspsend the EBs in NIM so that each well will receive 200μL of the cell suspension, and add cells to 6-well plate(s) accordingly. For one plate, cells would be resuspended in 1.2ml of NIM.

4. Add 250 μL (10%) FBS to each well to allow for cell attachment to the culture plate.

5. Transfer plates to the incubator, agitating plates in a side-to-side and then front-to-back manner to ensure an even distribution of cells within each well.

6. The following day, aspirate medium containing FBS and add fresh NIM to each well (2mL/well) without FBS.

7. Medium should be changed every other day until day 16 of differentiation is reached, by which point these cells will have acquired a primitive anterior neuroepithelial fate.

2.4 Basic protocol 3: Differentiation of primitive anterior neuroepithelial cells to a retinal pigment epithelial fate

During normal development, the RPE is the first retinal cell type to be specified from a more primitive source. The RPE layer develops in a manner that is distinctly separate from the neural retinal populations of cells, and is known to be specified in the absence of factors instrumental in directing a neural retinal fate [93–95]. Likewise, RPE cells generated from hPSCs are also found to differentiate through a similar process in which RPE cells are often found in close proximity to, although distinctly separate from, neural retinal populations [30, 96]. hPSC-derived RPE cells can be readily identified by their accumulation of pigmentation and their distinct hexagonal morphology (Figure 2.4), and have been successfully generated by many groups in recent years [10, 53, 75, 76, 80, 96–102].

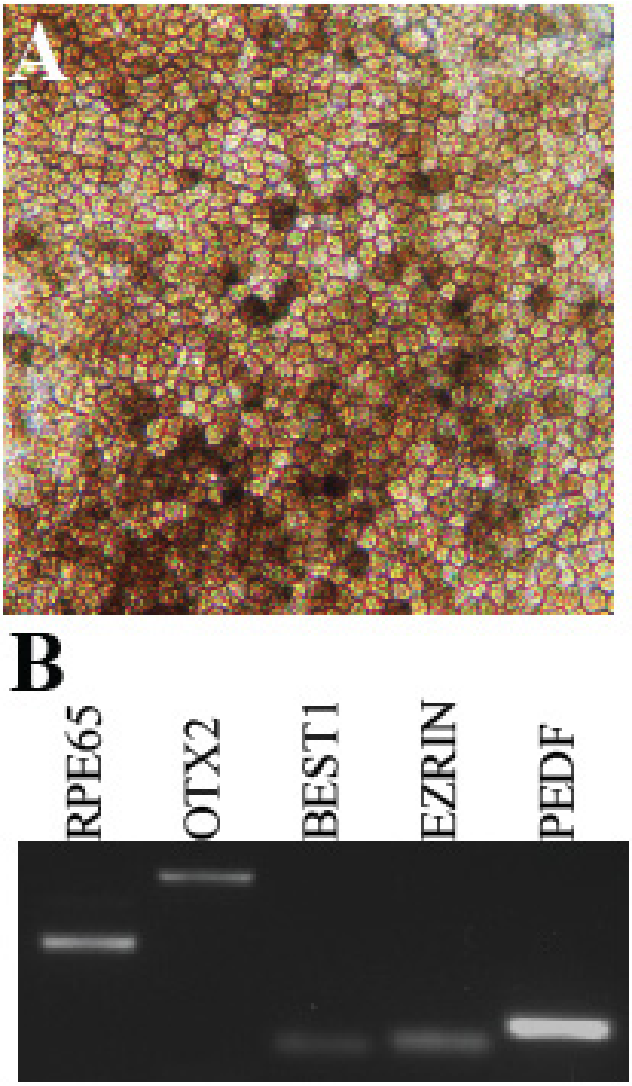

Fig. 2.4. Differentiation of hPSCs to retinal pigment epithelium.

hPSC-derived RPE-like cells expressed typical RPE associated markers when screened by RT-PCR (A). Under brightfield microscopy, these cells displayed proper morphological features distinct to RPE, including a hexagonal shape and areas of pigmentation (B).

2.4.1 Materials

- hPSC-derived neuroepithelial cells plated on 6-well plates (from Basic Protocol 2
- Retinal Differentiation Medium (see Reagents and Solutions unit)
- poly D-ornithine/Laminin-coated coverslips in a 4 or 24 well plate (see Support Protocol 2.7.1)
- Inverted light microscope
- FGF2 (working concentration of 20 ng/ml)
- EGF (working concentration of 20 ng/ml)
- Heparin (working concentration of 2 μg/ml)

2.4.2 Differentiation of hPSCs to retinal pigment epithelium.

hPSC-derived primitive anterior neuroepithelial cells on 6-well plates can also be used to generate a highly pure population of RPE, characterized by a cobblestone-like morphology as well as dark pigmentation. Continued growth and differentiation of these cells should be maintained until an RPE morphology emerges, typically within the first 60 days of differentiation.

1. Once day 16 of differentiation is reached, medium should be switched from NIM to RDM and medium should be changed every 2-3 days until distinct populations of RPE cells are readily observed, typically within 60 total days of differentiation.
2. At day 60 of differentiation, RPE can be microdissected and isolated. To microdissect RPE, identify an area of RPE cells of suitable purity by pigmentation and morphology under the microscope.

3. Using a pointed object (e.g. tungsten needle, pipette tip, etc), gently scratch away an area around the region of cells to be microdissected, freeing up the RPE cells.

4. Using a P100 pipette, transfer this cluster of freed RPE cells with 50μL of medium to a laminin/poly-D-ornithine-coated coverslip in a 4 or 24 well plate, and repeat this process for as many coverslips as needed (see support protocols for coating coverslips). Typically, one cluster of RPE cells should be sufficient per coverslip.

5. Transfer the plate to incubator and allow RPE to attach to coverslip overnight.

6. The next day, RPE cell clusters should have adhered to the coverslips. Add 500μL of RDM supplemented with EGF (20 ng/ml), FGF2 (20 ng/ml), and heparin to allow for proliferation of RPE cells. Replace medium and growth factors every 2 days.

7. Within 7-10 days, RPE cells should have lost most pigmentation and their hexagonal shape, and will have occupied most of the coverslip.

8. To allow for maturation and reacquisition of RPE morphology, remove medium containing EGF, FGF2, and heparin and replace with RDM. Maintain in this state for 2-3 weeks, or until a desired stage of RPE maturation is reached.

2.5 Basic protocol 4: Differentiation and long-term maintenance of retinal progenitor cells

During in vivo development, after cells have adopted a primitive anterior neural phenotype, a subset of cells are known to acquire a retinal fate and are characterized by numerous retinal-associated features that distinguish these cells from other neural lineages [103–106]. Once this retinal identity has been established, all mature retinal cell types (cones, rods, retinal ganglion cells, etc.) will eventually arise. Likewise,

hPSCs can acquire a retinal progenitor fate (Figure 2.5), eventually yielding all of the major cell types of the retina [10, 53, 80, 96, 107]. To accomplish this differentiation event, cells are lifted and maintained in floating suspension with RDM after approximately 16 days total days of differentiation. Retinal and non-retinal cells can then be manually separated and maintained until the desired stage of differentiation is reached.

2.5.1 Materials

- Primitive neuroepithelial cells maintained in 6 well plates (from Basic Protocol 2)
- Retinal Differentiation Medium (see Reagents and Solutions unit)
- 60mm x 15mm polystyrene petri dishes
- 6 well plates (Falcon)

2.5.2 Generation of neurospheres from primitive anterior neuroepithelial cells

At day 16 of differentiation, cells should be lifted from culture plates to allow for the development of a three-dimensional OV-like structures.

1. Using a P1000 pipetman, draw up 1 ml of medium from a well of cells and dislodge the center of each aggregate from the plate by vigorously pipetting the medium directly at the center of each aggregate. The center of each aggregate will dislodge, leaving behind a ring of peripheral cells possessing a flattened appearance. It is better to pipette forcefully 5-6 times instead of gently pipetting any more than this, as excessive pipetting results in cell death and reduced yield of neurospheres.

2. After dislodging the cells from the plates, transfer aggregates to a 15ml conical tube. Allow the cell aggregates to settle by gravity or by centrifugation for 1 minute at 800rpm.

3. Aspirate the supernatant and resuspend the cells in 5ml of RDM.

4. Transfer the cell suspension to a 60mm dish and return cells to the incubator. Cells at this stage should have their medium changed every 2-3 days.

2.5.3 Manual enrichment of retinal neurospheres

5. By day 20-25 of differentiation, two populations of neurospheres will begin to emerge from the primitive anterior neuroepithelial cells - those possessing a golden ring around the outside (retinal neurospheres) and those with a darker appearance lacking this golden ring (non-retinal forebrain neurospheres). These morphological differences can easily be observed with an inverted microscope under a 4x objective. By 30 total days of differentiation, distinct transcriptional profiles emerge that distinguish these two populations (Figure 2.5).

6. Enrichment of retinal neurospheres should be performed by day 25 of differentiation. While viewing the cells under an inverted light microscope with a 4x objective, swirl the plate gently in a circular motion to collect cells in the middle of the dish.

7. Looking at the neurospheres through the microscope, gently gather retinal neurospheres based on their bright outer ring appearance using a P20 pipetman and transfer these neurospheres to a 15ml conical tube containing 5ml of RDM. Repeat until all retinal neurospheres have been collected in the same 15 ml conical tube.

8. After collecting retinal neurospheres, transfer this population along with the medium to a 60mm dish and return cells to the incubator. Non-retinal neu-

rospheres may be similarly maintained for neuronal cultures if desired, or discarded at this stage.

2.5.4 Maintenance of retinal neurospheres

9. From this point forward, medium will need to be replaced every other day until the desired stage of retinal differentiation is reached.

10. Tilt the plate towards you to allow the medium and neurospheres to collect on the bottom half of the plate.

11. Using a P1000 pipetman, transfer 1 ml of medium containing as many neurospheres as possible to a 15ml conical tube while still maintaining the tilt of the plate.

12. Collect the remaining medium and rinse over the entire surface of the plate to collect any remaining neurospheres that may remain in the plate.

13. Transfer this remaining medium to the 15ml conical tube.

14. Allow neurospheres to settle to the bottom of the tube and then aspirate the supernatant.

15. Resuspend neurospheres in 5ml of fresh RDM and transfer this cell suspension back to the dish. The dish should be stored in the incubator for further use.

2.6 Basic protocol 5: Induction of retinal progenitors to specific retinal subtypes

Previous studies have demonstrated the ability to yield all of the major classes of retinal cells from hPSC-derived retinal progenitor cells, including photoreceptors [10, 30, 32, 53, 77, 78, 108] and retinal ganglion cells [10, 30, 77, 80]. In order to derive these various types of retinal cells, retinal neurospheres must be maintained in

differentiating cultures for extended periods of time. Within 90 days of total differentiation, neural retinal cell types including photoreceptors and retinal ganglion cells can be identified (Figure 2.6). In order to analyze cells by immunocytochemistry, neurospheres should be dissociated with accutase and then plated onto poly-D-ornithine and laminin-coated coverslips (See Support Protocol 2.7.1 for coating coverslips). At this point, cells demonstrate the presence of a wide variety of retinal specific transcription factors and distinct neuroretinal morphologies such as neurite outgrowth and/or axonal/dendritic arborization typical of retinal ganglion cell or photoreceptors (Figure 2.6).

2.6.1 Materials

- Retinal Neurospheres at 40 days total differentiation (from Basic protocol 4)
- Retinal Differentiation Medium (see Reagents and Solutions unit)
- Poly-D-ornithine and laminin-coated coverslips (see Support protocols)
- Accutase (BD Biosciences)
- Inverted light microscope

2.6.2 Dissociation and plating of retinal neurospheres

1. Place the plate of retinal neurospheres in suspension under a microscope and swirl in a circular motion to gather cells towards the center of the field of view.
2. Gather neurospheres that will be used for dissociation and plating in a 1.5mL tube. Note: For plating coverslips, 2-3 neurospheres/coverslip typically provide enough density for sufficient plating and microscopy.
3. Allow neurospheres to settle at the bottom and gently remove excess medium with a pipette.

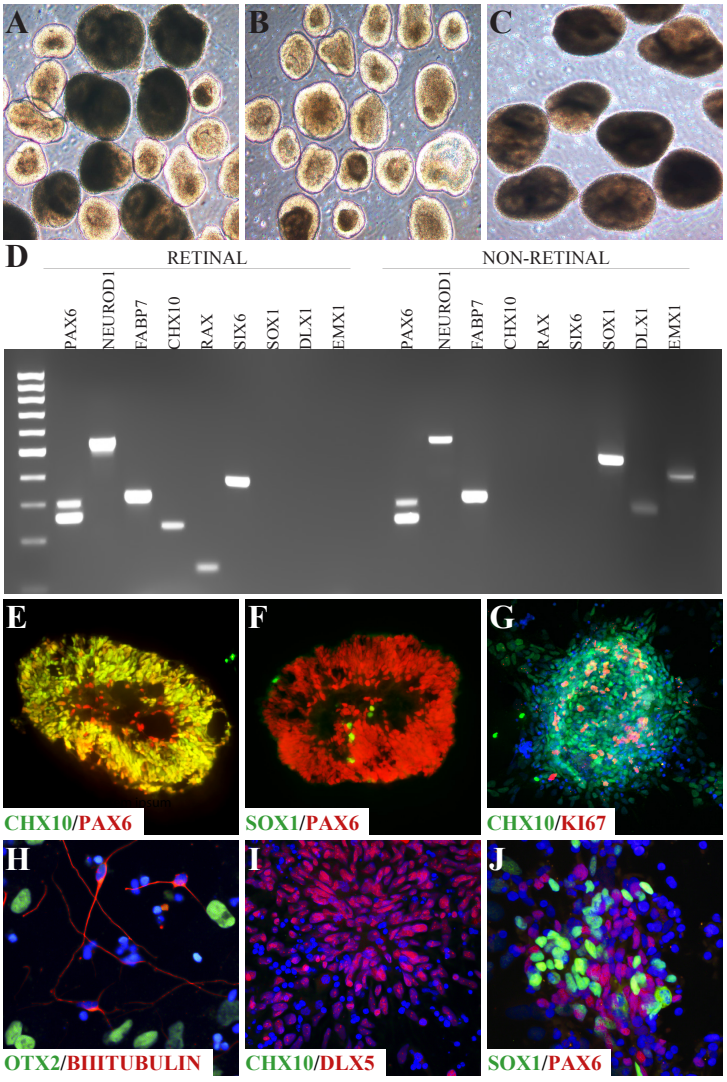

Fig. 2.5. Identification, enrichment, and characterization of retinal progenitor cells.

After 30 days of differentiation, hPSCs were isolated into two morphologically distinct populations (A). Retinal neurospheres were characterized by a bright ring (B) and a non-retinal neural population displayed a more uniform appearance (C). RT-PCR analysis revealed that both populations expressed neural associated transcription factors. Retinal neurospheres exhibited markers of retinal progenitors while the non-retinal neural cells expressed forebrain-associated transcription factors (D). Retinal neurospheres widely expressed retinal progenitor markers (E), but largely lacked the expression of the forebrain-associated marker SOX1 (F). hPSC-derived retinal progenitors remained highly proliferative (G). Non-retinal neural populations displayed typical features of emerging forebrain neurons (H) but lacked the retinal progenitor marker CHX10 (I). Non-retinal neural cells retained the expression of both PAX6 and SOX1 (J).

4. Add 100 μL of accutase.

5. Transfer to 37 °C water bath for 10 minutes.

6. Every 10 minutes, remove tube from water bath and forcefully agitate cells about 4 or 5 times with a P100 (50 μL setting) pipetman to break up the cells.

7. Repeat steps 5 and 6 if clusters need further dissociation.

8. Once retinal neurospheres have been dissociated to aggregates of a desired size, centrifuge cell suspension for 1 minute at 800 rpm. Viability is greatly increased if cells are dissociated to yield small aggregrates of cells rather than a single cell suspension.

9. Gently remove supernatant with a pipet and resuspend in enough RDM to ensure each coverslip receives 50μL of cell suspension.

10. Pipet 50μL of cell suspension onto each poly-D-ornithine and laminin-coated coverslip (see support protocol 2.7.1).

11. Transfer to incubator and allow cells to adhere overnight.

12. If cells are to be maintained on coverslips for further differentiation, add 500μL of RDM the following day and every other day thereafter until the desired stage of differentiation is reached. If cells are to be fixed immediately for immunocytochemistry, no additional medium should be added.

2.7 Support protocols

2.7.1 Coating coverslips with poly-D-ornithine and laminin

This brief protocol will explain how to coat the coverslips for use in Basic Protocols 3 and 5. While the poly-D-ornithine increases adhesion of cells to the coverslip,

the laminin promotes cell growth. Cells grown on poly-D-ornithine and laminin-coated coverslips can easily be utilized for immunocytochemical analysis and readily transferred to slides for visualization by microscopy.

2.7.2 Materials

- 24- and/or 4-well plates
- EtOH washed and subsequently autoclaved glass coverslips (12 mm)
- Stock of poly-D-ornithine (see Reagents and Solutions)

1. Transfer one coverslip to each well and ensure it lies flat on the bottom of the well.
2. Pipet 100 μL poly-D-ornithine into the center of each coverslip. Let sit at room temperature for 30 minutes, ensuring the poly-D-ornithine remains on the coverslip.
3. Remove poly-D-ornithine and wash each well with 1mL of sterile water. Repeat two more times.
4. After removing the third wash, check coverslips under microscope to make sure any precipitate is washed away. Continue rinsing if any residue remains.
5. Remove last wash and allow coverslips to air dry in the biological safety cabinet overnight. Be sure to leave the hood fan on and the sash slightly open.
6. The following day, remove dry coverslips from hood and store at room temperature for future use.

2.7.3 Laminin-coating of coverslips

1. Add 50 μL of laminin (20 μg/ml in DMEM) directly to the center of each coverslip previously coated with poly-D-ornithine.

2. Transfer plates to the incubator and let stand for at least 4 hours or overnight.

3. After incubation to allow for thorough coating of coverslips with laminin, aspirate excess laminin just before addition of cell suspension.

2.8 Reagents and solutions

All solutions should be made in a biological safety cabinet and filtered through a steriflip or bottle top filter to ensure solutions are sterile.

2.8.1 Dispase

- warm DMEM F/12
- 2mg/mL dispase powder.

Combine reagents and filter. Store up to 2 weeks at 4 °C

2.8.2 NIM (Neural Induction Medium)

- 489.5mL DMEMF/12
- 5mL N2 supplement
- 5mL MEM NEAA
- 0.5mL Heparin (2 mg/ml)

Combine reagents and filter. Store up to 1 month at 4 °C

2.8.3 RDM (Retinal Differentiation Medium)

- 240mL DMEMF/12
- 240mL DMEM

- 10mL B27 Supplement
- 5mL MEM Non-essential amino acids
- 5mL antibiotics

Combine reagents and filter. Store up to 1 month at 4 °C

2.8.4 Laminin

Staring with a 1mg/mL stock, dilute laminin 1:50 in cold DMEM to a final concentration of 20μg/mL. Store up to 1 month at 4 °C.

2.8.5 Matrigel

Dilute according to the manufacturers specifications in cold DMEM.

2.8.6 Poly-D-ornithine

- poly-D-ornithine (10mg Sigma)
- Sterile H_20
- 250 mL autoclaved beaker
- 50 mL conical tubes
- Steriflip 0.2 mm filtering device

1. Tap the bottle of poly-D-ornithine on the surface of the hood and open carefully as to not lose any powder.
2. Slowly pipet 1mL of sterile water into the bottle, put the top back on, and shake vigorously. Remove cap carefully and transfer to the beaker.
3. Repeat process about 4 more times to remove trace amounts from the bottle.

4. To the beaker, add sterile water up to a volume of 100mL. Pipet up and down to mix thoroughly.

5. Transfer 50mL into each conical tube. Sterile filter each using a Steriflip 0.2μm filtering device.

2.9 Discussion

The ability to direct the differentiation of hPSCs to a retinal fate represents a limitless source of retinal cells for in vitro studies of human retinogenesis, as well as a unique and exciting tool with which to study retinal disease progression, screen compounds for potential therapeutic efficacy, and even provide a source of replacement cells for transplantation purposes. For the above reasons, several groups have explored the ability to differentiate hPSCs to a retinal fate [8, 10, 11, 30, 32, 53, 76, 78, 80, 97], with the traditional focus upon the differentiation of photoreceptors and RPE cells due to the availability of unique and specific characteristics with which to identify these cells.

The protocol described within this manuscript not only details a method to differentiate retinal cells from a pluripotent stem cell population, but this protocol is significant due to the ability to faithfully identify and enrich for cells at all of the major stages of retinal development [10, 53, 80]. Starting from an undifferentiated population of hPSCs, cells are efficiently differentiated to a primitive anterior neuroepithelial fate in high purity after as little as 10 days of differentiation (Figure 2.3). From this point, differentiating cells yield neurosphere populations representing either forebrain progenitor cells or OV-like retinal progenitor cells, the latter of which exclusively gives rise to more mature retinal phenotypes including photoreceptor cells and retinal ganglion cells [10,80]. The ability to readily identify cells at each of the major stages of retinal development is unique to the method outlined in this manuscript, and helps to establish hPSCs as a valuable in vitro model of human retinogenesis.

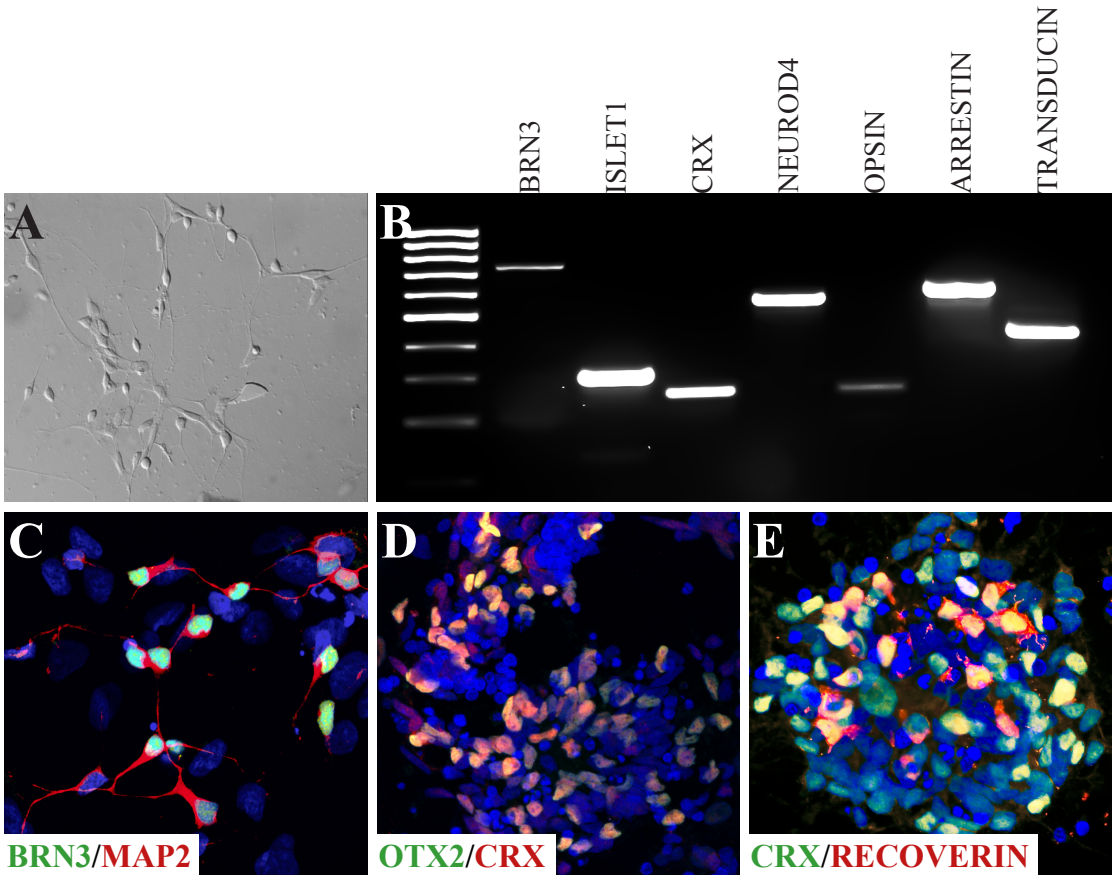

Fig. 2.6. Differentiation of hPSCs to retinal neurons.

Within 90 total days of differentiation, hPSC-derived retinal cells displayed typical neuronal morphologies under DIC microscopy (A). Analysis by RT-PCR illustrated an array of retinal-associated transcription factors including those associated with ganglion cells (BRN3 and Islet1), as well as those associated with photoreceptors (CRX and NeuroD4). Furthermore, proteins associated with phototransduction could also be identified (B). Immunocytochemistry analysis confirmed the expression of BRN3-positive retinal ganglion cells extending Map2-positive dendrites (C) as well as photoreceptor-like phenotypes including the expression of CRX, OTX2 and Recoverin (D, E).

The ability to morphologically identify and isolate retinal progenitor neurospheres within the first 20-25 days of differentiation is noteworthy for a variety of reasons (Figure 2.5). First, the use of morphological cues to identify and isolate retinal progenitor neurospheres represents a novel method of enrichment of retinal cells apart from other cellular lineages that may be found in such cultures, effectively yielding highly enriched populations of retinal progenitor cells that can readily differentiate into all of the major cell types of the retina [10, 30]. Furthermore, this ability to highly enrich for retinal progenitor cells allows for the more definitive identification of mature retinal cell types, including retinal ganglion cells. Within the retina itself, retinal ganglion cells are often identified by the expression of the transcription factor BRN3 [109–111]. However, this transcription factor is also expressed in other neural cell types, including some auditory neurons [110, 112] as well as many somatosensory neurons [39, 113]. Thus, when starting with a pluripotent stem cell source that has the potential to give rise to any cell type of the body, the expression of BRN3 by itself is not sufficient to definitively identify cells as retinal ganglion cells. However, due to the ability to enrich for retinal progenitor cells from hPSCs as described by the current protocol, traditional markers such as BRN3 can be utilized to identify these retinal cells as other non-retinal cell types will be effectively eliminated from the culture system. The ability to identify BRN3-positive cells from a highly enriched retinal progenitor population allows for the more definitive identification of these cells as retinal ganglion cells.

Due to the ease of hPSC differentiation described in this protocol, including the minimal culture conditions required to achieve this differentiation event, this procedure allows for the application of hPSCs as a novel model for in vitro studies of human retinogenesis [10, 30, 53, 80, 96, 107]. The ability to identify each of the major stages of retinal development has led to the recent use of this method as a means of studying the molecular basis for cell fate determination in the retina between those cells of the neural retina and the retinal pigment epithelium [96, 107]. Not only are these results significant due to the ability to study these events in human cells, but these

cell fate determination events are known to occur at stages of development that would otherwise be inaccessible to experimental investigation. Furthermore, recent studies have expanded upon this method to generate three-dimensional stratified retinal-like structures in vitro [30, 114], allowing for future studies of cell fate determination and subsequent maturation of retinal cells.

The ability to derive a full complement of retinal cell types from hPSCs also allows for the study of human inherited diseases of the retina, particularly those leading to blindness such as age-related macular degeneration (AMD), retinitis pigmentosa, and optic neuropathies including glaucoma. Owing to the ability to enrich for retinal progenitor cells with this protocol, large numbers of retinal cells are readily obtainable from patient-derived induced pluripotent stem cells, and this ability has recently been utilized as an effective in vitro model for a variety of blinding disorders, including gyrate atrophy and Best disease [10, 82]. The use of hPSCs to generate RGCs and model glaucoma has been relatively ignored due to issues identifying RGCs from a pluripotent source. As such, the characterization and exploration of hPSC-derived RGCs as a model for glaucomatous neurodegeneration is explored in the next chapter. The potential also exists for pharmacological screening of novel compounds for therapeutic efficacy using patient-derived cells. This was originally described in disorders affecting the RPE [10, 82] and has been expanded to disorders affecting other retinal cell types such as and glaucoma, as discussed in chapter 3. hPSCs are an effective complement to traditional model systems and thus bridge an important gap for both basic and translational research between traditional model systems and the existing human condition.

2.10 Critical paramaters

2.10.1 Passaging hPSCs

It is crucial to minimize the amount of pipetting as even a little excessive pipetting can result in a dramatic decrease in the yield of EBs. Cells that have been treated with dispase should lift off with little effort.

When cells have been collected into their respective tubes (expansion or differentiation), allow at least 5 minutes for cells to fully settle at the bottom to ensure no cells are being aspirated with the supernatant.

2.10.2 Plating embryoid bodies with 10% FBS

EBs must be plated at a critical density to ensure the proper differentiation into neuroepithelium. Without close proximity to neighboring cells, cell survival decreases. When plated at too high of a density, cells will lack the space they require to develop properly. Agitation of plates when placed into the incubator also helps in achieving a uniform distribution of cells within the well.

2.10.3 Manually separating retinal neurospheres

Separation of retinal neurospheres by day 25 is critical to ensure that morphology can be definitively used to separate retinal and non-retinal cells. After day 25, the retinal morphology may begin to disappear as the neurospheres continue proliferating.

2.10.4 Maintenance of retinal neurospheres

When changing medium of cells in suspension, unnecessary cell loss can be avoided by rinsing the well or dish with extra medium. This ensures all cells are collected and receive fresh medium in a timely manner.

2.10.5 Anticipated results

The use of this procedure yields a 90% pure population of CHX10-positive retinal progenitor cells that can be further differentiated into every retinal cell type.

2.10.6 Time considerations

With practice, passaging of hPSCs can take as little as 20 minutes once the necessary supplies and reagents have been prepared. When EBs are ready to be plated down, this process should take about 10 minutes for three plates. Manually separating retinal neurospheres from a mixed population can take anywhere from 30 minutes to an hour, depending on the yield of neurospheres and the experience of the researcher. Using accutase to disassociate neurospheres can take anywhere from 10 minutes to 40 minutes, with varying neurosphere size and the degree to which spheres are meant to be disassociated.

2.11 Acknowledgements

Sarah K. Ohlemacher: Conception and design, financial support, collection and/or assembly of data, data analysis and interpretation, manuscript writing, final approval of manuscript.

Clara L. Iglesias: Conception and design, collection and/or assembly of data, data analysis and interpretation.

Akshayalakshmi Sridhar: Conception and design, collection and/or assembly of data, data analysis and interpretation.

David M. Gamm: Conception and design, financial support.

Jason S. Meyer: Conception and design, financial support, collection and/or assembly of data, data analysis and interpretation, manuscript writing, final approval of manuscript.

3. STEPWISE DIFFERENTIATION OF RETINAL GANGLION CELLS FROM HUMAN PLURIPOTENT STEM CELLS ENABLES ANALYSIS OF GLAUCOMATOUS NEURODEGENERATION

3.1 Introduction

Human pluripotent stem cells offer the unique and unprecedented ability to study the differentiation of specific cellular lineages, particularly at those stages of development that would otherwise be inaccessible to investigation. As such, they have been demonstrated to serve as powerful in vitro models for human ontogenesis [115, 116]. When derived from specific patient populations, human induced pluripotent stem cells are capable of serving as in vitro models of disease progression [10, 61, 82, 117–119], effectively bridging the gap between basic and translational research. Among the diseases that may be effectively modeled with hiPSCs, those affecting the retina have been of particular interest [10, 82, 120–122] as a number of methods exist to derive all of the major cell types of the retina [10–12, 30, 32, 53, 77, 78, 80, 123] and no effective treatments and cures exist for many blinding disorders.

While many previous studies have focused upon the ability to derive and utilize retinal cells such as photoreceptors and RPE [10–12, 30, 32, 53, 77, 78, 80, 82, 123, 124], RGCs have been largely overlooked to date. As the projection neurons of the retina, RGCs effectively serve as the connection between the eye and the brain. Furthermore, RGCs are the predominant affected cell type in a group of diseases known as optic neuropathies, the most common of which is glaucoma with a current incidence of over 60 million individuals worldwide [56, 125]. Within the context of the retina, RGCs are often identified by the expression of a limited set of markers that are specific to these cells. However, when derived from a pluripotent cell source, these markers are

no longer specific for RGCs as they are expressed elsewhere in the nervous system. To date, the detailed description and utilization of hPSC-derived RGCs has been largely lacking due to the shortage of reliable markers with which to definitively identify these cells. Thus, a systematic, detailed analysis of hPSC-derived RGCs is warranted in order to serve as a comprehensive in vitro model of RGC development, as well as the application of patient-derived RGCs for disease modeling.

To this end, efforts were undertaken to comprehensively detail the differentiation of RGCs, with subsequent application of these approaches to a glaucoma patient-derived line of hiPSCs. Lines of hPSCs were directed to differentiate in a stepwise manner specifically toward a retinal lineage and highly enriched populations of retinal progenitor cells were readily identified and isolated, yielding a highly purified population. Upon further differentiation of these retinal progenitor cells, presumptive RGCs were identifiable within a total of 40 days of differentiation and were characterized for morphological, phenotypic, and physiological features of native RGCs. These cells were found to express all of the observed features associated with in vivo RGCs and importantly, the possibility was excluded to have differentiated into alternate lineages bearing similar phenotypic markers. Furthermore, hPSC-derived cells possessed expected physiological properties of RGCs [31, 126]. Following the conclusive identification and characterization of hPSC-derived RGCs, similar approaches were undertaken for hiPSCs derived from a glaucoma patient possessing an E50K mutation in the Optineurin gene, responsible for some familial forms of glaucoma [127–133]. The E50K mutation in OPTN are dominant but relatively rare, occurring in approximately 3-13% of patients with POAG [127,128]. E50K hiPSCs were differentiated to an RGC fate, at which point their ability to serve as an in vitro model for studies of disease progression and drug screening were tested. The results of these studies support a role for hPSCs as an effective in vitro model for human RGC development and functionality, as well as for use in studies of cellular mechanisms underlying disease progression in optic neuropathies.

3.2 Materials and methods

3.2.1 Maintenance of hPSCs

hPSCs were maintained as previously described [12, 80]. Briefly, three lines of control human pluripotent stem cells (H9, H7 and miPS2) were used, and three lines of patient-derived induced pluripotent stem cells from an OPTN E50K patient were derived. All cell lines were maintained in the pluripotent state with mTeSR1 medium (Stemcell Technologies, Vancouver, BC, Canada) on matrigel-coated 6-well plates. Cells were passaged upon reaching confluency of approximately 70%. Areas of spontaneous differentiation were initially identified by their distinct appearance and were mechanically removed. Colonies of hPSCs were then enzymatically lifted with dispase (2 mg/mL) for approximately 15 minutes and passaged at a ratio of 1:6 onto freshly-coated matrigel plates in mTeSR1 medium. Passaging of hPSCs typically occurred every 4-5 days.

3.2.2 Differentiation of hPSCs

Differentiation of hPSCs to a retinal lineage was performed with modifications to previously established protocols (see Chapter 2) [12, 53]. Briefly, EBs were generated from undifferentiated colonies of hPSCs by lifting adherent cultures with dispase. EBs were gradually transitioned into NIM consisting of DMEM/F12 (1:1), N2 supplement, MEM nonessential amino acids and heparin (2 μg/mL). After a total of 7 days of differentiation, EBs were plated onto uncoated 6-well plates and induced to adhere by the addition of 10% FBS overnight. The next day, NIM was replaced without FBS and medium was subsequently changed every other day until day 16. At this point, cells were lifted from plates by mechanical scraping or pipetting to dislodge colonies and generate neurospheres in suspension cultures. Neurospheres were maintained in RDM consisting of DMEM/F12 (3:1), MEM non-essential amino acids, B27 supplement, and antibiotics. Medium was replenished every 2-3 days thereafter until the

desired day of differentiation was reached. At this point, retinal neurospheres were isolated according to previously established protocols [10, 12, 30, 80, 107] based upon morphological cues exhibited by the neurospheres. As indicated in some experiments, E50K hiPSC-derived neurospheres were treated with either BDNF (100 ng/mL) or PEDF (100 ng/mL) from day 50 to day 70 of differentiation. Neurospheres were either harvested for RNA analysis, or partially dissociated with accutase and plated onto poly-D-ornithine/laminin-coated coverslips for immunocytochemical analysis.

3.2.3 Reprogramming of fibroblasts to hiPSCs

The generation of E50K glaucoma patient hiPSCs was performed using mRNA reprogramming strategies as previously described [134]. Synthetic mRNAs with a microRNA booster kit (Stemgent, San Diego, CA) were introduced into E50K fibroblasts through the use of Stemfect Transfection Reagent following manufacturers instructions. mRNAs were transfected daily for a total of 14 days. Within the first 20 days of reprogramming, some fibroblasts began to lose their elongated morphology and displayed the typical tightly packed morphology of hiPS cell colonies. Individual colonies of prospective hiPSCs were identified, manually isolated, and clonally expanded to yield lines of patient-specific hiPSCs. Newly established lines of hiPSCs were maintained as described above.

3.2.4 RT-PCR

RNA was isolated from retinal neurospheres using the Picopure RNA Isolation Kit (LifeTechnologies, Carlsbad, CA), with subsequent cDNA synthesis achieved utilizing the iScript cDNA synthesis kit (BioRad, Hercules, CA). PCR analysis was accomplished using Go-Taq PCR Master Mix (Promega, Madison, WI), while qPCR analysis was performed with SybrGreen (Life Technologies, Carlsbad, CA). For RT-PCR experiments, reactions were performed for 35 cycles and products were run

on 2% agarose gels. Primers for RT-PCR and qRT-PCR analysis can be found in Supplemental Table 6.2 and Supplemental Table 6.3.

3.2.5 Immunocytochemistry and data quantification

Samples were collected at indicated timepoints of differentiation and plated on poly-D-orinithine and laminin-coated coverslips. Cells were fixed in a 4% paraformaldehyde and PBS for 30 minutes. Alternatively, neurospheres were processed for cryostat sectioning as indicated. For this purpose, neurospheres were fixed in 4% paraformaldehyde and PBS for 45 minutes and then introduced into a 20% sucrose solution in PBS for equilibration overnight at 4 °C. The following day, sucrose solution was aspirated and changed to a 30% sucrose solution at 4 °C. Following equilibration, neurospheres were embedded in OCT, frozen in dry ice and stored at −80 °C until sectioning. Cryostat sections were cut at a thickness of 10μm and stored at −80 °C until use for immunocytochemistry.

For immunostaining of both coverslips and cryostat slides, samples were initially washed three times with PBS and permeabilized with 0.2% Triton X-100 for 10 minutes at room temperature. 10% donkey serum in PBS was used as a blocking agent for one hour at room temperature and primary antibodies (Supplemental Table 6.1) were applied in a solution consisting of 5% donkey serum and 0.1% Triton X-100 overnight at 4 °C. The next day, samples were washed with PBS and 10% donkey serum blocking agent was applied for 10 minutes at room temperature. Samples were treated with secondary antibodies diluted in a 5% donkey serum and 0.1% Triton X-100 solution for one hour at room temperature, followed by 3 washes with PBS. Samples were mounted onto slides and cells were imaged with either a Leica (Wetzlar, Germany) DM5500 fluorescence microscope or an Olympus (Shinjuku, Tokyo, Japan) Fluoview 2000 confocal microscope.

Quantification of cell counts was performed with ImageJ software using immunostained samples. For each experimental condition, three different lines of hPSCs were

utilized. Within these different cell lines, a minimum of three images were collected from at least three separate experiments performed at different passage number from each cell line. Each image was quantified to calculate the percentage of BRN3-positive cells, as well as the abundance of activated caspase-3 expression relative to the total number of BRN3-positive cells. ANOVA statistical analyses or students t-tests were performed with Prism software (Graphpad, La Jolla, CA) to determine statistically significant differences at a p-value of less than 0.05. Size of the Golgi complex was determined by GM130 staining similar to previous reports [107, 134, 135] by calculating the total area of GM130-positive staining utilizing ImageJ software, and then dividing this number by the total number of DAPI-positive nuclei. A minimum of three samples were analyzed per experiment to obtain the average Golgi area per cell. A students t-test was used to determine statistical significance using Prism software, and significant differences were identified at a p-value less than 0.05.

3.2.6 Electrophysiology

Whole-cell patch-clamp recordings were carried out at 21 °C as previously described [136] using an EPC-10 amplifier and the Pulse8.31 program (HEKA, Lambrecht/Pfalz, Germany). Fire-polished electrodes were fabricated from borosilicate capillary glass (1.2-mm outer diameter, 0.69-mm inner diameter; Sutter Instrument Co., Novato, CA) using a P-97 puller (Sutter Instrument Co., Novato, CA). After filling with the intracellular solution containing (in mM): KCl 140, $MgCl_2$ 5, EGTA 5, $CaCl_2$ 2.5, Hepes 10, ATP 4, GTP 0.3, Phosphocreatine 8, pH7.3 (adjusted with KOH), the access resistance of electrode pipettes ranged between 4 and 5 M. The bathing solution contained (in mM): NaCl 140, $MgCl_2$ 1, KCl 5, $CaCl_2$ 2, Hepes 10, Glucose 10, pH7.3 (adjusted with NaOH). After establishing the whole-cell recording configuration, cells were allowed to stabilize for 2-3 minutes in current-clamp mode before initiating ramp current injection to measure action potential activity. Cells were held at -100 mV to stabilize for 5 minutes in voltage-clamp mode before apply-

ing depolarizing voltage steps to measure potassium and sodium currents. A -P/4 subtraction protocol was used to remove linear leak current and capacitance artifact for all voltage clamp recordings. Voltage errors were minimized using more than 80% series resistance compensation. Membrane currents were filtered at 5 kHz and sampled at 20 kHz. Tetrodotoxin (TTX, 5μM) and tetraethylammonium (TEA, 100μM) stock solutions were made using the bathing solution. TTX or TEA was diluted into a 300 μL recording chamber to achieve the final concentration.

3.3 Results

3.3.1 Identification of hPSC-derived retinal ganglion cells

The definitive identification of RGCs from a pluripotent source has been complicated by the lack of specific markers to identify these cells. The expression of the transcription factor BRN3 has been widely utilized to identify cells with RGC-like characteristics [10–12, 20, 23, 30, 77, 78, 80, 114]. However, when derived from hPSCs, such markers lose their specificity as BRN3 is also expressed in other cell types of the central nervous system, particularly hair cells of the auditory system [40] as well as somatosensory neurons [39]. Thus, to conclusively establish the RGC nature of hPSC-derived RGCs, their derivation and identification necessitates the detailed stepwise differentiation through early neural and retinal progenitor intermediaries.

To this end, initial efforts were focused upon the differentiation and definitive identification of hPSC-derived RGCs. As a starting point, hPSCs were directed to differentiate to an optic vesicle-like stage of retinogenesis as previously described [10, 12, 30, 80, 114], at which point highly enriched populations of CHX10-positive retinal progenitor cells comprised 90.02% $\pm$ 1.95% of all neurospheres. These retinal populations were readily identified and isolated from their non-retinal forebrain counterparts based upon morphological cues (Figure 3.1A-C), allowing for the subsequent classification of further differentiated phenotypes to the retinal lineage. Within 40 total days of differentiation, enriched populations of optic vesicle-like retinal neuro-

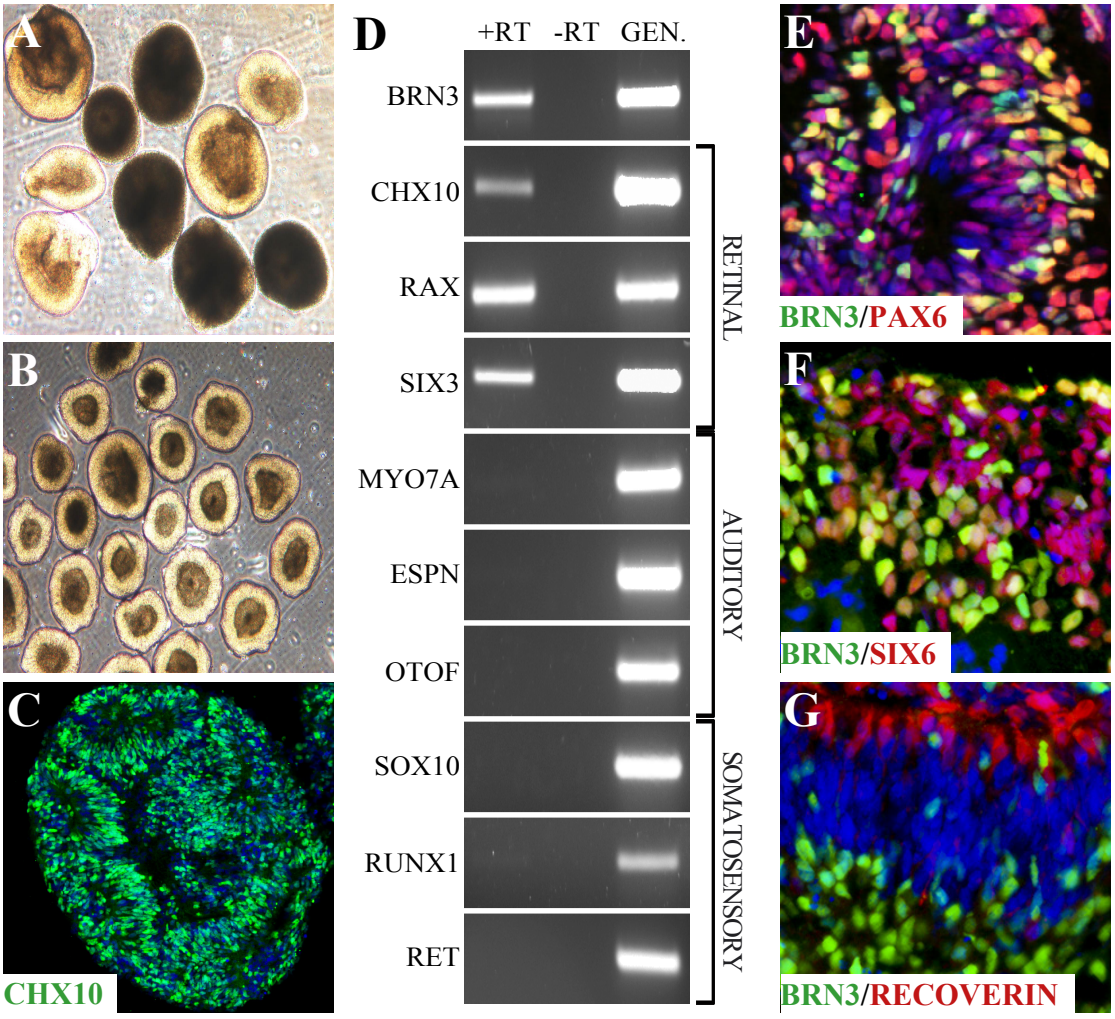

Fig. 3.1. Definitive identification of presumptive RGCs using BRN3 expression in differentiated cultures of hPSCs.

After 25 days of differentiation, two morphologically distinct populations of neurospheres were observed (A), from which optic vesicle-like neurospheres were identified and isolated based upon their phase-bright appearance (B). Isolated optic vesicle neurospheres were highly enriched for CHX10-expressing retinal progenitor cells (C). After a total of 40 days of differentiation, RT-PCR analysis demonstrated that presumptive RGCs expressed BRN3 in conjunction with other retinal markers, but not markers of other neuronal BRN3-expressing lineages (D). Genomic DNA (Gen.) served as a positive control for RT-PCR experiments. Immunocytochemical analysis confirmed expression of BRN3 localized with other retinal markers (E-F). BRN3 remained distinctly separate from Recoverin photoreceptors (G).

spheres began to express BRN3 as well as a compliment of other retinal-associated transcription factors when analyzed by RT-PCR (Figure 3.1D). Conversely, no expression of genes characteristic of the auditory [40] and somatosensory [39] lineages was detected. Taken together, these results confirm the retinal phenotype associated with these BRN3-positive cells. Immunocytochemistry analysis further confirmed the expression of BRN3 with other markers of the retinal lineage (Figure 3.1E-G). Specifically, BRN3 expression was often found colocalized with markers typically associated with retinal progenitor cells and some RGCs such as PAX6 and SIX6. However, colocalization of BRN3 with markers indicative of other retinal cell types such as MITF was not observed (Figure 3.2).

SCFig2.pdf

The temporal birth order of specific retinal cell types has been well characterized in vivo, with retinal progenitors giving rise to RGCs and cone photoreceptors early while rods and Muller glia emerge later [89, 137]. Through immunocytochemical analysis, early stages of this stepwise progression to an RGC fate could be observed (Figure 3.3A), with PAX6-positive neural progenitors the first stage in this differentiation process. Following the identification and isolation of retinal neurospheres, robust differentiation of CHX10-positive retinal progenitors was observed. The appearance of BRN3-expressing RGCs could be observed shortly thereafter, followed by the onset of recoverin-positive photoreceptor-like cells. RT-PCR analysis further confirmed this stepwise pattern of retinal fate determination (Figure 3.3B).

3.3.2 Characterization and functional analysis of hPSC-derived retinal ganglion cells

The expression of BRN3, along with the differentiation of hPSCs through the stepwise process of retinal differentiation, aided in the identification of resultant RGCs. Overall, approximately 36.1%±1.7% of cells expressed the RGC-associated transcription factor BRN3 within the first 40 days of differentiation (Figure 3.4A). Beyond

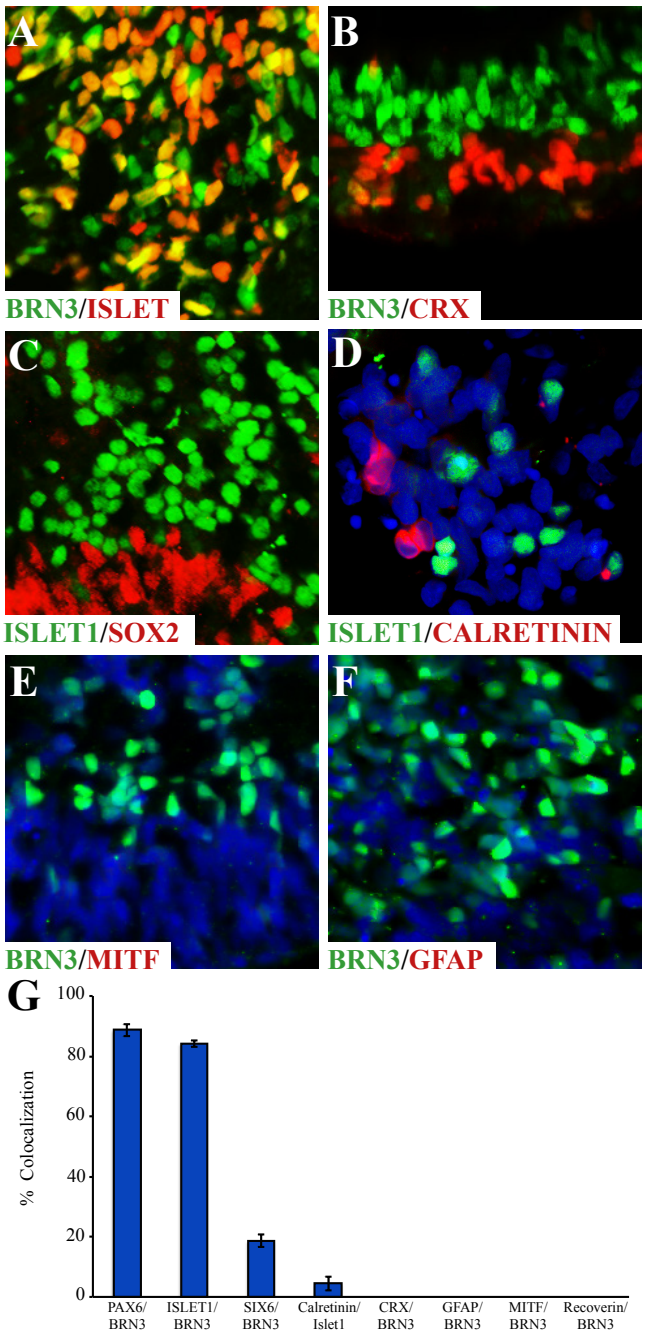

Fig. 3.2. Co-localization of RGC markers with markers of other retinal cell types.

BRN3 exhibited high-colocalization with the RGC-associated marker ISLET1 (A). RGCs labeled with BRN3 and ISLET1 showed very little co-expression with photoreceptors (B), glia (C), amacrine cells (D), RPE (E), or astrocytes (F). Quantification of BRN3 co-expression with RGC associated markers PAX6, ISLET1, and SIX6 and little to no co-expression with other retinal cell types (G). Error bars represent s.e.m.

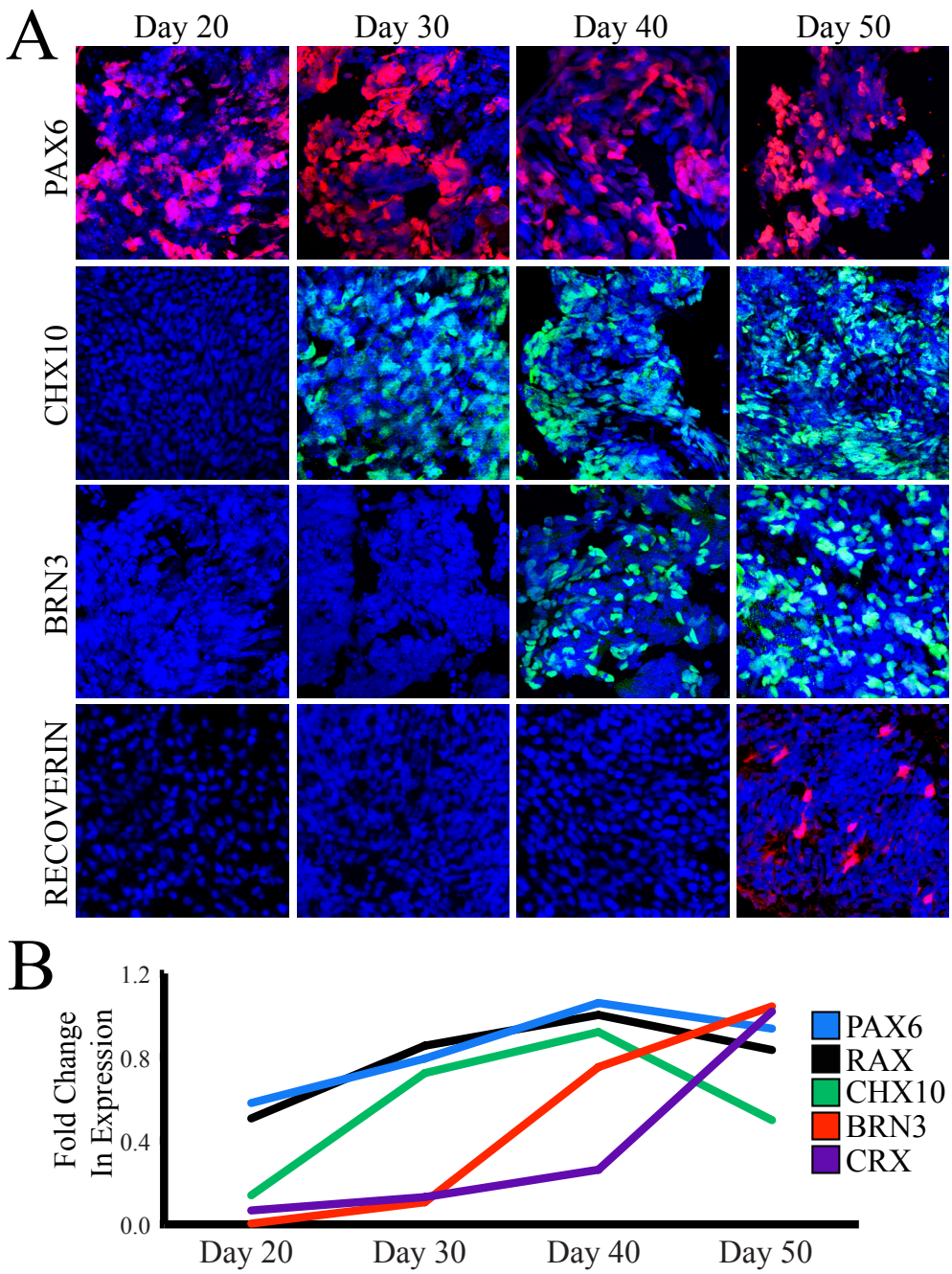

Fig. 3.3. hPSC-derived RGCs are generated in a temporally appropriate sequence.

Immunocytochemistry analysis revealed that BRN3-positive RGCs appeared subsequent to the establishment of neural (PAX6) and retinal (CHX10) progenitor fates, but prior to the generation of photoreceptor-like (Recoverin) cells (A). qRT-PCR analysis confirmed that genes associated with retinal and RGC development were expressed at developmentally-appropriate timepoints, with those genes associated with retinal progenitors expressed prior to the onset of RGC-specific genes (B).

the expression of BRN3, however, a variety of other features are associated with the development of RGCs. Upon differentiation, presumptive RGCs co-expressed a wide array of such factors associated with RGC specification (Figure 3.4B-E). Furthermore, maturation and morphological changes of these cells were readily observed, as BRN3-positive RGCs were found associated with MAP2-positive neurite extensions (Figure 3.4F). Interestingly, a small population of melanopsin-expressing cells were observed, indicative of ipRGCs, of which there are five subtypes, M1-M5. These cells expressed high levels of Melanopsin (Figure 3.4G) and largely lacked BRN3 expression (Figure 3.4G insert), typical of the M1 class of ipRGCs, which are one of the few RGC subtypes that do not express BRN3 [138–140].

The ability to exhibit lengthy neurite outgrowths is a defining characteristic of RGCs when compared to other neurons of the retina. Following prolonged growth in vitro, extensive neurite outgrowth was readily observed from BRN3-expressing RGCs (Figure 3.4H). Cytoskeletal components became compartmentalized with clear separation of MAP2 expression in somatodendritic regions and Tau expression confined to axonal extensions that fasciculated and extended over long distances. The progressive acquisition of RGC characteristics, as well as the differential expression of these characteristics apart from non-retinal forebrain cells, was further characterized by qRT-PCR analysis (Figure 3.4I-J). In comparison to retinal progenitor cells identified at earlier stages of differentiation, RGC populations exhibited a robust increase in the expression of RGC-associated genes, along with a significant decrease in the expression of retinal progenitor-associated genes (Figure 3.4I). Furthermore, when compared to age-matched non-retinal forebrain populations as indicated above (Figure 3.4A), a significant increase was observed in the expression of retinal and RGC-associated genes (Figure 3.4J).

As projection neurons connecting the eye with the brain, and unlike most other neurons of the retina, RGCs transmit visual information via elicitation of action potentials through the use of voltage-gated ion channels [31]. To confirm whether hPSC-derived RGCs are capable of similar physiological activity, prospective RGCs

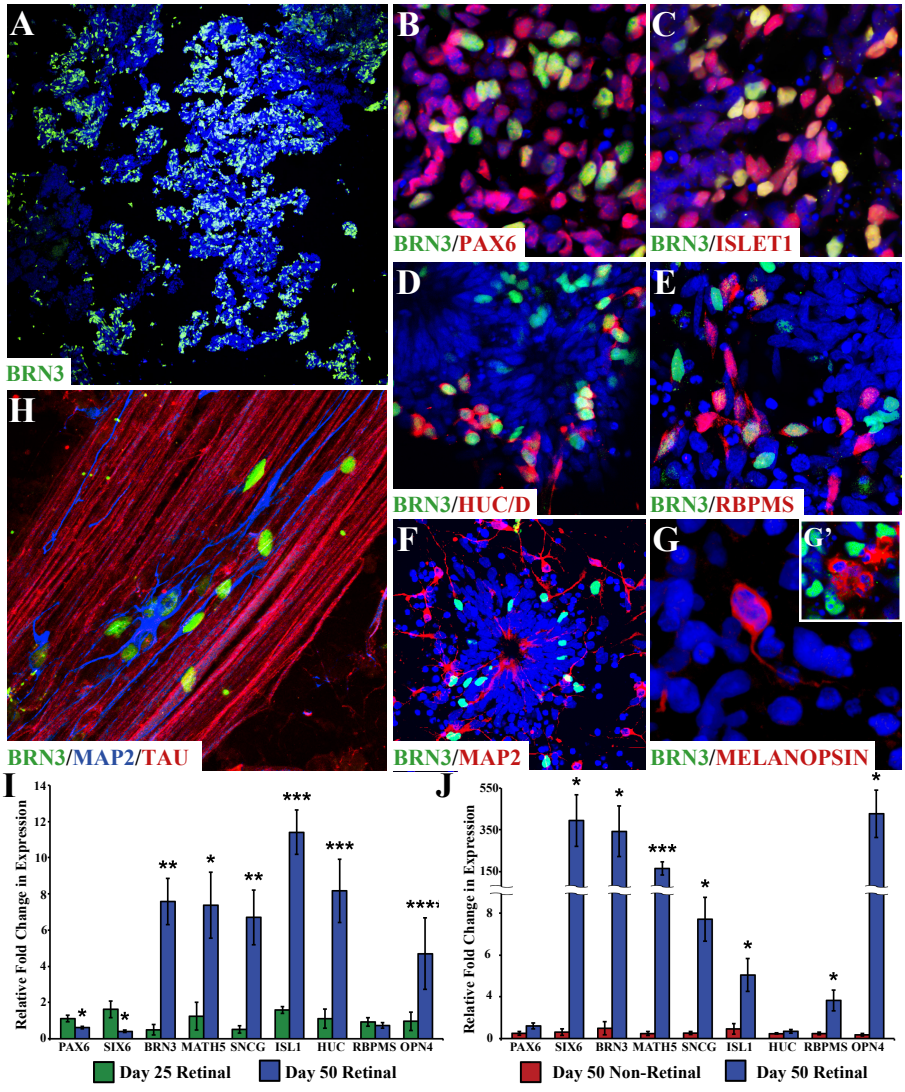

Fig. 3.4. Phenotypic characterization of hPSC-derived RGCs.

After 40 days of differentiation, BRN3-positive RGCs comprised approximately 36.1 ± 1.7% of the total differentiated population (A). BRN3-positve RGCs expressed numerous RGC-associated markers (B-E), and began to extend MAP2-positive neurites (F) within a total 70 days of differentiation. A small subset of intrinsically photosensitive melanopsin-positive RGCs were observed that were BRN3-negative (G) by 70 days of differentiation. Prolonged differentiation gave rise to elaborate RGC-like morphologies exhibiting compartmentalized expression of MAP2 and TAU, including fasciculated TAU-positive axons (H) within 100 total days of differentiation. qRT-PCR analysis revealed that BRN3-expressing cells exhibited increased expression of RGC-associated transcripts compared to their retinal progenitor precursors (I), as well as their age-matched non-retinal forebrain counterparts (J). Significant differences indicated as * = $p<0.05$, ** = $p<0.01$, *** = $p<0.005$, **** = $p<0.001$.

were first morphologically identified for electrophysiological analysis based upon extensive neurite outgrowth (Figure 3.5A) typical of these cells [12, 141].

Electrophysiological activity of hPSC-derived RGCs was then analyzed by patch clamp analysis, and recorded cells were filled with Lucifer Yellow for subsequent immunocytochemical analysis for BRN3 expression to definitively identify analyzed cells as RGCs (Figure 3.5B). hPSC-derived RGCs demonstrated the ability to fire action potentials (Figure 3.5C) and exhibited a hyperpolarized resting membrane potential (RMP) (Figure 3.5D). These electrophysiological properties were associated with ionic currents, including outward flow that could be blocked by the addition of TEA, indicating the presence of voltage-gated K+ channels (Figure 3.5E-F), as well as inward current flow that was sensitive to the voltage-gated Na+ channel blocker TTX (Figure 3.5G-H). Furthermore, both K+ and Na+ ionic currents were shown to be voltage-dependent in nature.

3.3.3 In vitro modeling of optic neuropathies using patient specific hiPSCs

The ability to derive RGCs from an hPSC source has important implications beyond studies of developmental biology [115, 116]. Translational applications include [10,61,82,118] in vitro disease modeling and pharmacological screening [142–144] when derived from specific patient sources. Mutations in the OPTN gene have been extensively documented to result in severe RGC degeneration associated with POAG [127–132] and therefore, should provide an effective in vitro tool for studies of underlying disease mechanisms, as well as subsequent pharmacological screening. To this end, skin fibroblasts from a patient possessing an E50K missense mutation in the OPTN gene were reprogrammed to pluripotency, exhibiting robust expression of a full complement of pluripotency-associated factors (Figure 3.6) and the ability to give rise to cell types of all three germ layers (Figure 3.7).

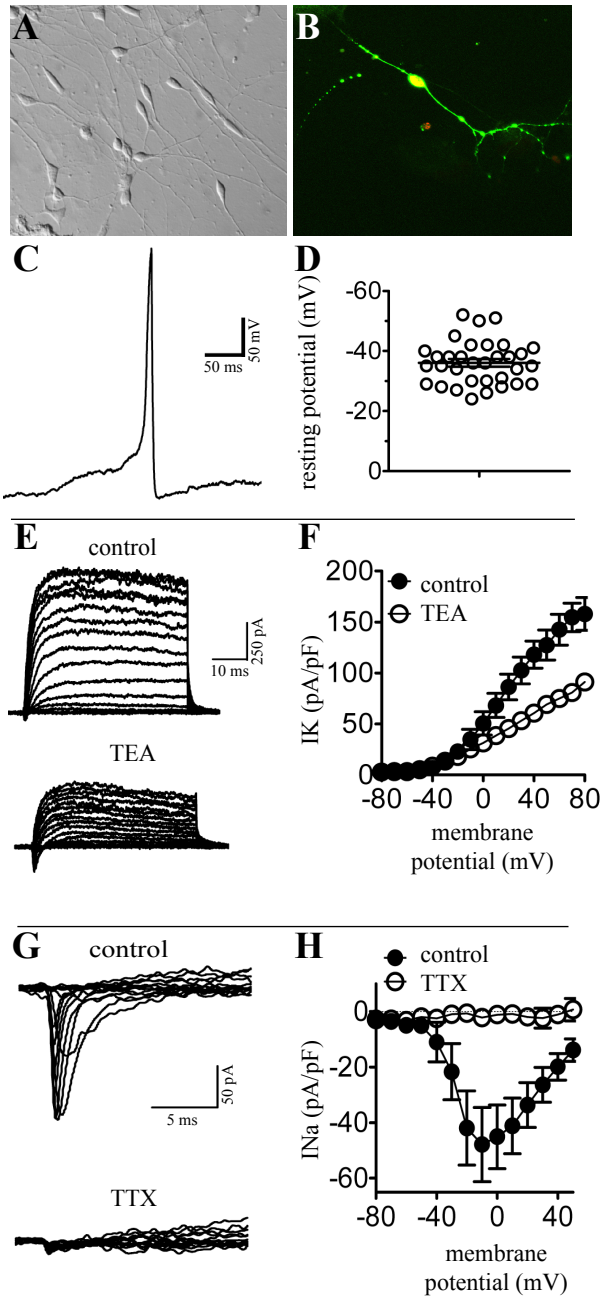

Fig. 3.5. Physiological analysis of hPSC-derived RGCs.

Patch clamp analysis was performed and retinal ganglion cell morphologies were highlighted by DIC microscopy, including long neurite outgrowth in RGCs derived between 80-90 total days of differentiation (A). Recorded cells were filled with Lucifer Yellow for subsequent immunocytochemical confirmation of their RGC identity (B). hPSC-derived RGCs demonstrated the ability to fire action potentials (C) and exhibited a hyperpolarized resting membrane potential (D). These features were associated with the conductance of potassium and sodium through voltage-gated channels, which could be blocked by the addition of either TEA (E-F) or TTX (G-H).

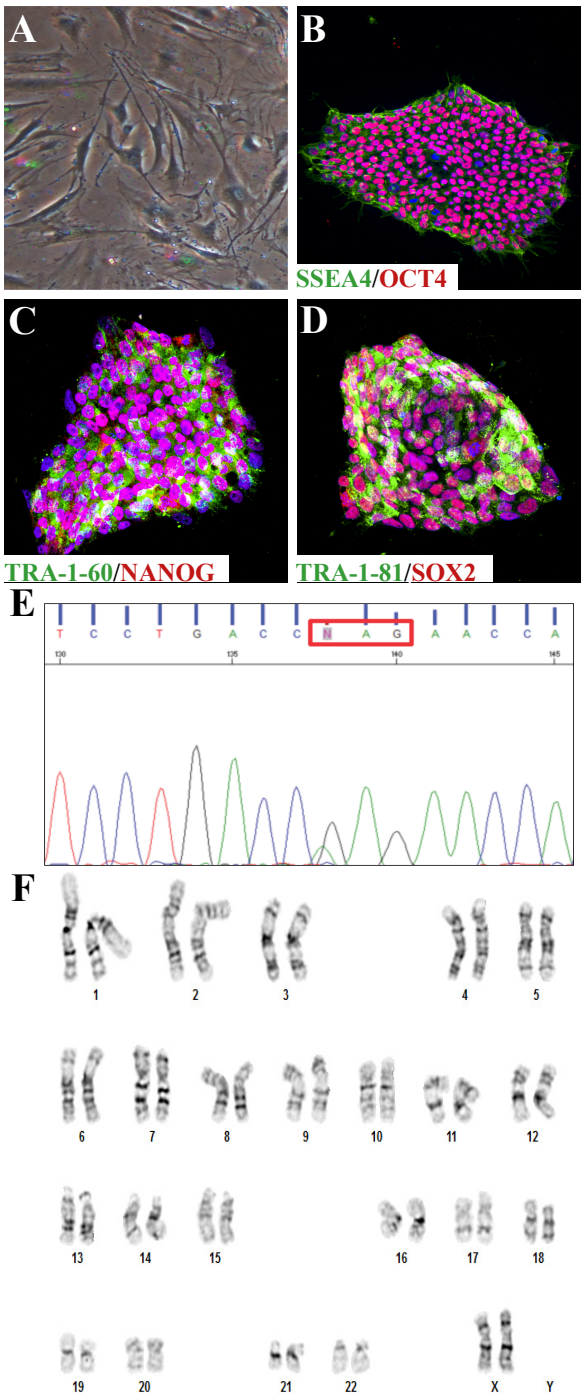

Fig. 3.6. Establishment of E50K patient-specific hiPSCs.

Fibroblasts from a glaucoma patient exhibiting an E50K mutation in the OPTN gene (A) were reprogrammed to yield hiPSCs, with resultant cells demonstrating immunoreactivity to pluripotency-associated transcription factors including OCT4, SOX2, and Nanog as well as the cell surface antigens SSEA4, Tra-1-60 and Tra-1-81 (B-D). Sequence analysis confirmed the presence of the E50K mutation in patient cells (E). Karyotype analysis of E50K hiPSCs exhibited no abnormalities in resultant cell lines (F).

Upon differentiation, enriched populations of E50K hiPSC-derived retinal neurospheres (Figure 3.8A) were characterized by robust expression of CHX10 (Figure 3.8B), indicative of a retinal progenitor state [10,105,107]. Subsequent differentiation of these retinal progenitors yielded BRN3-positive cells that could be definitively identified as RGCs due to their retinal lineage. These RGCs exhibited elaborate MAP2-positive neuronal morphologies and formation of complex neural networks (Figure 3.8C-D). To further examine the applicability of E50K hiPSC-derived RGCs as an in vitro model for glaucoma, the activation of caspase-3 was analyzed and quantified via immunocytochemistry in comparison to unaffected control lines. In undifferentiated cultures, little activation of caspase-3 was observed and no significant differences were seen between control and E50K hiPSCs (Figure 3.8E-G). Upon differentiation of these cells to the affected RGC cell type, caspase-3 activation was minimal in control hiPSC-derived RGCs but was significantly increased in E50K hiPSC-derived RGCs (Figure 3.8H-J). Given these increased levels of apoptosis, the ability of these cells to serve as a tool for pharmacological screening was subsequently tested, utilizing factors previously identified as neuroprotective in other systems [145–150]. Upon treatment of E50K hiPSC-derived RGCs with either BDNF or PEDF, a significant reduction in caspase-3 activation was observed (Figure 3.8K-M).

Interestingly, undifferentiated E50K hiPSCs also exhibited a disorganized Golgi morphology that led to a significant increase in size (Figure 3.9A-C), as previously reported [130, 131, 136]. However, differentiation to the affected RGC phenotype yielded no significant difference in the size and organization of the Golgi of E50K RGCs compared to control RGCs (Figure 3.9D-F).

3.4 Discussion

The results presented here demonstrate the robust derivation and definitive identification of RGCs from hPSCs as identified by the combination of morphological, phenotypic, and physiological measures. Furthermore, these efforts were applied to

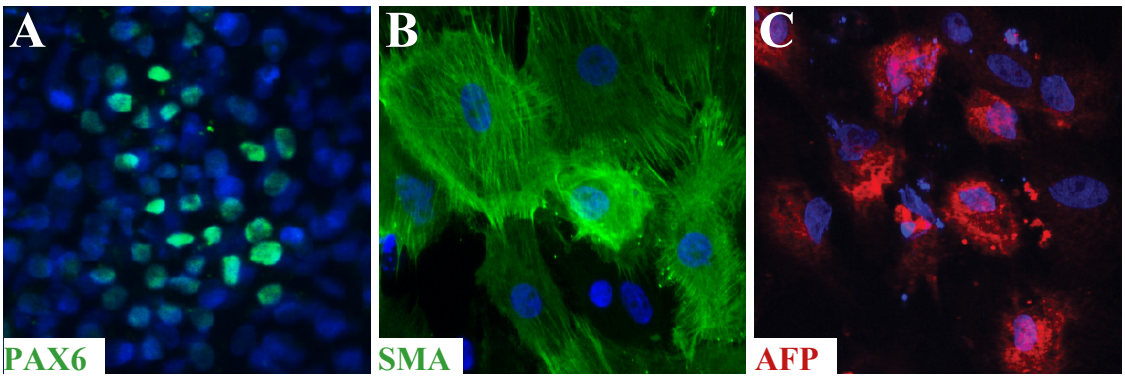

Fig. 3.7. Confirmation of pluripotency by differentiation analysis.

Upon spontaneous differentiation, E50K hiPSCs were capable of giving rise to cellular lineages of each of the three germ layers, including ectoderm (A), mesoderm (B), and endoderm (C).

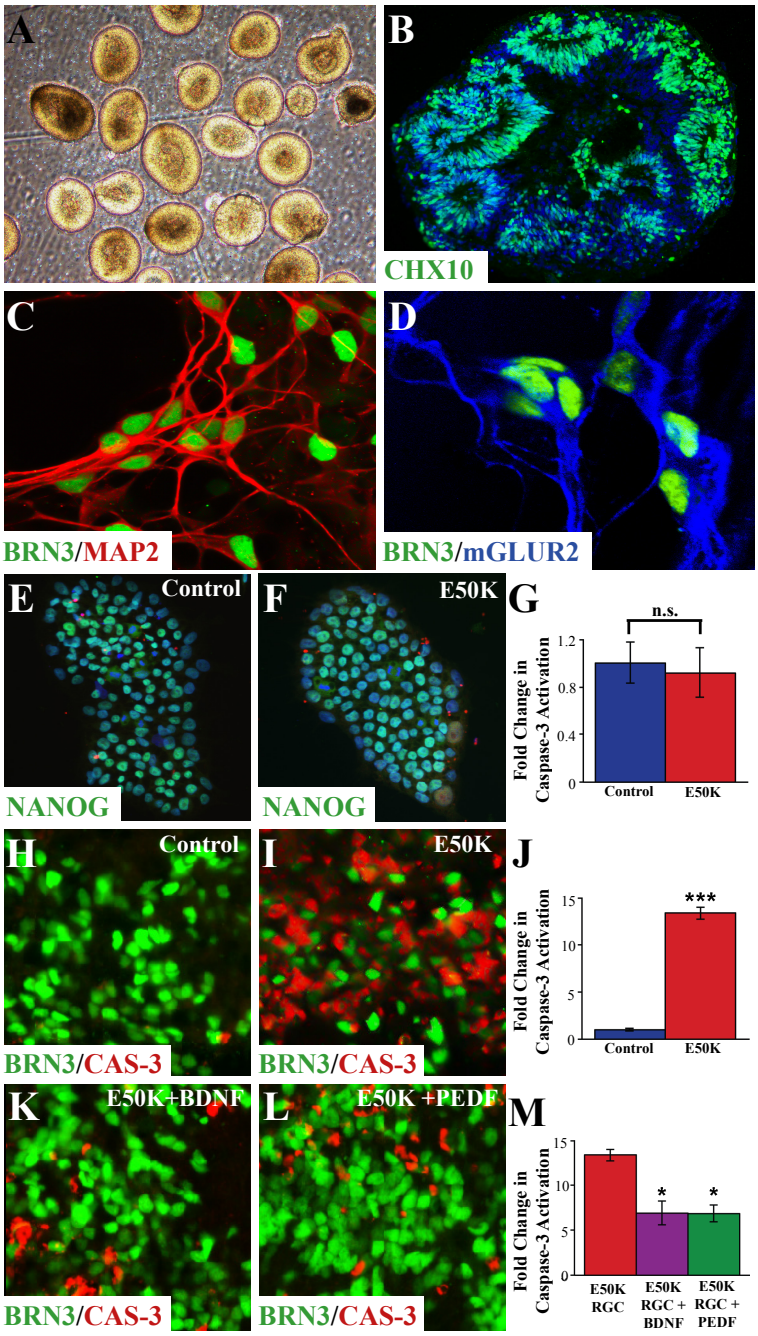

Fig. 3.8. Patient-derived hiPSCs can be utilized as an effective model of RGC neurodegeneration.

E50K patient hiPSCs were directed to differentiate to a retinal progenitor fate (A-B). Retinal ganglion cells were subsequently differentiated and characterized by the expression of BRN3 and the development of complex neural networks (C-D). In the pluripotent state, control and E50K hPSCs exhibited no significant differences in apoptosis (E-G). Following differentiation for 70 days, E50K RGCs demonstrated significantly increased apoptosis (H-J), which could be significantly reduced by treatment with select neuroprotective factors (K-M). Significant differences indicated as * = $p<0.05$, *** = $p<0.005$.

establish an in vitro model of glaucoma using patient-derived hiPSCs. This allowed for the ability to study associated underlying features of the disease itself, as well as provide a platform for pharmacological screening [142].

Although previous reports have demonstrated that hPSCs can acquire retinal characteristics upon differentiation [10, 12, 30, 53, 78, 80, 114], including features of retinal ganglion cells [10–12, 20, 22, 23, 30, 53, 54, 77, 78, 80, 114], many markers used to identify RGCs, particularly BRN3, are also expressed in other neural cells, including some auditory neurons [40] as well as somatosensory neurons [39]. Thus, efforts to unequivocally assign an RGC identity are complicated without thorough and systematic characterization. Moreover, BRN3 exists in three different forms, BRN3A, BRN3B, and BRN3C [109, 151]. While the current studies analyzed the overall expression of BRN3, it is likely that most of the cells expressed BRN3B, as this form is known to play a critical role in the differentiation and survival of RGCs, and is also known to be expressed earlier in development than other forms of BRN3.

In the current study, multiple approaches were undertaken to ensure that presumptive RGCs had indeed adopted this fate. First, retinal differentiation proceeded through a retinal progenitor stage that could be readily identified and isolated, yielding highly enriched populations of CHX10-expressing retinal progenitor cells, with subsequent expression of BRN3 allowing for more definitive identification of RGCs. Additionally, BRN3 expression was often found expressed in close association with other retinal cell types, while expression of markers associated with auditory and somatosensory lineages was not observed. Thus, the data presented provides the strongest evidence to date of the ability to conclusively differentiate RGCs from hPSCs.

Intrinsically photosensitive retinal ganglion cells are a specific subtype of RGC that function in non-visual phototransduction processes including circadian entrainment and pupillary responses [138–140]. The data presented within the current study is the first to demonstrate the differentiation of ipRGCs from hPSCs, as detected by the expression of the phototransduction protein melanopsin. While the derivation of

these cells was exceedingly rare, the presence of these cells allows for future investigation into the developmental specification of ipRGCs, as well as studies analyzing the damage and loss of ipRGCs in a variety of injuries and degenerative disorders of the retina.

Beyond phenotypic features, these hPSC-derived RGCs also possessed appropriate morphological and physiological features. After prolonged growth in vitro, hPSC-derived RGCs were capable of extensive neurite outgrowth, which was specifically directed toward other aggregates of cells, perhaps due to paracrine signaling. Further maturation of hPSC-derived RGCs was also observed in the compartmentalization of MAP2 and Tau, cytoskeletal proteins that are found widely expressed in immature neurons but whose expression becomes confined to somatodendritic and axonal regions, respectively, in mature neurons [152]. Furthermore, hPSC-derived RGCs exhibited the ability to function physiologically, with the ability to conduct sodium and potassium through voltage-dependent channels as well as the ability to fire action potentials. Although these features are characteristic of many types of neurons [31], in the retina these characteristics are specifically found within the RGCs as well as a subset of amacrine cells. While these cells exhibited a hyperpolarized resting membrane potential, this potential was recorded at an average of approximately -35 mV, indicating that these cells have not yet reached a fully mature state. Future experiments will necessitate the development of methods to derive fully mature hPSC-derived RGCs.

Efforts were also focused on the development of hiPSC-based models of optic neuropathies. Glaucoma is the most prevalent of the optic neuropathies, with a current incidence of more than 60 million individuals worldwide [56, 125]. However, a variety of factors exist which are causative or at least associated with the onset of glaucomatous neurodegeneration [153, 154]. Mutations in the OPTN gene were selected for study, particularly the E50K mutation which has been previously demonstrated to result in a particularly severe neurodegenerative phenotype [127, 128, 130]. While the results obtained with these cells will be of significance for future studies of this glaucoma-associated genotype, these results could also prove to be more profound

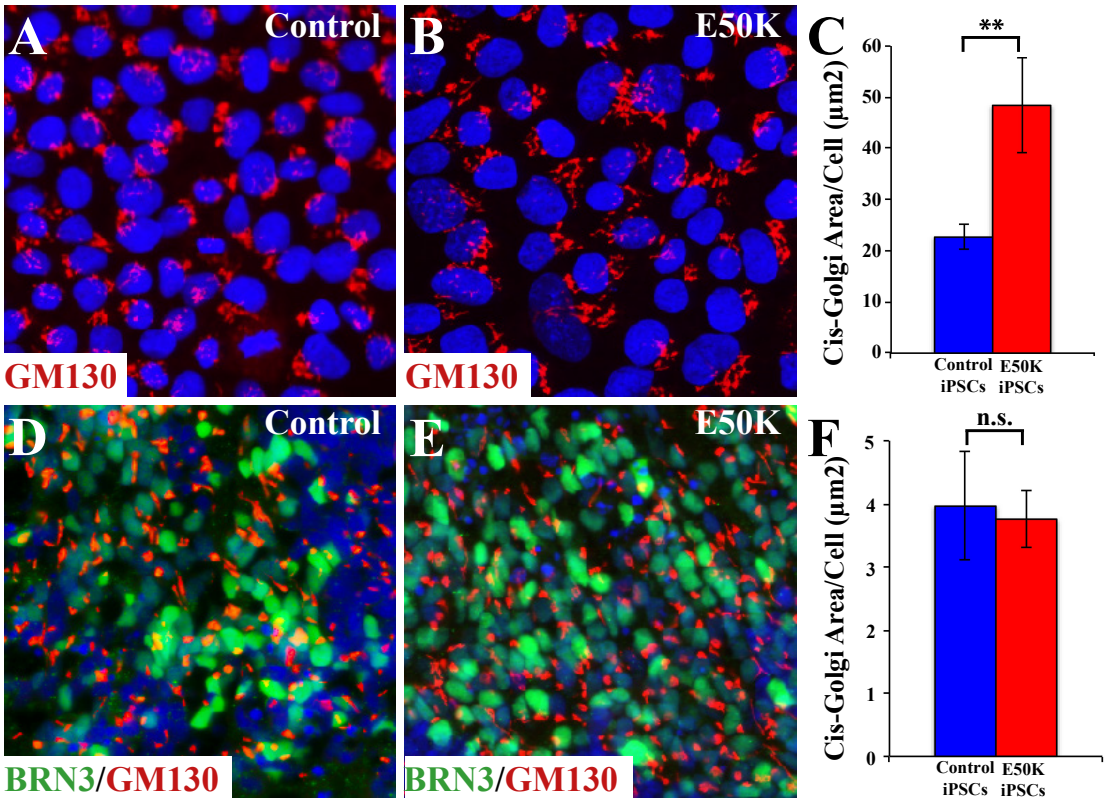

Fig. 3.9. Lack of Golgi deficits in E50K hiPSC-derived RGCs.

Fragmentation of the Golgi complex was detected in undifferentiated cultures of E50K hiPSCs compared to control hiPSCs (A-C). Upon differentiation to the affected RGC cell type, no significant differences in Golgi size were observed between control and E50K hiPSC-derived RGCs (D-F). Significant differences indicated as ** = $p<0.01$

for other glaucoma phenotypes as well. As other factors such as elevated intraocular pressure have been suggested to serve as a trigger for subsequent degeneration of RGCs [154], mutations in genes including OPTN could provide a similar trigger, with downstream effects mimicking features of glaucoma common to many underlying causes.

Whereas previous studies have analyzed features of glaucoma in RGCs by utilizing animal models or non-affected cell types in vitro [136, 155, 156], the development of a human induced pluripotent stem cell model of glaucoma allows for precise analysis of the affected cell type. The ability to study features of the disease process in human cells from the affected cell type is of utmost importance, as some previous studies have identified disruptions in the Golgi complex as a hallmark of certain mutations in OPTN, including the E50K mutation [130, 131, 136]. While this phenotype was recapitulated in undifferentiated E50K hiPSCs, this Golgi fragmentation was not observed upon differentiation to RGCs, the cell type directly affected by the disease process. Thus, disruptions to the Golgi complex may not have any direct connection to the health and survival of RGCs and consequently, may not play a role in glaucomatous neurodegeneration observed in patient samples. Such a result underscores the importance of hiPSC-based models of inherited diseases and the ability to differentiate these cells to the affected cell type. The increased apoptosis observed in E50K cells appeared to be specific for RGCs, the affected cell type, as no significant differences were observed in undifferentiated E50K hiPSCs compared to control cell lines. As such, the development of this in vitro model of glaucoma will allow for future studies analyzing precise mechanisms underlying glaucomatous neurodegeneration. The results of these studies also highlight the potential of hiPSCs to serve as a tool for pharmacological screening [142–144], as treatment of E50K hiPSC-derived RGCs with either BDNF or PEDF was able to partially rescue these cells from apoptosis. While many growth factors have been shown to play a role in RGC survival, recent work has demonstrated that BDNF and PEDF are especially important in the rescue of glaucomatous RGCs [157–161]. In vivo RGCs receive BDNF from the

LGN and PEDF from Muller glia [157, 158, 162–165]. Interestingly, treatment with these neuroprotective factors yielded similar levels of cell survival. While the reason for this similarity is not known, the possibility exists for overlap in these two signaling pathways. While both BDNF and PEDF are known to inhibit the apoptotic pathway [146–148, 150], they also affect transcription through MEK/ERK signaling pathways [144]. Thus, the similar net effects produced by BDNF and PEDF could be due to convergence of these signaling pathways within the cell.

3.5 Conclusion

Taken together, the results of the current study represent the most comprehensive description of RGC derivation from an hPSC source as well as the ability to utilize these approaches for studies of optic neuropathies such as glaucoma. On a broader level, this study establishes the suitability of hPSCs to analyze critical stages of RGC development from a human source. Furthermore, these results demonstrate the applicability of hPSC-derived RGCs for disease modeling and pharmacological screening for a host of optic neuropathies, both complementing existing animal models as well as narrowing the gap to clinical applications. However, the primary limitation of the current approach is that hPSC-derived RGCs grown in culture have not displayed all the proper electrophysiological characteristics as demonstrated by in vivo RGCs, including a complement of mature electrophysiological properties and the establishment of pre- and postsynaptic connections. Adult RGCs degenerate in optic neuropathies. As such, to better serve as physiologically relevant models of disease, the capacity of hPSC-derived RGCs to fully mature and recapitulate features of adult, in vivo RGCs is explored in the next chapter.

3.6 Acknowledgements

Sarah K. Ohlemacher: Conception and design, financial support, collection and/or assembly of data, data analysis and interpretation, manuscript writing, final approval of manuscript.

Akshayalakshmi Sridhar: Conception and design, collection and/or assembly of data, data analysis and interpretation.

Yucheng Xiao: Collection and/or assembly of data, data analysis and interpretation, manuscript writing.

Mansoor Sarfarazi: Conception and design, provision of study patient samples.

Theodore R. Cummins: Conception and design, financial support, data analysis and interpretation.

Jason S. Meyer: Conception and design, financial support, collection and/or assembly of data, data analysis and interpretation, manuscript writing, final approval of manuscript.

4. SYNAPTIC MATURATION OF HUMAN PLURIPOTENT STEM CELL- DERIVED RETINAL GANGLION CELLS

4.1 Introduction

The retina is linked to the brain by the optic nerve, a complex bundle of RGC axons, astrocytes, vasculature and oligodendrocytes. Damage of the optic nerve leads to common forms of blindness termed optic neuropathies, the most common of which is glaucoma [56, 166] . Onset of these disorders tends to be gradual and upwards of 50% of RGC axons have irreversibly degenerated by the time a patient observes any vision changes [4, 58]. Furthermore, RGCs possess no capacity for regeneration into adulthood. This necessitates the development of neuroprotective strategies for early stages of disorders and cell replacement therapies for end stages of diseases once RGCs have degenerated. hPSCs can provide an unlimited supply of RGCs for generation of cell replacement and drug screening therapies for optic neuropathies [5, 6, 52].

In order for hPSC-derived RGCs to be used for therapeutic applications, they must be able to fully recapitulate the features of the affected cell type, including the ability to develop mature phenotypic and functional characteristics. Previous studies have demonstrated the ability to generate hPSC-derived RGCs through various methods with great success [9, 10, 12, 13, 21, 30, 50, 167]. These cells have exhibited some capacity to mimic in vivo retinal ganglion cells, including recapitulating proper developmental timing and compartmentalized structure [13]. hPSC-derived RGCs have also been shown to fire APs [13,20,21,25,26,168], maintain a hyperpolarized RMP [13], respond to neurotransmitters like glutamate [21], and conduct ions through voltage gated channels [13, 20, 21, 25, 26]. Properties of fully mature in vivo RGCs include the maturation of intrinsic membrane properties such as voltage gated sodium and potas-

sium channels [126, 169, 170]. The development of voltage gated channels is essential as many properties of a mature RGC are governed by these channels including large amplitude APs [169,170] and repetitive AP firing [126,170]. Mature RGCs also display a resting membrane potential ranging from -55 to -60mV [126, 169, 171]. RGCs posses the largest somas within the retina, ranging from 70μm^2 to 400μm^2 [18, 172] and intricate neurites that increase in size and complexity as development proceeds [173]. However, it is unknown when these characteristics emerge and hPSC-derived RGCs that display a full complement of mature features have been scarce to date.

To address these shortcomings, experiments were undertaken to characterize the phenotypic maturation and functional capacity of hPSC-derived RGCs in short term (<2 weeks post-plating) and long term (>2 weeks post-plating) culture. Short term culture was used to monitor the emergence of neurite complexity while long term culture was utilized to observe the onset of electrophysiological properties, which are known to develop more slowly [174]. Additionally, one aspect of this research that has been largely ignored to date is the effect of astrocytes on RGC development. Within the retina, the cell bodies of astrocytes reside in the nerve fiber layer and optic nerve head [175, 176]. Astrocytes surround the axons of RGCs as they exit the optic nerve head to form the optic nerve. In the retina, astrocytes are essential for many functions, including reuptake of neurotransmitters [177], maintenance of the blood-retina barrier [178], provision of neurotrophic support [179], and importantly, guidance of synaptogenesis [180, 181]. As such, efforts were untaken to generate hPSC-derived astrocytes for co-culture with hPSC-derived RGCs to determine the effect upon phenotypic development and functional maturation in vitro. Results were compared to RGCs grown in the absence of astrocytes or in the presence of astrocyte conditioned medium (ACM) to determine if the effects of astrocytes were paracrine or contact mediated. hPSC-derived RGCs displayed some features associated with mature in vivo RGCs. However, the presence of hPSC-derived astrocytes increased RGC synaptic complexity and enhanced functional characteristics. The results of this study are the first of its kind to characterize the phenotypic and functional development of

hPSC-derived RGCs over time and explore how hPSC-derived astrocytes modulate the maturation of hPSC-derived RGCs.

4.2 Materials and methods

4.2.1 Maintenance of hPSCs

hPSCs were grown as previously described [10, 12, 13, 50]. In short, hPSCs were maintained using hESC qualified matrigel (Fisher Scientific, Hampton, NH) on six-well plates with mTeSR1 medium (StemCell Technologies, Vancouver, Canada) in incubators containing 5% CO_2 at 37 °C. Once colonies reached approximately 70% confluency, cells were passaged (every 4-5 days). Before passaging, areas of spontaneous differentiation were marked according to their unique morphology and mechanically removed. Passaging occurred by enzymatically lifting colonies using dispase (2mg/mL) for approximately 15 minutes. Colonies were then split in a 1:6 ratio. Multiple hPSC-lines were used throughout this study including h7-BRN3:tdTomato-Thy1.2, TiPS5, and miPS2.

4.2.2 Differentiation of hPSCs into RGCs

hPSCs were differentiated to a retinal fate using previously described protocols with minor modifications [10, 12, 13, 50]. Briefly, enzymatic lifting of pluripotent colonies yielded EBs. Over a time course of three days, cells were transitioned from mTeSR1 medium into NIM (Dubelcos Modified Eagle Medium (DMEM)/F12 (1:1), 100x N2 supplement, MEM nonessential amino acids, heparin (2μg/mL), and antibiotics). At 7 days of differentiation, cells were transferred into a six-well plate with NIM and adhered by the addition of 10% FBS. The following day, FBS was removed and fresh NIM was added and then replaced every other day until day 16. Plated colonies at day 16 were mechanically lifted and transferred into a suspension culture containing RDM (DMEM/F12 (3:1), MEM nonessential amino acids, B27,

and antibiotics). Suspension cultures were fed every two days with fresh RDM. After 30 days of differentiation, early retinal organoids could be readily identified by the bright ring surrounding the periphery. Retinal organoids were isolated from forebrain neurospheres. At day 45, retinal organoids were dissociated using accutase for 20 minutes. Following dissociation, single cells were immunopurified for RGCs with the Thy1.2 surface receptor using the MACs magnetic cell separation kit (Miltenyi Biotec, Bergisch Gladbach, Germany). Purified RGCs were plated on poly-D-ornithine, laminin-coated coverslips at a density of 10,000 cells/coverslip and maintained in BrainPhys Neuronal Media (StemCell Technologies, Vancouver, Canada) supplemented with 20ng/mL CNTF. Coverslips were then fixed at 1, 4, 7, and 10 days post-plating and used to analyze RGC phenotypic maturation.

4.2.3 Immunopurification

hPSC-RGCs were purified using a MACS kit based on the Thy1.2 surface receptor driven by the expression of BRN3 in the h7-BRN3:tdTomato-Thy1.2 hPSC line. Briefly, at 45 days of total differentiation, retinal organoids were dissociated for 20 minutes using accutase. Single cells were then incubated with the CD90.2 microbeads specific for Thy1.2 for 15 minutes at 4 °C in the dark at a ratio of 10μL of beads: 90μL of MACs Rinsing Buffer per 10 million cells. The cell suspension was pipetted into the MACs MS magnetic column. RGCs were trapped in the magnetic field based on the attachment of the Thy1.2 microbeads and non-RGCs flowed through the apparatus. The cell suspension was washed 3 times with MACs Rinsing Buffer. To flush out the RGCs, the MS column was removed from the magnetic field and 1mL of MACs Rinsing Buffer was added to the column and a plunger was used to push RGCs out of the column into a collection tube. The MS column was placed back in the magnetic field, and the 1mL purified RGC cell suspension was re-loaded to the column and the previous steps were repeated to increase the purity of RGCs. Purified RGCs were centrifuged, counted, and plated at a density of 10,000 cells/coverslip.

4.2.4 Differentiation of hPSCs into astrocytes

hPSCs were differentiated to astrocytes using previously described protocols [182, 183]. At 7 days of differentiation, EBs were adhered onto laminin-coated 6 well plates supplemented with NIM. At day 16, colonies were mechanically lifted using a P1000 pipette tip and placed in a suspension culture of RDM. Within 40 days of differentiation, early astrospheres were supplemented with 10 ng/mL EFH (FGF2, EGF and Heparin). Astrospheres were chopped and expanded using a mechanical tissue chopper to a size of 200μm every 2 weeks for up to 12 months. Between 9 and 12 months, glial astrospheres were dissociated using accutase for 20 minutes. Single cells were plated at a density of 20,000 astrocytes/coverslip and supplemented with BrainPhys Neuronal Media with the addition of 20ng/mL of CNTF to yield GFAP positive astrocytes. Within 3 weeks of plating, co-cultures of RGCs and astrocytes were established. 10,000 purified RGCs were plated on top of adhered astrocytes to create a substrate bound co-culture. Additionally, ACM was collected from plated astrocytes. ACM was added every second day to RGC cultures at a dilution of 1:1 with fresh BrainPhys as previously described [184] to create a secreted co-culture environment. Co-culture experiments were fixed 10 days post-plating and analyzed for RGC maturation.

4.2.5 Histology and immunocytochemistry

hPSC-derived RGC coverslips were collected at 1, 4, 7, and 10 days post-plating. Samples were fixed with 4% paraformaldehyde for 30 minutes. In preparation for immunostaining, samples were washed 3 times with PBS and permeabilized in 0.2% Triton X-100 for 10 minutes at room temperature. This was followed by blocking in 10% donkey serum for one hour at room temperature. Primary antibodies (Supplemental Table 6.1) were diluted in 5% donkey serum and 0.1% Triton X-100 solution and applied to samples overnight at 4 °C. The following day, cells were washed 3 times with PBS and blocked with 10% donkey serum for 10 minutes at room temper-

ature. Secondary antibodies were diluted in 5% donkey serum and 0.1% Triton X-100 solution and added for 1 hour at room temperature. Cells were washed 3 times with PBS and mounted appropriately. Immunofluorescent images were obtained using a Leica (Wetzlar, Germany) DM5500 fluorescence microscope.

4.2.6 Quantification and statistical analyses of RGC maturation

Purified RGCs at 1, 4, 7, and 10 days post-plating as well as co-culture experiments at 10 days post-plating were analyzed for RGC maturation based on soma size and the number of primary neurites. Numerous biological replicates (n=5) were obtained at each time point. Immunofluorescent images were captured and analyzed by the expression of tdTomato driven by BRN3. Using ImageJ plugins, the RGC soma size area and the number and length of primary neurites were quantified and recorded. Statistical analyses were performed using One-Way ANOVA followed by Tukey's post hoc. Statistical differences were determined based on a p value of less than 0.05.

4.2.7 Western blot

RGCs were collected and sonicated in a 2% SDS solution. Protein concentration was determined using a BCA assay (ThermoScientific, Waltham, MA) and samples were normalized so that equal amounts of protein were loaded into each well. Lysates were mixed with 4x Sample Buffer plus DTT and loaded onto 4-15% gradient gels. Gels were transferred to nitrocellulose using the Trans-Blot Turbo system (BioRad, Hercules, CA), blocked with 5% milk in tris buffered saline (TBS) plus 0.1% tween and blotted with primary antibodies (see Supplemental Table 6.1) overnight at 4 °C. After washing with 5% milk in TBS plus 0.1% tween, secondary antibody was applied for one hour using donkey anti-mouse 790, donkey anti-mouse 680, or donkey anti-rabbit 790 (Jackson ImmunoResearch, West Grove, PA). Blots were washed with TBS and imaged using the Li-COR Odyssey CLx imaging system (LI-COR Biosciences, Lincoln, NE). ERK1/2 served as a loading control. To generate a normalized fluo-

rescence value, fluorescence intensity for each protein of interest at each time point was normalized to its corresponding ERK1/2 loading control factor. The normalized fluorescence value was divided by the +2 week normalized value to obtain the relative fluorescence intensity for each time point.

4.2.8 Electrophysiological recordings

Whole cell patch clamp recordings were made at room temperature (21 °C) using HEKA EPC 10 amplifier and Patchmaster data acquisition software (HEKA, Lambrecht/ Pfalz, Germany). Recording pipettes with the tip resistance of 4-7 MΩ were fabricated from borosilicate capillary glass (1.2-mm outer diameter, 0.60-mm inner diameter; Sutter Instrument Co., Novato, CA) using a P-1000 puller (Sutter Instrument Co.,). The bathing solution contained (in mM): NaCl 140, $MgCl_2$ 1, KCl 5, $CaCl_2$, HEPES 10, Glucose 10, pH7.3 (adjusted with NaOH). For current-clamp recordings, pipettes were filled with internal solution containing (in mM): KCL 140, $MgCl_2$ 5, $CaCl_2$ 2.5, EGTA 5, HEPES 10, pH 7.3 (adjusted with KOH) and for voltage-clamp recordings, the internal solution contained (in mM): CsF 130, NaCl 10, HEPES 10, CsEGTA (EGTA in CsOH) 1. Inward sodium currents were recorded in the voltage-clamp mode with the holding potential of -80 mV. Spontaneous action potential activity was recorded in current-clamp mode without any current injection, using 3 sweeps of 1 min each starting from the holding potential of -80 mV. RMP was recorded in current-clamp mode at 0 pA immediately after establishing whole-cell configuration. For evoked action potentials, the cells were allowed to stabilize in the whole-cell configuration for 2 min before initiating ramp current injection with depolarization from 0 to 40 pA for 1s. Action potential threshold was estimated from ramp current injection. In addition to ramp depolarization, AP threshold was also determined from 500 ms step current injections at RMP, with increments of 10pA AP threshold, using dV/dt method. AP amplitude was measured as the height of the peak from threshold and duration was measured as the width at the threshold.

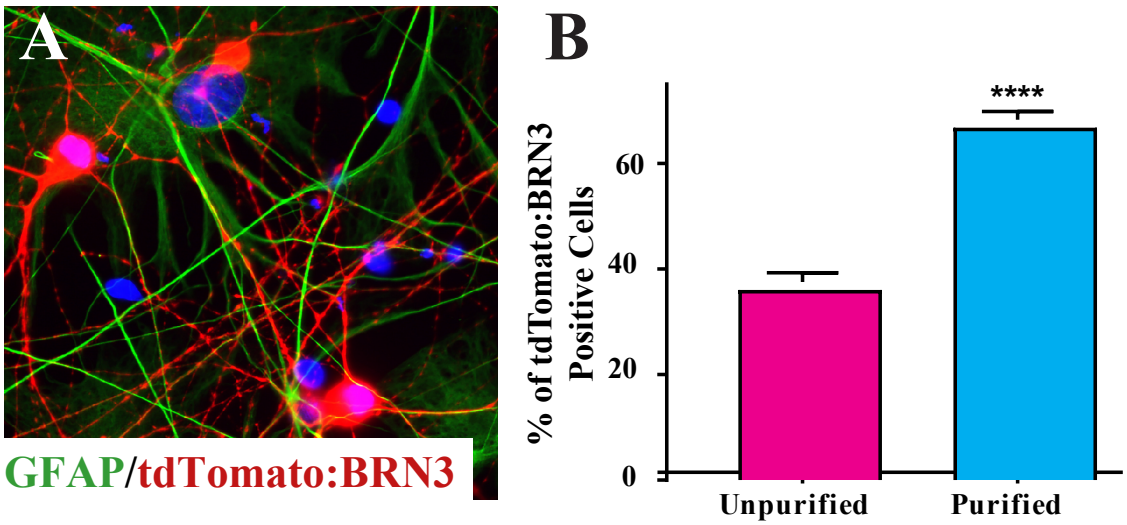

Fig. 4.1. Purification and quantification of MACS purified RGCS.

BRN3-tdTomato-Thy1.2 lines were immunopurified using expression of Thy1.2. Purified hPSC-derived RGCs were plated on laminin or in the presence of hPSC-derived astrocytes (A). Quantification revealed 66.87% ± 1.51% purified population of hPSC-derived RGCs (B). A Students t-test was used to compare conditions, n=5 and significant differences indicated as ****<0.0001. Error bars represent s.e.m.

When necessary, a small bias current was injected to maintain a similar baseline membrane potential (near -70 mV) before depolarizing current injections. Spontaneous postsynaptic currents were measured in the voltage-clamp mode at -80mV.

4.3 Results

4.3.1 Characterization of hPSC-derived RGCs

To date, studies have demonstrated that hPSC-derived RGCs posses voltage gated sodium and potassium currents ranging from 1pA to 2nA [13, 20, 21, 25, 26], are responsive to glutamate [21], and can fire spontaneous action potentials [13, 21]. While many of these characteristics are indicative of developing neurons, the ability to derive

hPSC-RGCs that possess a variety of mature phenotypic and functional features has eluded researchers to date. Mature in vivo RGCs across many species demonstrate a full complement of characteristics including large cell body sizes ranging from 70μm^2 to 400μm^2 [18, 172], complex neurite outgrowths [173], repetitive spontaneous firing [170], a RMP between -55 and -60 mV [126, 169], large amplitude/high frequency APs [169, 170], and nA of voltage gated currents [126, 170]. As such, experiments were undertaken to elucidate the time course of hPSC-derived RGC maturation to determine the onset of phenotypic and functional features in short ($<$ 2 weeks) and long term culture ($>$2 weeks).

BRN3-tdTomato-Thy1.2 reporter lines were differentiated using a stepwise protocol as previously described [10, 12, 13, 50]. hPSC-derived RGCs appeared around day 45 of differentiation, at which time they were purified by magnetic activated cell sorting (MACS) using expression of Thy1.2 on the cell surface of RGCs (Figure 4.1A). This resulted in a 66.87%$\pm$1.51% purified population of hPSC-derived RGCs (Figure 4.1B). The resultant cells were plated on a laminin substrate to observe neurite outgrowth in short term culture.

10 days post-plating, hPSC-derived RGCs displayed features of developing neurons, including robust and complex neurite outgrowth (Figure 4.2 A-D). Soma size increased from 46.63μm^2 to 98.24μm^2 in 10 days (Figure 4.2E) and RGC neurites grew significantly in length, extending 142.51μm on average (Figure 4.2F). During short term culture, the number of primary, secondary, tertiary and quaternary neurites more than doubled (Figure 4.2G). RGC neurites also displayed a 662.8% increase in the number of branch points over this time period (Figure 4.2H). These data indicated that in short term culture, RGCs generated increasingly complex neurite outgrowths as observed in vivo.

In addition to morphological maturation, hPSC-derived RGCs were characterized further for their electrophysiological maturation over a 4-week time course after plating on laminin. Voltage-clamp recordings from hPSC-derived RGCs exhibited an increase in peak sodium conductance as neurons matured from week 1 to week

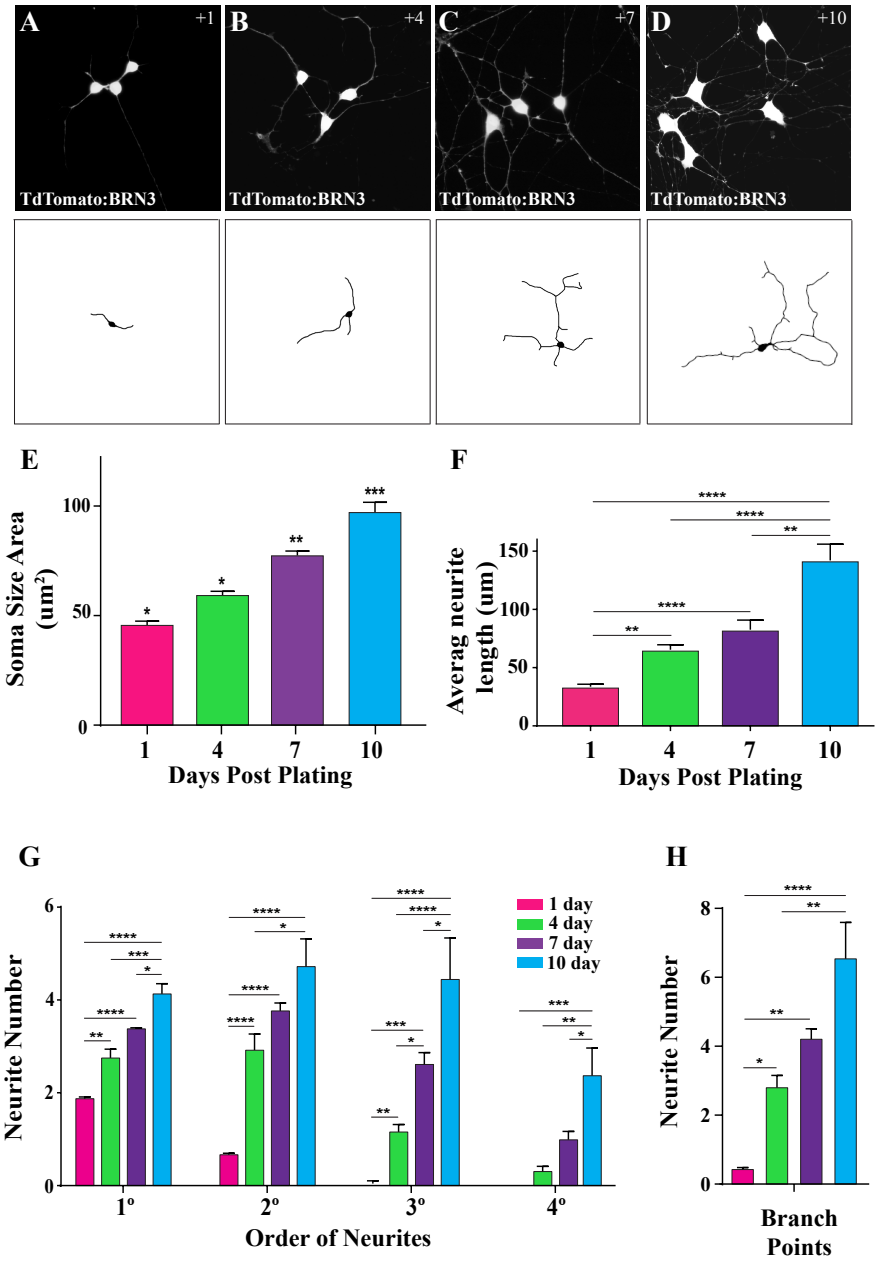

Fig. 4.2. hPSC-derived RGCs developed complex neurites in short term culture.

Immunocytochemistry and representative tracings of hPSC-derived RGCs demonstrated emerging complex morphologies over 10 days post-plating (A-D). Cell body size increased from 46.63μm^2 to 98.24μm^2 (E). RGC neurites extended an average of 142.2μm in 10 days (F). Neurites of RGCs grew increasingly complex as indicated by the significant increase in the number of primary, secondary, tertiary and quaternary neurites (G) and number of branch points (H). One-way ANOVA was used to compare timepoints, n=5 and significant differences indicated as *<0.05, ** <0.01, ***<0.001, ****<0.0001. Error bars represent s.e.m.

4 post-plating (Figure 4.3A, B), with an average conductance of - 0.38 ± 0.03 nA (n=10) at week 1; at week 2 = - 0.81 ±0.04 nA (n=8); at week 3 = -1.15 ± 0.03 nA (n=6) and at week 4 = -1.48 ± 0.06 nA (n=9). Currents were elicited using a series of depolarizations from the holding potential of -80 mV (Figure 4.3B, inset). There was a significant hyperpolarized shift in $V_{0.5}$ of activation (at week 1: V0.5 = 20.9 ± 1.3 mV, n=5; at week 2: $V_{0.5}$ = 29.9 ± 0.9 mV, n=5; at week 3: $V_{0.5}$ = 31.4 ± 1.6 mV, n=5 and at week 4: $V_{0.5}$= 35.6 ± 0.9 mV, n=5) (Figure 4.3C) which signified functional maturation of hPSC-derived RGCs. Current density plots displayed an increase in sodium current, (week 1= -61.6 ±4.9 pA/pF, n=6; week 2= -136.7 ±7.1 pA/pF, n=4; week 3= -196.1 ±21.1 pA/pF, n=5 and week 4= -236.0± 20.8 pA/pF; n=6) demonstrating an increase in the expression of voltage-gated sodium channels as RGCs matured (Figure 4.3D). For the calculation of sodium current densities, steady-state inactivation protocol was used to estimate peak sodium conductance to minimize voltage-clamp errors.

hPSC-derived RGCs demonstrated the ability to fire spontaneous action potentials as early as 2 weeks post-plating and by 4 weeks post-plating, trains of spontaneous action potentials emerged (Figure 4.4A). By the end of 4 weeks post-plating, approximately 37% of RGCs measured could fire spontaneous APs (Figure 4.4B). hPSC-derived RGCs maintained a resting membrane potential of about -35.14±1.34mV and no significant changes were observed throughout long term culture (Figure 4.4C).

To determine if hPSC-derived RGCs were forming presumptive synaptic connections, the presence of pre- and postsynaptic proteins was analyzed at 2, 4, and 6 weeks post-plating. hPSC-derived RGCs demonstrated increasing levels of the presynaptic protein SV2 by immunocytochemistry (Figure 4.5A). Western blot revealed a potential trend of increasing presynaptic protein levels as indicated by Neurexin 1 (NRXN1) and Synapsin 1 (SYN1) (Figure 4.5B-C). Levels of the postsynaptic marker PSD95 remained relatively stable. Taken together, these data indicate the formation of presumptive synaptic connections in culture.

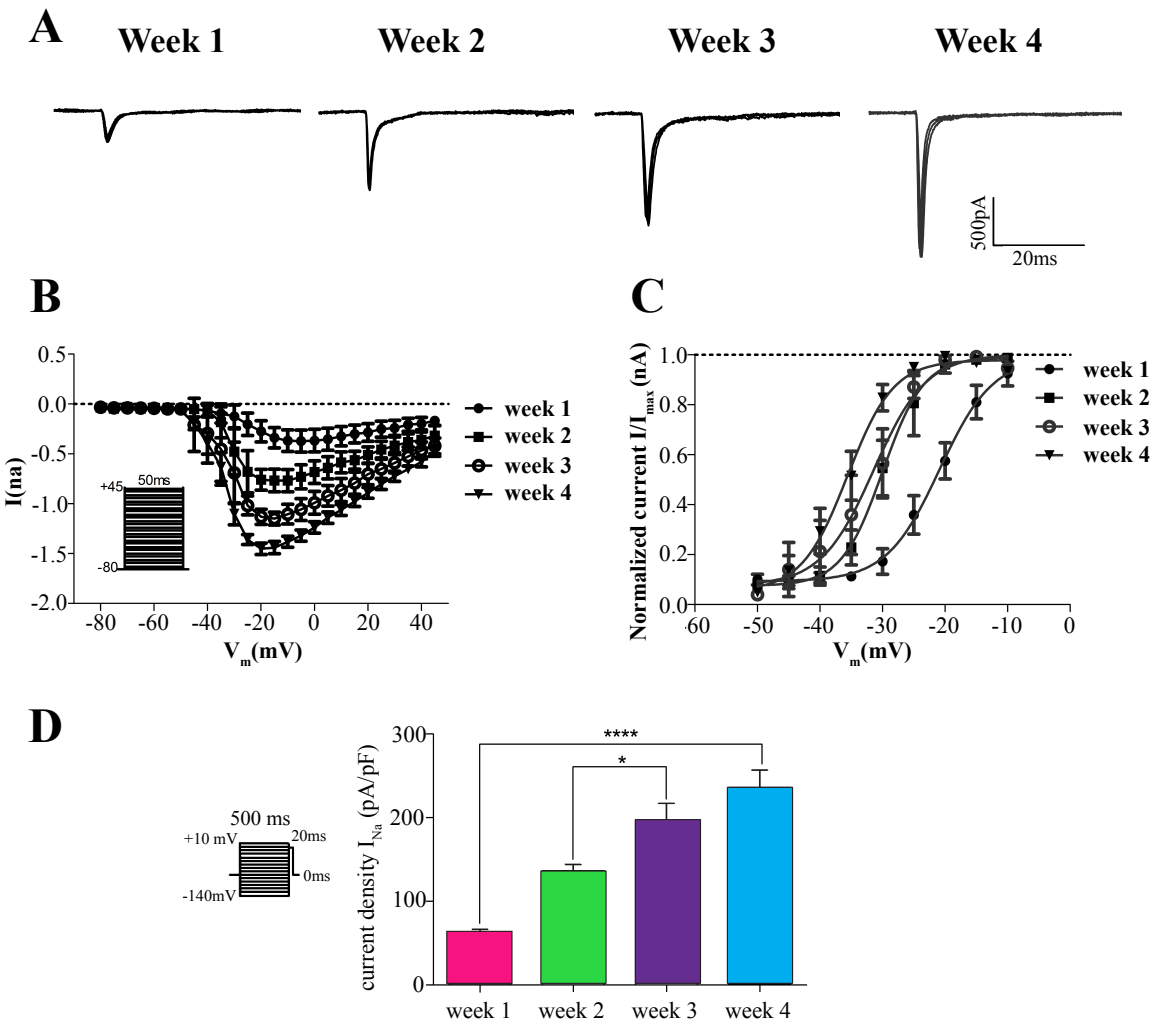

Fig. 4.3. hPSC-derived RGCs demonstrated increasingly mature functional characteristics in long term culture.

Patch clamp revealed an increase of inward voltage gated sodium currents from 400pA to 1.48nA over 4 weeks of plating (A). IV-curve displayed an increase in inward currents as RGCs matured (B). Voltage dependence of activation indicated a significant shift in the hyperpolarized direction with the progression of RGCs from week 1 to week 4 post-plating(C). Current density plot demonstrated an increase in sodium currents over 4 weeks, (week 1= -61.6 ± 4.9 pA/pF, n=6; week 2= -136.7 ± 7.1 pA/pF, n=4; week 3= -196.1 ± 21.1 pA/pF, n=5 and week 4= -236.0± 20.8 pA/pF; n=6) indicating an increase in the expression of voltage-gated sodium channels with RGC maturation (D). Significant differences indicated as *<0.05, ****<0.0001. Error bars represent s.e.m.

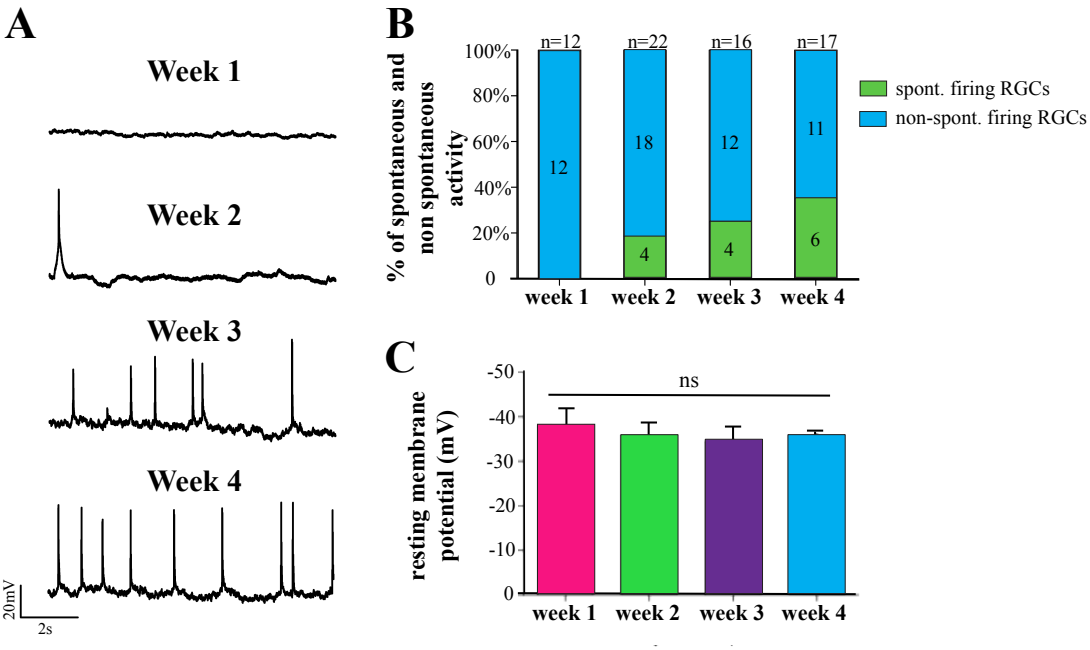

Fig. 4.4. hPSC-derived RGCs exhibited the ability to fire spontaneous action potentials in long term culture.

RGCs demonstrated an increase in the ability to fire spontaneous APs when analyzed by patch clamp over 4 weeks post-plating (V_{hold}=-80mV) (A-B). hPSC-derived RGCs maintained a RMP of -35.14±1.34mV (n=7) and no significant changes were observed throughout long term culture (C). Error bars represent s.e.m.

4.3.2 Enhanced phenotypic and functional maturation of hPSC-derived RGCs co-cultured with hPSC-derived astrocytes

During short and long term culture, hPSC-derived RGCs generated complex neurites, cell body sizes up to 98.24μm^2, spontaneous action potentials and presumptive synaptic connections. Astrocytes are known to modulate CNS maturation and previous studies have demonstrated the capacity for astrocytes to influence the synaptic development of neurons in culture [184–186]. As such, astrocyte co-culture was employed as a strategy to enhance phenotypic and functional maturation of hPSC-derived RGCs.

Multiple lines of hPSCs were differentiated to astrocytes following previously established protocols [182, 183], leading to a 88.26±2.13% pure population of mature hPSC-derived astrocytes after 9 months of differentiation (Figure 4.6). Mature astrocytes were co-cultured with immunopanned RGCs at 45 days of differentiation. Co-cultures were grown in short and long term culture to observe changes in phenotypic and functional development. Co-cultures were compared to control hPSC-derived RGCs grown on laminin or in the presence of ACM.

10 days post-plating, RGCs maintained on laminin displayed robust neurite outgrowth, which significantly increased when these cells were co-cultured on astrocytes (Figure 4.7 A-C). Astrocyte co-culture led to a 25% increase in RGC soma sizes (Figure 4.7D) and over 200% longer neurites (Figure 4.7E). RGCs co-cultured with astrocytes displayed significantly complex neurite outgrowths, demonstrated by the increase in number of primary, secondary, tertiary and quaternary neurites (Figure 4.7F) as well as increased neurite branching (Figure 4.7G). ACM generated no significant differences in soma size, neurite outgrowth, and complexity compared to control conditions, indicating the effect of astrocytes on hPSC-derived RGCs was primarily contact mediated.

Electrophysiological analysis was conducted on hPSC-derived RGCs grown on laminin or co-cultured with hPSC-derived astrocytes at 3 weeks post-plating. APs

were evoked using ramp current injection with depolarization from 0-40 pA (V_{hold} = -80 mV) (Figure 4.8A). Co-cultured RGCs demonstrated an increased AP amplitude (Figure 4.8B) as well as significantly increased numbers of APs (Figure 4.8C) that correlated with a significant decrease in AP duration(Figure 4.8D) when compared to laminin control. The resting membrane potential of these cells remained relatively stable, averaging -35.25±0.92 mV regardless of culture condition (Figure 4.8E).

Taken together, these results indicated that co-culture with astrocytes enhanced hPSC-derived RGC phenotypic complexity and functional maturation compared to control and ACM conditions. RGCs co-cultured with astrocytes generated RGCs more closely resembling mature in vivo RGCs. Co-cultured RGCs displayed soma sizes around 119.2μm^2, complex neurites reaching 862.7μm, as well as nanoamps of voltage gated currents and large amplitude, high frequency trains of APs.

4.4 Discussion

The primary function of retinal ganglion cells is to transfer information from the retina to the proper synaptic targets in the brain through the firing and propagation of action potentials [187]. While electrical activity is vital to the function of adult RGCs, electrical activity within the context of neural development is imperative for cell survival, synaptic pruning, and the formation of phenotypic and functional characteristics [170, 188–190]. However, the mechanisms that underlie RGC maturation are not well understood, particularly within human RGCs. The ability to generate populations of hPSC-derived RGCs has greatly expanded our knowledge of human development and revolutionized the ability to produce novel therapies for patients with optic neuropathies. However, optic neuropathies involve degeneration of mature RGCs that express a full complement of electrophysiological and phenotypic features [191]. Thus, hPSC-derived RGCs must be able to mirror these features to serve as physiologically-relevant models for translational applications.

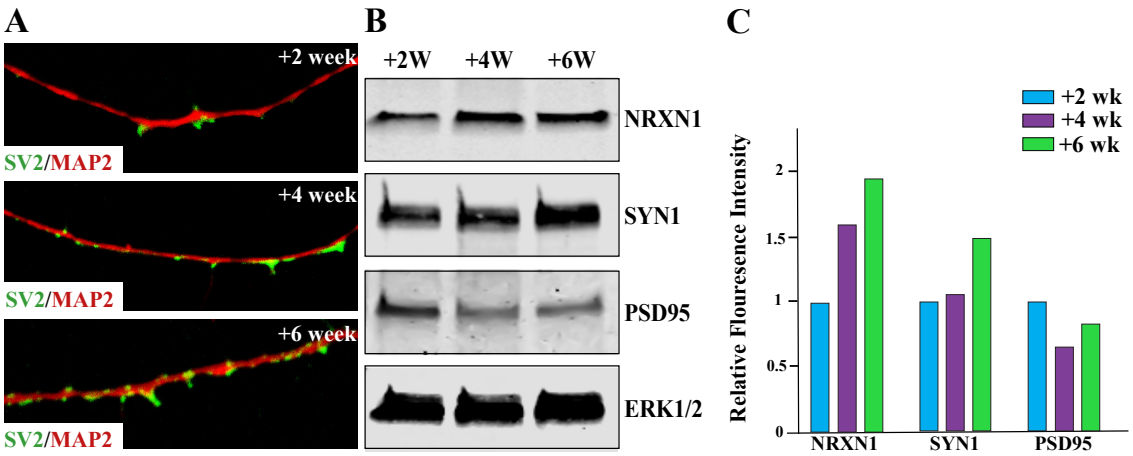

Fig. 4.5. hPSC-derived RGCs formed presumptive pre- and postsynaptic connections in long term culture.

hPSC-derived RGCs exhibited increasing expression of the presynaptic marker SV2 by immunocytochemistry (A). Western blot revealed the presence of additional presynaptic markers including Neurexin-1 (NRXN1), Synapsin-1 (SYN1), and the postsynaptic marker PSD95 (B). ERK1/2 served as the loading control and relative fluorescence intensity was calculated relative to the +2 week sample as described in the methods (C).

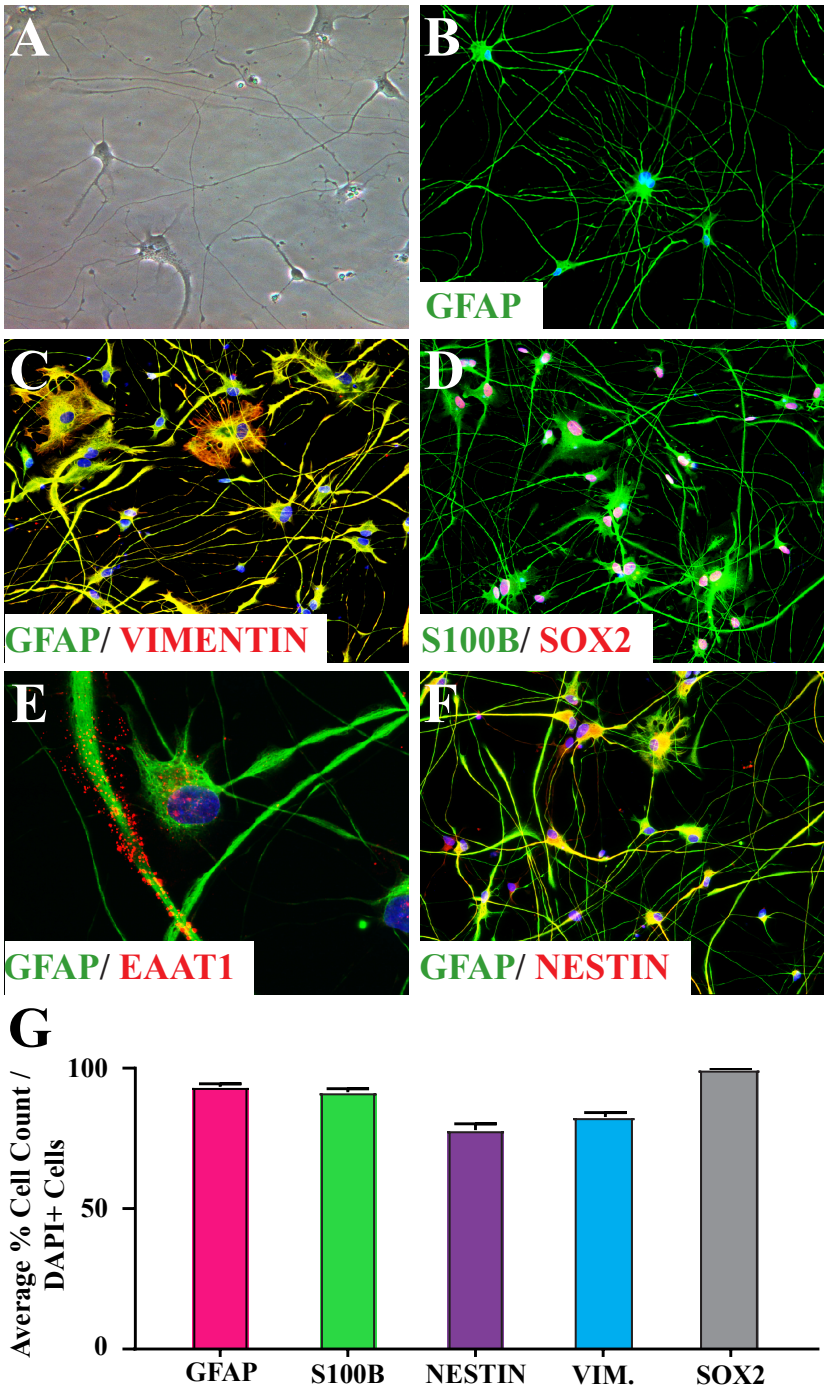

Fig. 4.6. Purification and quantification of hPSC-derived astrocytes.

Astrocytes demonstrated a typical star-like morphology under bright field microscopy after nine months of differentiation (A). Immunocytochemistry revealed robust expression of the mature astrocyte marker GFAP (B), co-localized with other astrocyte associated markers (C-F). Quantification of these markers indicated that 88.26% ± 2.13% of DAPI positive cells in culture expressed astrocyte markers, resulting in a highly pure population of hPSC-derived astrocytes (G). Error bars represent s.e.m.

The data presented in this manuscript demonstrates the ability to derive functionally active retinal ganglion cells with complex morphologies. Although mature in vivo RGCs exhibit a full complement of phenotypic and electrophysiological features, it is unclear to what extent hPSC-derived RGCs can mimic these characteristics. hPSC-derived RGCs were studied in short term culture to observe the generation of synaptic complexity. hPSC-derived RGCs displayed large cell body sizes up to 98.24μm^2. These cells also developed numerous complex and lengthy neurites over the course of short term culture. However, when hPSC-derived RGCs were co-cultured with hPSC-derived astrocytes, the onset of these features appeared more rapidly. 10 days post-plating, RGCs co-cultured with astrocytes displayed an average cell body size of 119.2μm^2 and developed a greater number of complex primary neurites compared to control RGCs. While control RGCs developed neurites reaching 244.4μm, co-cultured RGC neurites extended distances of up to 850.1μm in ten days.

hPSC-derived RGCs were maintained in long term culture to monitor the onset of electrophysiological features. To date, groups have demonstrated that hPSC-derived RGCs conduct sodium and potassium currents [13,20,21,25,26], and have the ability to fire APs [13,20,21,25,26,168]. However, very little is known about when these features emerge and to what extent hPSC-derived RGCs can develop mature functional characteristics. Nascent in vivo RGCs generate spontaneous activity early in development [170]. Spontaneous activity is important for refining early retinal circuitry and shaping the physiological development of mature RGCs [170,188–190]. As RGCs begin to mature, they develop intrinsic membrane properties such as large voltage gated currents [126,169,170], a hyperpolarized RMP [126,169,171], the ability to fire trains of APs [126,170], and cell body sizes ranging from 70μm^2 to 400μm^2 [18,172]. Sodium and potassium channel development have been shown across numerous studies to play a crucial role in maintenance of retinal circuitry [126,169–171]. During development, the ability of RGCs to regulate their ion channel kinetics is directly related to the ability of these cells to fire action potentials in response to stimulation [126,170,192]. As RGCs increase the ability to conduct sodium and potassium currents, the ability

to fire large amplitude, short half-width action potentials increases. In the presence of astrocytes, hPSC-derived RGCs generated trains of action potentials when stimulated compared to very little activity generated from control RGCs. Astrocytes promoted AP maturation as evidenced by an increase in the AP amplitude with a corresponding decrease in AP duration (width at threshold) which mirrors neuronal maturation in vivo. These data taken together indicate that hPSC-derived astrocytes significantly enhanced hPSC-derived RGC phenotypic and functional maturation. Previous groups have investigated RGC maturation in co-cultured rodent RGCs with rodent astrocytes due to limited availability of human samples [184, 186]. However, the experiments outlined in this manuscript are the first to utilize hPSCs to explore in depth maturation of human retinal ganglion cells and the effect of human astrocytes upon this process.

One result that proved confounding was the minor changes observed in the resting membrane potentials of these cells in long term culture. The average resting membrane potential of an mature RGC across most species is around -56.1± 7.8mv [126, 170, 171]. Despite long term culture with astrocytes, hPSC-derived RGCs demonstrated an average RMP of -35.14 mV with no significant changes during long term culture regardless of culture condition. Other studies exploring the development of electrophysiological characteristics in stem cell-derived neurons have reported similar findings. hPSC-derived neurons grown in long term culture displayed a RMP between -35mV and -50mV [185, 193–196]. The inability of RGCs to develop a mature RMP is likely due to limitations of the cell culture environment. Although culture conditions for RGC differentiation have been optimized, the synthetic in vitro environment is inherently different from the in vivo environment where RGCs mature naturally. Exploring ways to provide hPSC-derived RGCs with an in vivo-like environment might improve RMP. For instance, because neural circuitry development is dependent upon input into the system, external stimulation of RGCs might provide the exogenous activity necessary to push hPSC-derived RGCs to a more mature state [170, 188–190]. Moreover, the in vivo optic nerve is characterized by the

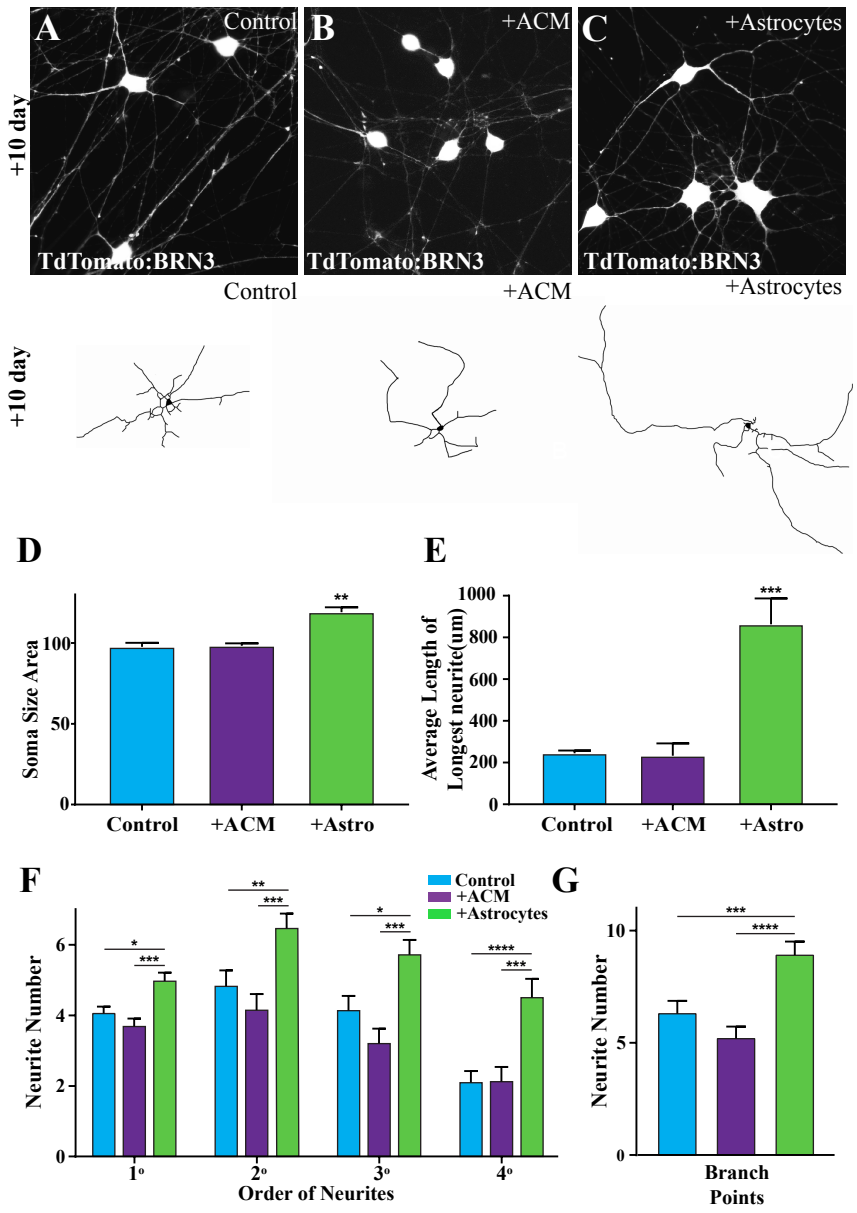

Fig. 4.7. hPSC-derived astrocytes enhanced phenotypic development of hPSC-derived RGCs.

10 days post-plating, RGCs co-cultured with astrocytes exhibited increased complex neurite morphologies compared to laminin control and ACM conditions as seen by immunocytochemistry and representative tracings (A-C). Astrocyte co-culture led to a significant increase in RGC soma size from an average of 95.21μm^2 in control and ACM conditions to an average of 119.22μm^2 in co-culture(D). hPSC-derived RGCs cultured with astrocytes also exhibited increased neurite length (E) and enhanced synaptic complexity(F). RGCs grown with astrocytes displayed an increase in neurite branching compared to control and ACM conditions (G). One-way ANOVA was used to compare conditions, n=5 and significant differences indicated as *<0.05, ** <0.01, ***<0.001, ****<0.0001. Error bars represent s.e.m.

presence of other cell types, including oligodendrocytes which form insulating myelin sheaths [197, 198]. Previous work has demonstrated that co-culturing rodent RGCs with oligodendrocyte progenitor cells (OPCs) can generate myelin sheaths surrounding RGC axons [199]. Interestingly, the presence of astrocytes in this study promoted rapid myelination of RGC axons in OPC co-culture. Future studies should be conducted exploring the role of OPC co-culture in hPSC-dervied RGC development. Lastly, perhaps -35mV is the maximum RMP hPSC-derived RGCs can attain in culture. If this is the case, RMP is established during the first week of plating, much earlier in hPSC-derived RGC development than anticipated. Future work should be done to elucidate the exact developmental timing of RMP onset.

Astrocytes play an essential and often underappreciated role within the central nervous system. It is becoming increasingly clear that astrocytes are not passive participants in neural development, but play instructive roles in shaping phenotypic and functional maturation [181, 200, 201]. Within the retina, astrocytes and RGCs lie closely associated in the nerve fiber layer and optic nerve [202]. Previous work has established that astrocytes play a critical role in the formation of tripartite synapses which contain the pre- and postsynaptic membrane closely associated with an astrocyte [200, 201, 203–205]. In fact, recent studies have shown one astrocyte can associate with multiple neurons and can have wide reaching effects on up to 100,000 synapses [204, 206, 207].

In the current study, hPSC-derived astrocytes demonstrated effects on hPSC-derived RGC maturation primarily through contact mediated signaling. hPSC-derived RGCs grown in direct contact with astrocytes displayed a significant increase in neurite length and complexity. In addition, astrocytes enhanced hPSC-derived RGC functional properties by increasing the frequency of APs and generating large amplitude, short half width APs. Previous studies have uncovered that direct contact of neurons and astrocytes can increase functional activity of developing neurons, leading to larger voltage gated currents and expedited AP maturation [201, 206, 208]. Although paracrine mediated signaling has been shown to play a role in RGC mat-

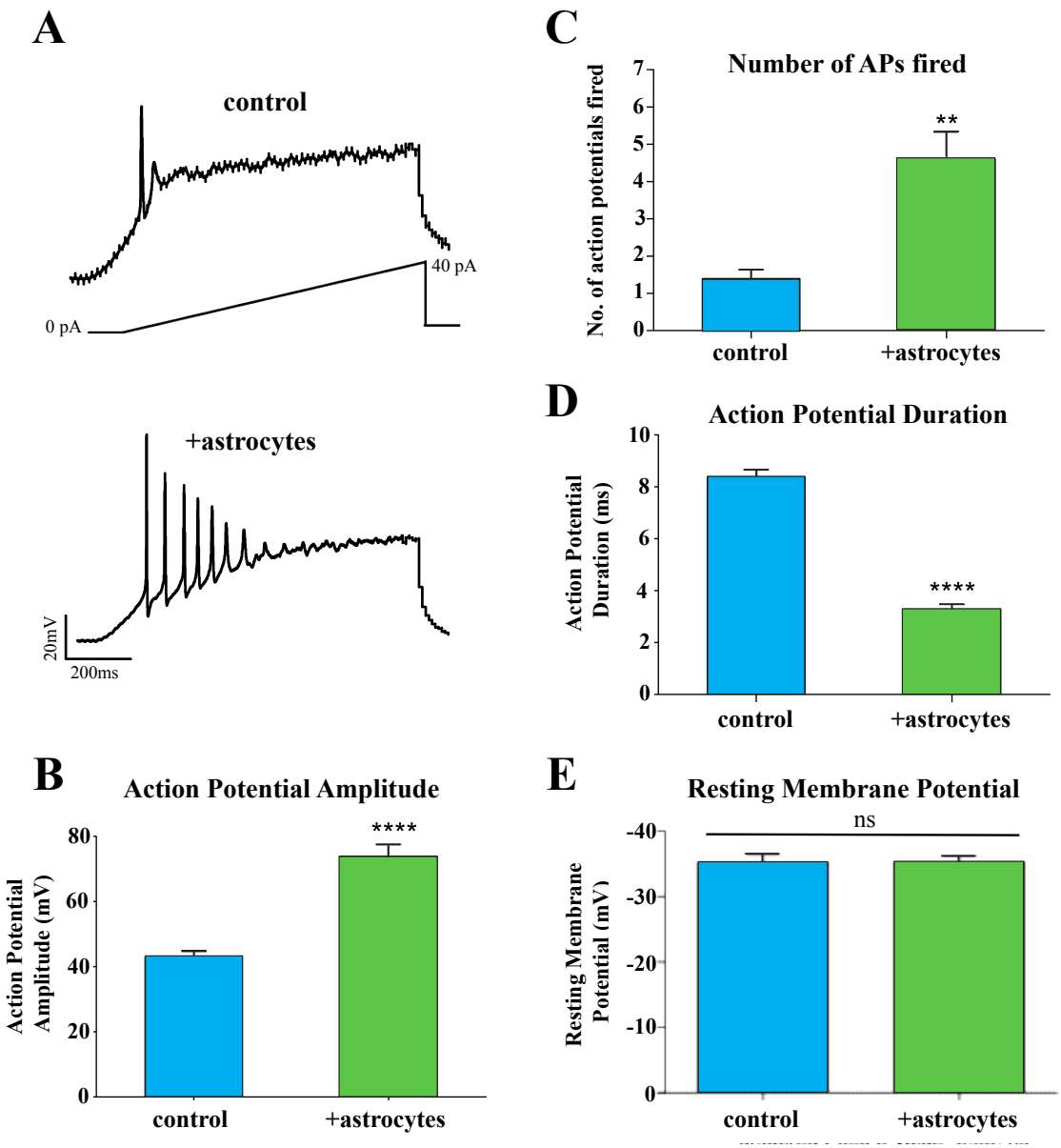

Fig. 4.8. hPSC-derived astrocytes enhanced functional maturation of hPSC-derived RGCs.

Representative traces of AP firing recorded from hPSCs-derived RGCs grown without and with astrocytes 3 weeks post-plating. APs were evoked using ramp current injection with depolarization from 0-40 pA (V_{hold} = -80 mV) (A). Summarized data for AP maturation demonstrated that AP amplitude (B) and AP firing (C) increased significantly and correlated with a significant decrease in AP duration (D) for RGCs co-cultured with astrocytes. Regardless of culture conditions, the resting membrane potential of remained relatively stable across at approximately -35mV (n=8) (E). Significant differences indicated as ** p=0.005; **** p<0.0001. Error bars represent s.e.m.

uration, numerous studies have indicated that soluble factors secreted by astrocytes might be more important in the generation of inhibitory and excitatory synapses and maintenance of these synapses, [201, 206, 209, 210] which was not quantified in this study. However, it is important to note that previous work has suggested that direct contact of RGCs and astrocytes is necessary for RGCs to respond to soluble factors released from astrocytes [201, 208]. Without this initial contact, ACM may not have the capacity to influence hPSC-derived RGCs. Future work should be carried out to determine to what extent hPSC-derived RGCs can respond to soluble factors released from astrocytes.

Given the influence of astrocytes in the CNS, it would also be useful to understand the role astrocytes play in the disease process. While astrocytes are typically thought to exert a positive influence on the nervous system, their effects can be detrimental if they become reactive when injured or diseased [211–214]. Experiments aimed at uncovering the interplay between diseased astrocytes and healthy RGCs would aid in understanding the mechanisms underlying optic neuropathies and present additional therapeutic targets. Groundbreaking studies from the field of amyotrophic lateral sclerosis (ALS) have shown that diseased astrocytes can negatively impact healthy neurons [213, 215]. hPSC-astrocytes derived from patients with genetic and sporadic forms of ALS were co-cultured with hPSC-derived motor neurons from healthy, non-ALS subjects. Both populations of diseased astrocytes were similarly toxic to motor neurons, indicating a non-cell autonomous contribution of astrocytes to the disease process [213]. Conversely, healthy hPSC-derived astrocytes have been shown to confer some degree of protection to hPSC-derived motor neurons derived from ALS patients [216–218]. Future studies should explore the role of astrocytes in the onset and development of optic neuropathies.

4.5 Conclusion

The data presented here demonstrates that hPSC-derived RGCs mirror many of the phenotypic and functional features of in vivo RGCs. Furthermore, the clear contribution of astrocytes to enhanced RGC maturity are in close agreement with previous data suggesting the importance of astrocytes in RGC maturation. The finding that hPSC-derived RGCs can recapitulate many features of in vivo RGCs will contribute to the overall goal of developing efficacious therapies for patients suffering from optic neuropathies.

4.6 Acknowledgements

Sarah K. Ohlemacher: Conception and design, financial support, collection and/or assembly of data, data analysis and interpretation, manuscript writing, final approval of manuscript.

Kirstin B. Langer: Conception and design, financial support, collection and/or assembly of data, data analysis and interpretation, manuscript writing, final approval of manuscript.

Ridhima Vij: Conception and design, collection and/or assembly of data, data analysis and interpretation, manuscript writing, final approval of manuscript.

Elyse M. Feder: Data analysis and interpretation.

Clarisse M. Fligor: Data analysis and interpretation.

Michael C. Edler: Conception and design, collection and/or assembly of data, data analysis and interpretation, manuscript writing, final approval of manuscript.

AJ Baucum II: Conception and design, collection and/or assembly of data, data analysis and interpretation, final approval of manuscript.

Theodore R. Cummins: Conception and design, financial support, collection and/or assembly of data, data analysis and interpretation, final approval of manuscript.

Jason S. Meyer: Conception and design, financial support, collection and/or assembly of data, data analysis and interpretation, manuscript writing, final approval of manuscript.

5. DISCUSSION

Human pluripotent stem cells possess the remarkable ability to self renew and differentiate into virtually any cell type of the body [5, 6]. This makes hPSCs powerful tools for novel translational applications. hPSCs allow for investigation into some of the earliest time points in human embryonic development. The generation of human cell lines allows for the development of models that reveal mechanisms of human disease, thereby bridging the gap in the translation of therapies from animal models to human patients. hPSCs also allow for the generation of millions of patient specific cells for cell replacement therapy and high-throughput drug screening.

The retina is an ideal place to study translational applications of hPSCs because it is can be manipulated easily. It can be monitored using non-invasive techniques, which is difficult for other locations in the brain and spinal cord. Its structure is also well characterized, containing defined neuronal types. Although the retina is small in size, the visual system accounts for approximately 80% of the sensory information that is processed by the brain [219, 220].

Many protocols have been developed to generate retinal neurons from hPSCs, primarily based on information gathered from developmental studies in animal models and the limited data obtained from postmortem human retinal tissues [8–13, 21, 53]. It is well established that retinal development occurs in a stepwise manner through the interplay of different signaling pathways that instruct retinal generation in a chronological and stepwise fashion [7]. The retina begins as two outgrowths from the early neural tube. These outgrowths invaginte to form optic cup structures, which eventually develop into stratified retinal tissue.

Many hPSC differentiation protocols seek to mimic in vivo development in a cell culture environment by exogenously activating the proper signaling pathways using expensive growth factors and small molecules [8,21,26,54,221]. However, the protocol

developed by the Meyer Lab relies on the ability of hPSCs to intrinsically differentiate towards a neural lineage in the absence of extrinsic signaling, also called default differentiation [10,53,222]. This default differentiation protocol generates populations of optic vesicle-like structures, which are >95% enriched for CHX10 expressing retinal progenitor cells. Optic vesicles give rise to retinal organoids, which recapitulate the spatial and temporal organization of an in vivo retina [9, 30]. Retinal ganglion cells are specified first, followed shortly by cone photoreceptors and amacrine cells, while later-born cell types such as rods and Muller glia arise near the end of organoid development. Furthermore, retinal ganglion cells develop on the inner layers of retinal organoids, while photoreceptors emerge along the outer layers.

However, the development and characterization of RGCs had been relatively ignored in the field of hPSC retinal cell biology because of difficulties in cell type identification. Due to the limited availability of specific markers for RGCs, studies instead focused on the generation of RPE and photoreceptors, cell types residing in the outer retina [100,223]. These cells have a unique morphology and exhibit specific genetic markers to identify them from a pluripotent source. As such, the study of disorders affecting the outer retina- such as AMD- were the initial focus of efforts in the field while studies of inner retinal disorders and subsequently affected cell types (such as RGCs) lagged behind.

Thus, efforts in the lab prioritized the definitive identification of retinal ganglion cells from a pluripotent source. One of the most reliable markers of RGCs is BRN3, which is also found in somatosensory and auditory neurons [36, 37, 39, 40]. Lack of specificity complicated efforts to assign an identity to a BRN3 positive cell differentiated from hPSCs. However, the ability to generate and isolate purified organoids that contained a highly enriched population of retinal progenitor cells allowed BRN3 to be used as a definitive marker of RGCs. Once a cell has become specified as a CHX10-positive retinal progenitor, it is locked into its retinal fate and cannot differentiate into anything other than a retinal neuron [32]. Extensive characterization using the Meyer protocol demonstrated that BRN3 was expressed in conjunction with other

RGC-associated markers [10,13,13,50,53,80,167]. Analyzing the spatial organization of human retinal organoids, BRN3 was found restricted to the inner layers, further confirming its use as a marker for RGCs.

As in vivo retinal ganglion cells develop, they extend neurites into the environment to explore their surroundings. As these cells begin to make rudimentary connections with neighboring neurons, RGC neurites will undergo compartmentalization, including development of a defined axon, multiple dendrites and the soma [224]. Compartmentalization is imperative for the proper physiological function of a neuron. RGC dendrites receive input from retinal interneurons and pass this information to the brain in the form of APs that propagate along their axons [187]. The axons of RGCs bundle together in the nerve fiber layer to form the optic nerve, which travels into the brain to synapse with the LGN or SC.

hPSC-derived RGCs recapitulated many in vivo features, including the generation of many neurites that eventually compartmentalized into a polarized neuron with multiple dendrites, a soma and a single axon [13]. hPSC-derived RGC axons exhibited the capacity to fasciculate in an optic-nerve like manner and extended distances of up to 1.5mm in a 24 hour period. In addition, these cells possessed the ability to fire APs [20, 21, 25, 26], maintained a hyperpolarized RMP [13], and conducted ions through voltage gated channels [13, 20, 25, 26]. Although hPSC-derived RGCs lacked features of a bona fide optic nerve, such as oligodendrocytes, astrocytes and vasculature, the ability of these cells to mirror the basic structure and function of in vivo RGCs is remarkable.

After successful generation and characterization of hPSC-derived RGCs, these cells were used to establish a model for glaucoma [13]. Glaucoma can be divided into two broad categories, primary open angle glaucoma and closed angle glaucoma (CAG) [166,225]. POAG is the most common form of the disorder and is traditionally associated with an elevated intraocular pressure [58,166,225]. However, elevated IOP is no longer a defining characteristic of POAG [59, 166, 226], although it remains a risk factor for the disease. In fact, normal IOP has been observed in up to 50% of

POAG patients [3, 57, 227]. As such, glaucoma has recently been recharacterized as a disorder that causes slow and progressive loss of RGCs via apoptosis, leading to deficits in the visual field [159, 166, 225].

Although the mechanism underlying RGC degeneration has not been uncovered, recent studies suggest that axonal transport in RGCs is perturbed in POAG [161, 189, 228]. Axonal transport is critical to RGC survival due to the neuroprotective signals these cells receive from their synaptic targets. Muller glia endfeet are closely associated with the ganglion cell layer and have been shown to provide CNTF, PEDF, GDNF, and BDNF to RGCs [157,158,162,229] while synaptic targets in the brain such as the LGN supply BDNF, NGF, and NT4/5 retrogradely to RGCs [162–165]. Recent studies have suggested that blockage of axonal transport due to injury obstructs signaling of neuroprotective factors [161, 228, 230, 231]. Once signaling cascades are blocked, the ganglion cells are triggered to self destruct through apoptosis [166, 232]. Supplementing animals with BDNF has shown to rescue retinal ganglion cells in rodent glaucoma models [159, 160, 233]. Interestingly, this same mechanism is reminiscent of early development, wherein RGCs that fail to reach the proper target in the brain do not receive this protective signaling and degenerate [161, 234, 235].

It is hypothesized that the mechanism of degeneration is similar across all forms of glaucoma, even if the inciting event that causes the damage varies from person to person [166,226]. As such, a glaucoma model does not necessarily need to recreate the initial stressor that induces damage, but instead should recapitulate the primary phenotype observed- specifically a targeted loss of RGCs by apoptosis. As such, we aimed to establish a genetic model of glaucoma using fibroblasts obtained from a patient with an E50K mutation in the OPTN gene, causative for normal tension POAG [131]. E50K mutations in OPTN are relatively rare, occurring in approximately 3-13% of patients with POAG [236, 237]. However, investigating the mechanism of RGC degeneration in E50K hPSC-derived RGCs might have wide-ranging implications for all forms of POAG, serve as a complement to existing animal models and help narrow the gap in generating translational therapies.

E50K patient-derived RGCs displayed increased apoptosis compared to control hPSC-derived RGCs. Interestingly, apoptosis in E50K RGCs was diminished with the treatment of neuroprotective factors BDNF and PEDF. In vivo RGCs receive BDNF from the LGN and PEDF from Muller glia [157, 161, 162]. These results support the importance of neuroprotective signaling in disease states and displayed a proof of principle that E50K RGCs could serve as a platform for high-throughput drug screening in future studies. Although it is clear that this model recapitulates apoptotic cell death of RGCs, the precise interplay of OPTN in glaucoma is still unknown. OPTN is an autophagy receptor and it is hypothesized that autophagy dysregulation plays a role in many forms of neurodegeneration [238, 239].

While treatment of E50K RGCs with neuroprotective factors appeared to reduce apoptosis, neuroprotective therapies remain difficult to translate to patients. These proteins have a half-life of approximately 10 minutes in the circulatory system, meaning that systemic delivery is not an optimal route of administration [240, 241]. Moreover, the blood-retina barrier functions in much the same way as the blood-brain barrier, presenting further obstacles to effective systemic drug delivery. Although the eye is relatively easy to access via intravitreal injections, sustained delivery of neuroprotective factors in this way is simply unrealistic. Studies have explored the possibility of engineering astrocytes to express high levels of neuroprotective factors [242–244]. Engineered astrocytes can be transplanted into the retina and serve as a local source of these proteins. Other strategies include the use of gene therapy to express neuroprotective factors in RGCs or Muller glia [245, 246]. Combinations of gene therapy and cell mediated delivery of neuroprotective factors have shown promising results in animal models [240, 247]. It is unknown how well these therapies will translate to human patients.

Furthermore, hPSC models contain their own set of limitations. hPSCs allow for generation and the straightforward analysis of one human cell type in a dish. However, differentiated cells exist outside the ecosystem of a tissue or organism. While hPSCs may help determine what drugs are efficacious for specific cell types, it is difficult

to determine side effects or elucidate the complex pharmacokinetics of compounds without a whole organism.

However, it must be noted that adult RGCs degenerate in optic neuropathies. Therefore, to serve as a more physiologically relevant model, hPSC-derived RGCs should replicate the phenotypic and functional features of mature, in vivo RGCs. As such, methods were explored to improve the E50K disease model by investigating the capacity of hPSC-derived RGCs to become phenotypically and functionally mature. Preliminary evidence suggested that prolonged culture of hPSC-derived RGCs generated neurons that could fire single APs [13, 20, 21, 25, 26], maintain a hyperpolarized RMP of about -35mV [13] and conduct picoamps of current through voltage gated channels [13, 20, 25, 26]. However, these features were typical signs of an immature RGC. Mature mammalian RGCs have the capacity to fire trains of APs in response to stimuli [126, 170], maintain a RMP between -55 and -60mV [126, 169, 171], and develop complex and lengthy neurites that eventually form pre- and postsynaptic connections [173]. As such, methods were explored to generate mature hPSC-derived RGCs. Approaches included optimizing cell culture conditions and exploring the role of astrocytes to enhance RGC maturation.

Astrocytes play an underappreciated role within the nervous system. It is becoming increasingly clear that astrocytes are not passive participants in neural development, but play instructive roles in shaping phenotypic and functional maturation [181, 200, 201]. hPSC-derived RGCs co-cultured with hPSC-derived astrocytes displayed enhanced synaptic and electrophysiological maturation. These cells exhibited nA of voltage gated currents, trains of action potentials in response to stimuli, and complex neurite morphology. While astrocytes are typically thought to exert a positive influence on the nervous system, their effects can be detrimental if they become reactive when injured or diseased [211–214]. Recent studies have demonstrated that when hPSC-astrocytes derived from patients with genetic and sporadic forms of ALS were co-cultured with hPSC-derived motor neurons from healthy subjects, both populations of diseased astrocytes were similarly toxic to motor neurons [213]. These

data indicate a non-cell autonomous contribution of astrocytes to the disease process. Conversely, healthy hPSC-derived astrocytes have been shown to confer some degree of protection to hPSC-derived motor neurons derived from ALS patients [216–218]. Future experiments aimed at uncovering the interplay between diseased astrocytes and healthy RGCs are the next step in glaucoma disease modeling. Co-culturing E50K astrocytes with wild type RGCs would help elucidate the non-cell autonomous contributions of astrocytes to glaucoma. The establishment of healthy hPSC-derived astrocytes co-cultured with E50K RGCs might confer some level of protection of diseased RGCs and present additional therapeutic targets.

Drug screening platforms to identify neuroprotective agents and therapeutic targets are useful in early stages of neurodegeneration. However, once neurons in the central nervous system are lost, they have no capacity for regeneration. Moreover, the CNS has an extraordinary capacity for adaptation and as such, vision loss is usually not evident in patients until 50% of the retinal ganglion cells are lost [3, 4, 58, 248]. Clinical screening for glaucoma can only detect gross changes to retinal architecture that occur once a large population of the ganglion cells have irreversibly degenerated [166]. This necessitates the need for cell replacement therapies for patients who have lost a significant portion of their RGCs to degeneration.

Cell replacement therapy requires the successful completion of numerous steps. Transplanted neurons must first integrate to the proper position within the retina and make presynaptic connections with appropriate cells, primarily amacrine and bipolar cells. Once neurons have integrated into the ganglion cell layer, they must extend their axons from the retina to the LGN, a distance of approximately 110mm in humans [19]. After hPSC-derived RGC axons traverse this distance, they must navigate to the proper synaptic target in the brain and establish functional postsynaptic connections.

Integration into the retina is challenging due to retinal injury and immune responses, as well as missing developmental cues RGCs normally receive during neurogenesis and synaptogenesis. However, ongoing research suggests that hPSC-derived neurons and RGCs display some capacity to integrate into rodent retinas [72–74, 249],

with approximately 3.2% of cells surviving one week after transplant [74, 249]. Retinal progenitors and newly specified RGCs demonstrate greater capacity for survival after transplant than adult RGCs. Interestingly, it appears that integration is more successful in mouse models of RGC degeneration compared to healthy mice, although the mechanisms underlying this phenomenon remain unknown. Furthermore, multiple studies have demonstrated that less than 1% of integrated neurons can make the journey from the RGC layer to the LGN and form synapses [73, 74].

Recent studies have demonstrated that hPSC-derived RGCs possess the capacity to respond to growth cues and and can travel up to 1.5mm in just 24 hours. In addition, hPSC-derived RGCs exhibit target specificity, preferentially targeting explants of SC over non-target tissues such as the olfactory bulb [25]. Current work indicates that hPSC-derived RGCs develop functional properties similar to those of in vivo RGCs. Taken together, it is clear that hPSC-derived RGCs possess some capacity for in vivo cell replacement. More research is needed to optimize the steps involved in successful cell replacement therapy. Future experiments include exploring the expression of specific guidance receptors expressed by hPSC-derived RGCs throughout their growth and development. Once the precise developmental timing of these receptors is known, ways in which to guide RGC outgrowths to a target, such as a LGN explant, should be explored. Lastly, once hPSC-derived RGCs synapse with an ex vivo target tissue in vitro, the ability of RGCs to form functional synaptic connections can be analyzed. Optogenetic stimulation of hPSC-derived RGCs and subsequent calcium imaging of the target tissue would be one way to conduct such an experiment.

Another obstacle to development of successful therapies is the time, cost, and labor needed to generate populations of hiPSCs for individual patients. One way to overcome this challenge is to generate human leukocyte antigen (HLA) and ABO blood group matched hiPSCs in combination with immunosuppressants. The same methods are used to ensure successful organ transplants between individuals [250,251]. A recent study in the United Kingdom determined that the generation of 150 lines

from O negative donors of varying HLA types would be compatible for approximately 80% of the British population [252].

The eye is uniquely immune privileged. In fact, many corneal transplant recipients often to do not undergo HLA matching, yet 90% of them are accepted with few complications [253]. This does not mean that transplants into the eye suffer from no rejection; only that immune rejection within the eye is significantly reduced. Recent data suggests that transplanted retinal progenitor cells are likely to be rejected if they cannot integrate and differentiate to the appropriate cell type [254,255]. However, the transplant of differentiated retinal neurons experience little immune rejection [72].

5.0.1 Conclusion

Since the first description of hPSCs two decades ago, hPSC technology has advanced quickly. The work presented in this dissertation demonstrates the first in depth characterization of RGCs from a pluripotent source, largely ignored in the field of retinal stem cell biology. hPSC-derived RGCs exhibited the ability to generate lengthy neurites and compartmentalize into RGCs with many functional characteristics. Using this knowledge, a glaucoma disease model was generated from a patient with an E50K mutation in the OPTN gene, causative for POAG. Patient-derived RGCs demonstrated an increase in apoptosis as observed across all forms of POAG. Treatment with neuroprotective factors reduced cell death, indicating that diseased RGCs could serve as a platform for high-throughput screening in future studies. However, to serve as physiologically relevant models for translational applications, hPSC-derived RGCs were assayed for their ability to mirror in vivo RGC phenotypic and functional maturation, which could be greatly enhanced by the presence of hPSC-derived astrocytes. Taken together, these data contribute to the greater understanding of the ways in which hPSC-derived RGCs could be used for drug screening, cell replacement therapies, and disease modeling applications to enhance our knowledge of human development and generate novel therapies for optic neuropathies.

6. SUPPLEMENTAL TABLES

Table 6.1.: Primary antibodies used for immunocytochemistry and western blot

Antibody	Source	Catalog Number	Dilution
Activated Caspase-3	Promega	G748A	1:500
AFP	Santa Cruz Biotechnology	SC-15375	1:50
BIIITubulin	Covance	PRB-435P	1:100
BRN3	Santa Cruz Biotechnology	SC-6026	1:50
Calretinin	Millipore	AB1550	1:500
CHX10	Santa Cruz Biotechnology	SC-21690	1:200
CRX	Abnova	H00001406-M02	1:100
DLX5	Abcam	Ab64827	1:200
EAAT1	Santa Cruz Biotechnology	SC-515839	1:100
ERK1/2	Santa Cruz Biotechnology	SC-514302	1:500
GFAP	Cell Signaling Technology	D1F4Q	1:200
GFAP	Millipore	MABA360	1:200
GM130	BD Pharmigen	560257	1:50
HuC/D	Life Technologies	A-21271	1:200
ISLET1	Developmental Studies Hybridoma Bank	40.2D6	1:200
LHX2	Santa Cruz Biotechnology	SC-19344	1:200
MAP2	Santa Cruz Biotechnology	SC-20172	1:200
mGluR2	Millipore	MAB397	1:500
MITF	Exalpha	X1405M	1:200
NANOG	R&D Systems	AF1997	1:100

Continued on next page.

Table 6.1.: *continued*

Antibody	**Source**	**Catalog Number**	**Dilution**
Nestin	Santa Cruz Biotechnology	SC-23927	1:10
Neurexin-1	Millipore	ABN161-I	1:1000
OCT4	Stemgent	09-0023	1:200
OPN4	ThermoFisher	PA1-781	1:500
OTX2	R&D Systems	AF1979	1:2000
PAX6	Developmental Studies Hybridoma Bank	PAX6	1:50
RBPMS	PhosphoSolutions	1830-RBPMS	1:500
Recoverin	Chemicon	AB5585	1:2000
RFP	Rockland	600-401-379	1:1500
S100β	Abcam	Ab11178	1:200
SIX6	Sigma-Aldrich	HPA001403	1:200
SMA	Millipore	CBL171	1:100
SNAP25	Millipore	MAB331	1:500
SOX1	R&D Systems	AF3369	1:1000
SOX2	R&D Systems	AF2018	1:1000
SSEA-4	Chemicon	09-0006	1:500
SV2	Developmental Studies Hybridoma Bank	SV2A	1:1000
Synapsin-1	Calbiochem	574777	1:1000
TAU	Santa Cruz Biotechnology	SC-21796	1:50
Tra-1-60	Chemicon	09-0010	1:1000
Tra-1-81	Chemicon	09-0011	1:1000
Vimentin	Santa Cruz Biotechnology	SC-6260	1:100
ZO-1	Zymed	61-7300	1:100

Table 6.2.: Primers used for RT-PCR.

Gene	Forward	Reverse	Size (bp)
alpha-fetoprotein	AGA ACC TGT CAC AAG CTG TG	GAC AGC AAG CTG AGG ATG TC	676
ARRESTIN	ACA AGC TAG GGG ACA ATG CC	TTG TGC TAG AGG CCA GGT TG	597
BEST1	GGT GTG GTT TGC CAA CCT GTC AAT	TGT TCA TCT CGT TCA GCA GGC TCT	92
BRACHYURY	ACC CAG TTC ATA GCG GTG AC	CAA TTG TCA TGG GAT TGC AG	218
BRN3	CTC ACA CTG TCC CAC AAT AAT A	CCG GCG GAA TAT TTC ATT CT	311
CHX10	ATT CAA CGA AGC CCA CTA CCC AGA	ATC CTT GGC TGA CTT GAG GAT GGA	229
CRX	TAT TCT GTC AAC GCC TTG GCC CTA	TGC ATT TAG CCC TCC GGT TCT TGA	253
DLX1	CAA CCA GCA AAT GTC TCC TTC TC	CGC ACT TCA CCG CCT TCC	282
EMX1	AGA CGC AGG TGA AGG TGT GG	CAG GCA GGC AGG CTC TCC	403
ESPN	GCT GGA CGT GCT GAG GT	TGC GAC AGC AGC CAC T	234
EZRIN	ACC ACC ATG GAT GCA GAG CTG GA	ACA CTT CCC GGA GGC CGA TAG T	100
FABP7	AGG CAG GTG GGA AAT GTG AC	CAT AGT GGC GAA CAG CAA CC	298
ISLET1	GTG TGA TCC GGG TCT GGT TT	AAT TAG AGC CCG GTC CTC CT	300
KLF4	AGT CCC GCC GCT CCA TTA CCA A	TGC TCG GTC GCA TTT TTG GCA C	316
LHX2	CAA GAT CTC GGA CCG CTA CT	CCG TGG TCA GCA TCT TGT TA	284
LIN28	AGT GGT TCA ACG TGC GCA TGG G	AGG TCC GGT GAC ACG GAT GGA T	203
MYO7A	CTG GGC TGC TCT GAT CTT G	CAG GGC CAC AAC ATA CTT AGA T	243
NANOG	CAA AGG CAA ACA ACC CAC TT	TCT GCT GGA GGC TGA GGT AT	158
NEUROD1	TAC TGC TGC AAA GTG CAA ATA C	AAG TGC TAA GGC AAC ACA ATA AC	539
NEUROD4	AGG TCT GGG CTC CCA AAA TG	GCC CCG GAG ACT GAT AGT TG	557

Continued on next page.

Table 6.2.: *continued*

Gene	Forward	Reverse	Size (bp)
OCT4	CGA GCA ATT TGC CAA GCT CCT GAA	TTC GGG CAC TGC AGG AAC AAA TTC	324
OPSIN	GAA GTT CAA GAA GCT GCG CC	TCT CAC ATT GCC AAA GGG CT	253
OTOF	GAT ACT CAG GAT GGC CCT A	CAG CTC AGC TCC TCC A	227
OTX2	CAA CAG CAG AAT GGA GGT CA	CTG GGT GGA AAG AGA GAA GC TG	429
PAX6	CGG AGT GAA TCA GCT CGG TG	CCG CTT ATA CTG GGC TAT TTT GC	300 (+5a) 258 (-5a)
PEDF	AGA TCT CAG CTG CAA GAT TGC CCA	ATG AAT GAA CTC GGA GGT GAG GCT	127
RAX	GAA TCT CGA AAT CTC AGC CC	CTT CAC TAA TTT GCT CAG GAC	279
RET	GCA TCA ACG TCC AGT ACA A	CCC TCC ACT GTT ACA AGC	214
RPE65	TAC CAC AGA AGG TTC ATC CGC ACT	GGG AAA GCA CAG GTG CCA AAT TCT	92
RUNX1	TGA CAG CGT TCA GCG A	GCC GTA GTA CAG GTG GTA G	245
SIX3	CGA GCA GAA GAC GCA TTG CTT CAA	CGG CCT TGG CTA TCA TAC ATC ACA	394
SIX6	ATT TGG GAC GGC GAA CAG AAG ACA	ATC CTG GAT GGG CAA CTC AGA TGT	385
SOX1	CAA TGC GGG GAG GAG AAG TC	CTC TGG ACC AAA CTG TGG CG	464
SOX2	CCC CCG GCG GCA ATA GCA	TCG GCG CCG GGG AGA TAC AT	448
SOX10	GGA GGA GCA GGA CCT ATC	TGA GCC CAC ACC ATG A	342
TRANSDUCIN	CAC GAT GCC CAA GGA GAT GT	GGT GGT TGC AGA TGC TGT TG	419

Table 6.3.: Primers used for quantitative RT-PCR.

Gene	**Forward**	**Reverse**	**Size (bp)**
BRN3	AGC GCT CTC ACT TAC CCT TAC ACA	AAA TGG TGC ATC GGT CAT GCT TCC	92
HuC	GCT GAG CCC ATC ACA GTC AA	GCT GGG TCT GAT GGT GTA GG	124
ISLET1	GGG ATC AAA TGC GCC AAG TG	GTG ATA CAC CTT GGA GCG GG	78
MATH5	ACT GCC TTC GAC CGC TTA C	CTG CAG GGT CTC GTA CTT GG	78
OPN4	ACA CGT CCT GAC ACC CTA CA	GCA ATG GCC ACC CTG TAC TT	88
PAX6	AGT GAA TCA GCT CGG TGG TGT CTT	TGC AGA ATT CGG GAA ATG TCG CAC	96
RBPMS	GCC TGC ACT TTA CCC CAG TA	AAG CGG GAT AGG TGA AAG CA	104
SIX6	GCC TGC ACT TTA CCC CAG TA	AAG CGG GAT AGG TGA AAG CA	104
SNCG	TGG GTG CGG TGG AAA AGA C	TTC TCG GCC ACT GAG GTC AC	127

REFERENCES

REFERENCES

[1] K. Mohan, H. Kecova, E. Hernandez-Merino, R. H. Kardon, and M. M. Harper, "Retinal ganglion cell damage in an experimental rodent model of blast-mediated traumatic brain injury," *Invest Ophthalmol Vis Sci*, vol. 54, no. 5, pp. 3440–3450, 2013.

[2] Y. You, V. K. Gupta, J. C. Li, A. Klistorner, and S. L. Graham, "Optic neuropathies: characteristic features and mechanisms of retinal ganglion cell loss," *Rev Neurosci*, vol. 24, no. 3, pp. 301–321, 2013.

[3] R. N. Weinreb and P. T. Khaw, "Primary open-angle glaucoma," *Lancet*, vol. 363, no. 9422, pp. 1711–1720, 2004.

[4] R. S. Harwerth, J. L. Wheat, M. J. Fredette, and D. R. Anderson, "Linking structure and function in glaucoma," *Prog Retin Eye Res*, vol. 29, no. 4, pp. 249–271, 2010.

[5] J. A. Thomson, J. Itskovitz-Eldor, S. S. Shapiro, M. A. Waknitz, J. J. Swiergiel, V. S. Marshall, and J. M. Jones, "Embryonic stem cell lines derived from human blastocysts," *Science*, vol. 282, no. 5391, pp. 1145–1147, 1998.

[6] K. Takahashi, K. Tanabe, M. Ohnuki, M. Narita, T. Ichisaka, K. Tomoda, and S. Yamanaka, "Induction of pluripotent stem cells from adult human fibroblasts by defined factors," *Cell*, vol. 131, no. 5, pp. 861–872, 2007.

[7] C. L. Cepko, C. P. Austin, X. Yang, M. Alexiades, and D. Ezzeddine, "Cell fate determination in the vertebrate retina," *Proc Natl Acad Sci U S A*, vol. 93, no. 2, pp. 589–595, 1996.

[8] Y. Hirami, F. Osakada, K. Takahashi, K. Okita, S. Yamanaka, H. Ikeda, N. Yoshimura, and M. Takahashi, "Generation of retinal cells from mouse and human induced pluripotent stem cells," *Neurosci Lett*, vol. 458, no. 3, pp. 126–131, 2009.

[9] M. Eiraku, N. Takata, H. Ishibashi, M. Kawada, E. Sakakura, S. Okuda, K. Sekiguchi, T. Adachi, and Y. Sasai, "Self-organizing optic-cup morphogenesis in three-dimensional culture," *Nature*, vol. 472, no. 7341, pp. 51–56, 2011.

[10] J. S. Meyer, S. E. Howden, K. A. Wallace, A. D. Verhoeven, L. S. Wright, E. E. Capowski, I. Pinilla, J. M. Martin, S. Tian, R. Stewart, B. Pattnaik, J. A. Thomson, and D. M. Gamm, "Optic vesicle-like structures derived from human pluripotent stem cells facilitate a customized approach to retinal disease treatment," *Stem Cells*, vol. 29, no. 8, pp. 1206–1218, 2011.

[11] T. Nakano, S. Ando, N. Takata, M. Kawada, K. Muguruma, K. Sekiguchi, K. Saito, S. Yonemura, M. Eiraku, and Y. Sasai, "Self-formation of optic cups and storable stratified neural retina from human ESCs," *Cell Stem Cell*, vol. 10, no. 6, pp. 771–785, 2012.

[12] S. K. Ohlemacher, C. L. Iglesias, A. Sridhar, D. M. Gamm, and J. S. Meyer, "Generation of highly enriched populations of optic vesicle-like retinal cells from human pluripotent stem cells," *Curr Protoc Stem Cell Biol*, vol. 32, pp. 1h.8.1–1h.8.20, 2015.

[13] S. K. Ohlemacher, A. Sridhar, Y. Xiao, A. E. Hochstetler, M. Sarfarazi, T. R. Cummins, and J. S. Meyer, "Stepwise Differentiation of Retinal Ganglion Cells from Human Pluripotent Stem Cells Enables Analysis of Glaucomatous Neurodegeneration," *Stem Cells*, vol. 34, no. 6, pp. 1553–1562, 2016.

[14] E. Herrera, L. Erskine, and C. Morenilla-Palao, "Guidance of retinal axons in mammals," *Semin Cell Dev Biol*, 2017.

[15] E. M. Martersteck, K. E. Hirokawa, M. Evarts, A. Bernard, X. Duan, Y. Li, L. Ng, S. W. Oh, B. Ouellette, J. J. Royall, M. Stoecklin, Q. Wang, H. Zeng, J. R. Sanes, and J. A. Harris, "Diverse Central Projection Patterns of Retinal Ganglion Cells," *Cell Rep*, vol. 18, no. 8, pp. 2058–2072, 2017.

[16] H. Kolb, R. Nelson, and A. Mariani, "Amacrine cells, bipolar cells and ganglion cells of the cat retina: a Golgi study," *Vision Res*, vol. 21, no. 7, pp. 1081–1114, 1981.

[17] B. Volgyi, S. Chheda, and S. A. Bloomfield, "Tracer coupling patterns of the ganglion cell subtypes in the mouse retina," *J Comp Neurol*, vol. 512, no. 5, pp. 664–687, 2009.

[18] R. Hebel and H. Hollander, "Size and distribution of ganglion cells in the human retina," *Anat Embryol (Berl)*, vol. 168, no. 1, pp. 125–136, 1983.

[19] M. Watanabe and R. W. Rodieck, "Parasol and midget ganglion cells of the primate retina," *J Comp Neurol*, vol. 289, no. 3, pp. 434–454, 1989.

[20] H. Riazifar, Y. Jia, J. Chen, G. Lynch, and T. Huang, "Chemically induced specification of retinal ganglion cells from human embryonic and induced pluripotent stem cells," *Stem Cells Transl Med*, vol. 3, no. 4, pp. 424–432, 2014.

[21] V. M. Sluch, C. H. Davis, V. Ranganathan, J. M. Kerr, K. Krick, R. Martin, C. A. Berlinicke, N. Marsh-Armstrong, J. S. Diamond, H. Q. Mao, and D. J. Zack, "Differentiation of human ESCs to retinal ganglion cells using a CRISPR engineered reporter cell line," *Sci Rep*, vol. 5, p. 16595, 2015.

[22] T. Tanaka, T. Yokoi, F. Tamalu, S. Watanabe, S. Nishina, and N. Azuma, "Generation of retinal ganglion cells with functional axons from human induced pluripotent stem cells," *Sci Rep*, vol. 5, p. 8344, 2015.

[23] Y. Maekawa, A. Onishi, K. Matsushita, N. Koide, M. Mandai, K. Suzuma, T. Kitaoka, A. Kuwahara, C. Ozone, T. Nakano, M. Eiraku, and M. Takahashi, "Optimized Culture System to Induce Neurite Outgrowth From Retinal Ganglion Cells in Three-Dimensional Retinal Aggregates Differentiated From Mouse and Human Embryonic Stem Cells," *Curr Eye Res*, vol. 41, no. 4, pp. 558–568, 2016.

[24] V. M. Sluch, X. Chamling, M. M. Liu, C. A. Berlinicke, J. Cheng, K. L. Mitchell, D. S. Welsbie, and D. J. Zack, "Enhanced Stem Cell Differentiation and Immunopurification of Genome Engineered Human Retinal Ganglion Cells," *Stem Cells Transl Med*, vol. 6, no. 11, pp. 1972–1986, 2017.

[25] P. Teotia, M. J. Van Hook, and I. Ahmad, "A Co-culture Model for Determining the Target Specificity of the de novo Generated Retinal Ganglion Cells," *Bio Protoc*, vol. 7, no. 7, 2017.

[26] P. Teotia, M. J. Van Hook, C. S. Wichman, R. R. Allingham, M. A. Hauser, and I. Ahmad, "Modeling Glaucoma: Retinal Ganglion Cells Generated from Induced Pluripotent Stem Cells of Patients with SIX6 Risk Allele Show Developmental Abnormalities," *Stem Cells*, vol. 35, no. 11, pp. 2239–2252, 2017.

[27] J. E. Dowling and B. B. Boycott, "Organization of the primate retina: electron microscopy," *Proc R Soc Lond B Biol Sci*, vol. 166, no. 1002, pp. 80–111, 1966.

[28] J. E. Dowling, "Organization of vertebrate retinas," *Invest Ophthalmol*, vol. 9, no. 9, pp. 655–680, 1970.

[29] C. A. Curcio and K. A. Allen, "Topography of ganglion cells in human retina," *J Comp Neurol*, vol. 300, no. 1, pp. 5–25, 1990.

[30] X. Zhong, C. Gutierrez, T. Xue, C. Hampton, M. N. Vergara, L. H. Cao, A. Peters, T. S. Park, E. T. Zambidis, J. S. Meyer, D. M. Gamm, K. W. Yau, and M. V. Canto-Soler, "Generation of three-dimensional retinal tissue with functional photoreceptors from human iPSCs," *Nat Commun*, vol. 5, p. 4047, 2014.

[31] T. J. Velte and R. H. Masland, "Action potentials in the dendrites of retinal ganglion cells," *J Neurophysiol*, vol. 81, no. 3, pp. 1412–1417, 1999.

[32] D. A. Lamba, M. O. Karl, C. B. Ware, and T. A. Reh, "Efficient generation of retinal progenitor cells from human embryonic stem cells," *Proc Natl Acad Sci U S A*, vol. 103, no. 34, pp. 12 769–12 774, 2006.

[33] K. F. Sullivan and D. W. Cleveland, "Identification of conserved isotype-defining variable region sequences for four vertebrate beta tubulin polypeptide classes," *Proc Natl Acad Sci U S A*, vol. 83, no. 12, pp. 4327–4331, 1986.

[34] R. K. Sharma and P. A. Netland, "Early born lineage of retinal neurons express class III beta-tubulin isotype," *Brain Res*, vol. 1176, pp. 11–17, 2007.

[35] M. Xiang, L. Zhou, J. P. Macke, T. Yoshioka, S. H. Hendry, R. L. Eddy, T. B. Shows, and J. Nathans, "The Brn-3 family of POU-domain factors: primary structure, binding specificity, and expression in subsets of retinal ganglion cells and somatosensory neurons," *J Neurosci*, vol. 15, no. 7 Pt 1, pp. 4762–4785, 1995.

[36] L. Erkman, R. J. McEvilly, L. Luo, A. K. Ryan, F. Hooshmand, S. M. O'Connell, E. M. Keithley, D. H. Rapaport, A. F. Ryan, and M. G. Rosenfeld, "Role of transcription factors Brn-3.1 and Brn-3.2 in auditory and visual system development," *Nature*, vol. 381, no. 6583, pp. 603–606, 1996.

[37] L. Gan, M. Xiang, L. Zhou, D. S. Wagner, W. H. Klein, and J. Nathans, "POU domain factor Brn-3b is required for the development of a large set of retinal ganglion cells," *Proc Natl Acad Sci U S A*, vol. 93, no. 9, pp. 3920–3925, 1996.

[38] F. M. Nadal-Nicolas, M. Jimenez-Lopez, P. Sobrado-Calvo, L. Nieto-Lopez, I. Canovas-Martinez, M. Salinas-Navarro, M. Vidal-Sanz, and M. Agudo, "Brn3a as a marker of retinal ganglion cells: qualitative and quantitative time course studies in naive and optic nerve-injured retinas," *Invest Ophthalmol Vis Sci*, vol. 50, no. 8, pp. 3860–3868, 2009.

[39] S. M. Chambers, Y. Qi, Y. Mica, G. Lee, X. J. Zhang, L. Niu, J. Bilsland, L. Cao, E. Stevens, P. Whiting, S. H. Shi, and L. Studer, "Combined small-molecule inhibition accelerates developmental timing and converts human pluripotent stem cells into nociceptors," *Nat Biotechnol*, vol. 30, no. 7, pp. 715–720, 2012.

[40] K. R. Koehler, A. M. Mikosz, A. I. Molosh, D. Patel, and E. Hashino, "Generation of inner ear sensory epithelia from pluripotent stem cells in 3D culture," *Nature*, vol. 500, no. 7461, pp. 217–221, 2013.

[41] J. Ericson, S. Thor, T. Edlund, T. M. Jessell, and T. Yamada, "Early stages of motor neuron differentiation revealed by expression of homeobox gene Islet-1," *Science*, vol. 256, no. 5063, pp. 1555–1560, 1992.

[42] R. J. Phillips, S. L. Hargrave, B. S. Rhodes, D. A. Zopf, and T. L. Powley, "Quantification of neurons in the myenteric plexus: an evaluation of putative pan-neuronal markers," *J Neurosci Methods*, vol. 133, no. 1-2, pp. 99–107, 2004.

[43] T. C. Schulz, S. A. Noggle, G. M. Palmarini, D. A. Weiler, I. G. Lyons, K. A. Pensa, A. C. Meedeniya, B. P. Davidson, N. A. Lambert, and B. G. Condie, "Differentiation of human embryonic stem cells to dopaminergic neurons in serum-free suspension culture," *Stem Cells*, vol. 22, no. 7, pp. 1218–1238, 2004.

[44] R. Genead, C. Danielsson, A. B. Andersson, M. Corbascio, A. Franco-Cereceda, C. Sylven, and K. H. Grinnemo, "Islet-1 cells are cardiac progenitors present during the entire lifespan: from the embryonic stage to adulthood," *Stem Cells Dev*, vol. 19, no. 10, pp. 1601–1615, 2010.

[45] H. N. Nguyen, B. Byers, B. Cord, A. Shcheglovitov, J. Byrne, P. Gujar, K. Kee, B. Schule, R. E. Dolmetsch, W. Langston, T. D. Palmer, and R. R. Pera, "LRRK2 mutant iPSC-derived DA neurons demonstrate increased susceptibility to oxidative stress," *Cell Stem Cell*, vol. 8, no. 3, pp. 267–280, 2011.

[46] J. F. Poulin, J. Zou, J. Drouin-Ouellet, K. Y. Kim, F. Cicchetti, and R. B. Awatramani, "Defining midbrain dopaminergic neuron diversity by single-cell gene expression profiling," *Cell Rep*, vol. 9, no. 3, pp. 930–943, 2014.

[47] A. R. Rodriguez, L. P. de Sevilla Muller, and N. C. Brecha, "The RNA binding protein RBPMS is a selective marker of ganglion cells in the mammalian retina," *J Comp Neurol*, vol. 522, no. 6, pp. 1411–1443, 2014.

[48] T. M. Schmidt and P. Kofuji, "Structure and function of bistratified intrinsically photosensitive retinal ganglion cells in the mouse," *J Comp Neurol*, vol. 519, no. 8, pp. 1492–1504, 2011.

[49] V. Jain, E. Ravindran, and N. K. Dhingra, "Differential expression of Brn3 transcription factors in intrinsically photosensitive retinal ganglion cells in mouse," *J Comp Neurol*, vol. 520, no. 4, pp. 742–755, 2012.

[50] K. B. Langer, S. K. Ohlemacher, M. J. Phillips, C. M. Fligor, P. Jiang, D. M. Gamm, and J. S. Meyer, "Retinal Ganglion Cell Diversity and Subtype Specification from Human Pluripotent Stem Cells," *Stem Cell Reports*, 2018.

[51] M. Grskovic, A. Javaherian, B. Strulovici, and G. Q. Daley, "Induced pluripotent stem cells–opportunities for disease modelling and drug discovery," *Nat Rev Drug Discov*, vol. 10, no. 12, pp. 915–929, 2011.

[52] A. D. Ebert and C. N. Svendsen, "Human stem cells and drug screening: opportunities and challenges," *Nat Rev Drug Discov*, vol. 9, no. 5, pp. 367–372, 2010.

[53] J. S. Meyer, R. L. Shearer, E. E. Capowski, L. S. Wright, K. A. Wallace, E. L. McMillan, S. C. Zhang, and D. M. Gamm, "Modeling early retinal development with human embryonic and induced pluripotent stem cells," *Proc Natl Acad Sci U S A*, vol. 106, no. 39, pp. 16 698–16 703, 2009.

[54] B. A. Tucker, F. Solivan-Timpe, B. R. Roos, K. R. Anfinson, A. L. Robin, L. A. Wiley, R. F. Mullins, and J. H. Fingert, "Duplication of TBK1 Stimulates Autophagy in iPSC-derived Retinal Cells from a Patient with Normal Tension Glaucoma," *J Stem Cell Res Ther*, vol. 3, no. 5, p. 161, 2014.

[55] I. Ferrer, A. Martinez, S. Boluda, P. Parchi, and M. Barrachina, "Brain banks: benefits, limitations and cautions concerning the use of post-mortem brain tissue for molecular studies," *Cell Tissue Bank*, vol. 9, no. 3, pp. 181–194, 2008.

[56] Y. C. Tham, X. Li, T. Y. Wong, H. A. Quigley, T. Aung, and C. Y. Cheng, "Global prevalence of glaucoma and projections of glaucoma burden through 2040: a systematic review and meta-analysis," *Ophthalmology*, vol. 121, no. 11, pp. 2081–2090, 2014.

[57] R. D. Fechtner and R. N. Weinreb, "Mechanisms of optic nerve damage in primary open angle glaucoma," *Surv Ophthalmol*, vol. 39, no. 1, pp. 23–42, 1994.

[58] R. N. Weinreb, T. Aung, and F. A. Medeiros, "The pathophysiology and treatment of glaucoma: a review," *Jama*, vol. 311, no. 18, pp. 1901–1911, 2014.

[59] H. A. Quigley, "New paradigms in the mechanisms and management of glaucoma," *Eye (Lond)*, vol. 19, no. 12, pp. 1241–1248, 2005.

[60] H. A. Quigley, R. W. Nickells, L. A. Kerrigan, M. E. Pease, D. J. Thibault, and D. J. Zack, "Retinal ganglion cell death in experimental glaucoma and after axotomy occurs by apoptosis," *Invest Ophthalmol Vis Sci*, vol. 36, no. 5, pp. 774–786, 1995.

[61] M. C. Marchetto, K. J. Brennand, L. F. Boyer, and F. H. Gage, "Induced pluripotent stem cells (iPSCs) and neurological disease modeling: progress and promises," *Hum Mol Genet*, vol. 20, no. R2, pp. R109–15, 2011.

[62] R. C. B. Wong, S. Y. Lim, S. S. C. Hung, S. Jackson, S. Khan, N. J. Van Bergen, E. De Smit, H. H. Liang, L. S. Kearns, L. Clarke, D. A. Mackey, A. W. Hewitt, I. A. Trounce, and A. Pebay, "Mitochondrial replacement in an iPSC model of Leber's hereditary optic neuropathy," *Aging (Albany NY)*, vol. 9, no. 4, pp. 1341–1350, 2017.

[63] Y. Kitazawa and T. Horie, "Diurnal variation of intraocular pressure in primary open-angle glaucoma," *Am J Ophthalmol*, vol. 79, no. 4, pp. 557–566, 1975.

[64] S. C. Sacca, M. Rolando, A. Marletta, A. Macri, P. Cerqueti, and G. Ciurlo, "Fluctuations of intraocular pressure during the day in open-angle glaucoma, normal-tension glaucoma and normal subjects," *Ophthalmologica*, vol. 212, no. 2, pp. 115–119, 1998.

[65] S. Williams, "Genetic mutations you want," *Proc Natl Acad Sci U S A*, vol. 5, no. 4, p. E2093, 2014.

[66] N. Shanks, R. Greek, and J. Greek, "Are animal models predictive for humans?" *Philos Ethics Humanit Med*, vol. 4, p. 2, 2009.

[67] R. Greek and N. Shanks, "Complex systems, evolution, and animal models," *Stud Hist Philos Biol Biomed Sci*, vol. 42, no. 4, pp. 542–544, 2011.

[68] H. Inoue and S. Yamanaka, "The use of induced pluripotent stem cells in drug development," *Clin Pharmacol Ther*, vol. 89, no. 5, pp. 655–661, 2011.

[69] D. S. Welsbie, K. L. Mitchell, V. Jaskula-Ranga, V. M. Sluch, Z. Yang, J. Kim, E. Buehler, A. Patel, S. E. Martin, P. W. Zhang, Y. Ge, Y. Duan, J. Fuller, B. J. Kim, E. Hamed, X. Chamling, L. Lei, I. D. C. Fraser, Z. A. Ronai, C. A. Berlinicke, and D. J. Zack, "Enhanced Functional Genomic Screening Identifies Novel Mediators of Dual Leucine Zipper Kinase-Dependent Injury Signaling in Neurons," *Neuron*, vol. 94, no. 6, pp. 1142–1154.e6, 2017.

[70] J. Assawachananont, M. Mandai, S. Okamoto, C. Yamada, M. Eiraku, S. Yonemura, Y. Sasai, and M. Takahashi, "Transplantation of embryonic and induced pluripotent stem cell-derived 3D retinal sheets into retinal degenerative mice," *Stem Cell Reports*, vol. 2, no. 5, pp. 662–674, 2014.

[71] H. Shirai, M. Mandai, K. Matsushita, A. Kuwahara, S. Yonemura, T. Nakano, J. Assawachananont, T. Kimura, K. Saito, H. Terasaki, M. Eiraku, Y. Sasai, and M. Takahashi, "Transplantation of human embryonic stem cell-derived retinal tissue in two primate models of retinal degeneration," *Proc Natl Acad Sci U S A*, vol. 113, no. 1, pp. E81–90, 2016.

[72] C. Jiang, H. Klassen, X. Zhang, and M. Young, "Laser injury promotes migration and integration of retinal progenitor cells into host retina," *Mol Vis*, vol. 16, pp. 983–990, 2010.

[73] J. R. Chao, D. A. Lamba, T. R. Klesert, A. Torre, A. Hoshino, R. J. Taylor, A. Jayabalu, A. L. Engel, T. H. Khuu, R. K. Wang, M. Neitz, J. Neitz, and T. A. Reh, "Transplantation of Human Embryonic Stem Cell-Derived Retinal Cells into the Subretinal Space of a Non-Human Primate," *Transl Vis Sci Technol*, vol. 6, no. 3, p. 4, 2017.

[74] J. Hertz, B. Qu, Y. Hu, R. D. Patel, D. A. Valenzuela, and J. L. Goldberg, "Survival and integration of developing and progenitor-derived retinal ganglion cells following transplantation," *Cell Transplant*, vol. 23, no. 7, pp. 855–872, 2014.

[75] D. E. Buchholz, B. O. Pennington, R. H. Croze, C. R. Hinman, P. J. Coffey, and D. O. Clegg, "Rapid and efficient directed differentiation of human pluripotent stem cells into retinal pigmented epithelium," *Stem Cells Transl Med*, vol. 2, no. 5, pp. 384–393, 2013.

[76] A. J. Carr, A. A. Vugler, S. T. Hikita, J. M. Lawrence, C. Gias, L. L. Chen, D. E. Buchholz, A. Ahmado, M. Semo, M. J. Smart, S. Hasan, L. da Cruz, L. V. Johnson, D. O. Clegg, and P. J. Coffey, "Protective effects of human iPS-derived retinal pigment epithelium cell transplantation in the retinal dystrophic rat," *PLoS One*, vol. 4, no. 12, p. e8152, 2009.

[77] D. A. Lamba, A. McUsic, R. K. Hirata, P. R. Wang, D. Russell, and T. A. Reh, "Generation, purification and transplantation of photoreceptors derived from human induced pluripotent stem cells," *PLoS One*, vol. 5, no. 1, p. e8763, 2010.

[78] F. Osakada, H. Ikeda, M. Mandai, T. Wataya, K. Watanabe, N. Yoshimura, A. Akaike, Y. Sasai, and M. Takahashi, "Toward the generation of rod and cone photoreceptors from mouse, monkey and human embryonic stem cells," *Nat Biotechnol*, vol. 26, no. 2, pp. 215–224, 2008.

[79] D. M. Gamm and J. S. Meyer, "Directed differentiation of human induced pluripotent stem cells: a retina perspective," *Regen Med*, vol. 5, no. 3, pp. 315–317, 2010.

[80] A. Sridhar, M. M. Steward, and J. S. Meyer, "Nonxenogeneic growth and retinal differentiation of human induced pluripotent stem cells," *Stem Cells Transl Med*, vol. 2, no. 4, pp. 255–264, 2013.

[81] Z. B. Jin, S. Okamoto, P. Xiang, and M. Takahashi, "Integration-free induced pluripotent stem cells derived from retinitis pigmentosa patient for disease modeling," *Stem Cells Transl Med*, vol. 1, no. 6, pp. 503–509, 2012.

[82] R. Singh, W. Shen, D. Kuai, J. M. Martin, X. Guo, M. A. Smith, E. T. Perez, M. J. Phillips, J. M. Simonett, K. A. Wallace, A. D. Verhoeven, E. E. Capowski, X. Zhang, Y. Yin, P. J. Halbach, G. A. Fishman, L. S. Wright, B. R. Pattnaik, and D. M. Gamm, "iPS cell modeling of Best disease: insights into the pathophysiology of an inherited macular degeneration," *Hum Mol Genet*, vol. 22, no. 3, pp. 593–607, 2013.

[83] K. J. Wahlin, J. Maruotti, and D. J. Zack, "Modeling retinal dystrophies using patient-derived induced pluripotent stem cells," *Adv Exp Med Biol*, vol. 801, pp. 157–164, 2014.

[84] L. S. Wright, M. J. Phillips, I. Pinilla, D. Hei, and D. M. Gamm, "Induced pluripotent stem cells as custom therapeutics for retinal repair: progress and rationale," *Exp Eye Res*, vol. 123, pp. 161–172, 2014.

[85] S. Al-Shamekh and J. L. Goldberg, "Retinal repair with induced pluripotent stem cells," *Transl Res*, vol. 163, no. 4, pp. 377–386, 2014.

[86] J. Stern and S. Temple, "Stem cells for retinal repair," *Dev Ophthalmol*, vol. 53, pp. 70–80, 2014.

[87] T. E. Ludwig, V. Bergendahl, M. E. Levenstein, J. Yu, M. D. Probasco, and J. A. Thomson, "Feeder-independent culture of human embryonic stem cells," *Nat Methods*, vol. 3, no. 8, pp. 637–646, 2006.

[88] J. Yu, M. A. Vodyanik, K. Smuga-Otto, J. Antosiewicz-Bourget, J. L. Frane, S. Tian, J. Nie, G. A. Jonsdottir, V. Ruotti, R. Stewart, Slukvin II, and J. A. Thomson, "Induced pluripotent stem cell lines derived from human somatic cells," *Science*, vol. 318, no. 5858, pp. 1917–1920, 2007.

[89] F. J. Livesey and C. L. Cepko, "Vertebrate neural cell-fate determination: lessons from the retina," *Nat Rev Neurosci*, vol. 2, no. 2, pp. 109–118, 2001.

[90] T. Marquardt and P. Gruss, "Generating neuronal diversity in the retina: one for nearly all," *Trends Neurosci*, vol. 25, no. 1, pp. 32–38, 2002.

[91] G. Oliver and P. Gruss, "Current views on eye development," *Trends Neurosci*, vol. 20, no. 9, pp. 415–421, 1997.

[92] S. S. Zhang, X. Y. Fu, and C. J. Barnstable, "Molecular aspects of vertebrate retinal development," *Mol Neurobiol*, vol. 26, no. 2-3, pp. 137–152, 2002.

[93] S. Fuhrmann, E. M. Levine, and T. A. Reh, "Extraocular mesenchyme patterns the optic vesicle during early eye development in the embryonic chick," *Development*, vol. 127, no. 21, pp. 4599–4609, 2000.

[94] J. R. Martinez-Morales, V. Dolez, I. Rodrigo, R. Zaccarini, L. Leconte, P. Bovolenta, and S. Saule, "OTX2 activates the molecular network underlying retina pigment epithelium differentiation," *J Biol Chem*, vol. 278, no. 24, pp. 21 721–21 731, 2003.

[95] S. Shibahara, K. Yasumoto, S. Amae, T. Udono, K. Watanabe, H. Saito, and K. Takeda, "Regulation of pigment cell-specific gene expression by MITF," *Pigment Cell Res*, vol. 13 Suppl 8, pp. 98–102, 2000.

[96] E. E. Capowski, J. M. Simonett, E. M. Clark, L. S. Wright, S. E. Howden, K. A. Wallace, A. M. Petelinsek, I. Pinilla, M. J. Phillips, J. S. Meyer, B. L. Schneider, J. A. Thomson, and D. M. Gamm, "Loss of MITF expression during human embryonic stem cell differentiation disrupts retinal pigment epithelium development and optic vesicle cell proliferation," *Hum Mol Genet*, 2014.

[97] D. E. Buchholz, S. T. Hikita, T. J. Rowland, A. M. Friedrich, C. R. Hinman, L. V. Johnson, and D. O. Clegg, "Derivation of functional retinal pigmented epithelium from induced pluripotent stem cells," *Stem Cells*, vol. 27, no. 10, pp. 2427–2434, 2009.

[98] M. Ferrer, B. Corneo, J. Davis, Q. Wan, K. J. Miyagishima, R. King, A. Maminishkis, J. Marugan, R. Sharma, M. Shure, S. Temple, S. Miller, and K. Bharti, "A Multiplex High-Throughput Gene Expression Assay to Simultaneously Detect Disease and Functional Markers in Induced Pluripotent Stem Cell-Derived Retinal Pigment Epithelium," *Stem Cells Transl Med*, vol. 3, no. 8, pp. 911–922, 2014.

[99] J. L. Liao, J. Yu, K. Huang, J. Hu, T. Diemer, Z. Ma, T. Dvash, X. J. Yang, G. H. Travis, D. S. Williams, D. Bok, and G. Fan, "Molecular signature of primary retinal pigment epithelium and stem-cell-derived RPE cells," *Hum Mol Genet*, vol. 19, no. 21, pp. 4229–4238, 2010.

[100] J. Maruotti, K. Wahlin, D. Gorrell, I. Bhutto, G. Lutty, and D. J. Zack, "A simple and scalable process for the differentiation of retinal pigment epithelium from human pluripotent stem cells," *Stem Cells Transl Med*, vol. 2, no. 5, pp. 341–354, 2013.

[101] T. J. Rowland, A. J. Blaschke, D. E. Buchholz, S. T. Hikita, L. V. Johnson, and D. O. Clegg, "Differentiation of human pluripotent stem cells to retinal pigmented epithelium in defined conditions using purified extracellular matrix proteins," *J Tissue Eng Regen Med*, vol. 7, no. 8, pp. 642–653, 2013.

[102] A. Vugler, A. J. Carr, J. Lawrence, L. L. Chen, K. Burrell, A. Wright, P. Lundh, M. Semo, A. Ahmado, C. Gias, L. da Cruz, H. Moore, P. Andrews, J. Walsh, and P. Coffey, "Elucidating the phenomenon of HESC-derived RPE: anatomy of cell genesis, expansion and retinal transplantation," *Exp Neurol*, vol. 214, no. 2, pp. 347–361, 2008.

[103] T. Belecky-Adams, S. Tomarev, H. S. Li, L. Ploder, R. R. McInnes, O. Sundin, and R. Adler, "Pax-6, Prox 1, and Chx10 homeobox gene expression correlates with phenotypic fate of retinal precursor cells," *Invest Ophthalmol Vis Sci*, vol. 38, no. 7, pp. 1293–1303, 1997.

[104] K. Bharti, W. Liu, T. Csermely, S. Bertuzzi, and H. Arnheiter, "Alternative promoter use in eye development: the complex role and regulation of the transcription factor MITF," *Development*, vol. 135, no. 6, pp. 1169–1178, 2008.

[105] D. J. Horsford, M. T. Nguyen, G. C. Sellar, R. Kothary, H. Arnheiter, and R. R. McInnes, "Chx10 repression of Mitf is required for the maintenance of mammalian neuroretinal identity," *Development*, vol. 132, no. 1, pp. 177–187, 2005.

[106] S. Rowan, C. M. Chen, T. L. Young, D. E. Fisher, and C. L. Cepko, "Transdifferentiation of the retina into pigmented cells in ocular retardation mice defines a new function of the homeodomain gene Chx10," *Development*, vol. 131, no. 20, pp. 5139–5152, 2004.

[107] M. J. Phillips, E. T. Perez, J. M. Martin, S. T. Reshel, K. A. Wallace, E. E. Capowski, R. Singh, L. S. Wright, E. M. Clark, P. M. Barney, R. Stewart, S. J. Dickerson, M. J. Miller, E. F. Percin, J. A. Thomson, and D. M. Gamm, "Modeling human retinal development with patient-specific induced pluripotent stem cells reveals multiple roles for visual system homeobox 2," *Stem Cells*, vol. 32, no. 6, pp. 1480–1492, 2014.

[108] P. Srinivasan, I. K. Zervantonakis, and C. R. Kothapalli, "Synergistic effects of 3D ECM and chemogradients on neurite outgrowth and guidance: a simple modeling and microfluidic framework," *PLoS One*, vol. 9, no. 6, p. e99640, 2014.

[109] T. C. Badea and J. Nathans, "Morphologies of mouse retinal ganglion cells expressing transcription factors Brn3a, Brn3b, and Brn3c: analysis of wild type and mutant cells using genetically-directed sparse labeling," *Vision Res*, vol. 51, no. 2, pp. 269–279, 2011.

[110] J. Bryant, R. J. Goodyear, and G. P. Richardson, "Sensory organ development in the inner ear: molecular and cellular mechanisms," *Br Med Bull*, vol. 63, pp. 39–57, 2002.

[111] M. Shi, S. R. Kumar, O. Motajo, F. Kretschmer, X. Mu, and T. C. Badea, "Genetic interactions between Brn3 transcription factors in retinal ganglion cell type specification," *PLoS One*, vol. 8, no. 10, p. e76347, 2013.

[112] J. Weir, M. Rivolta, and M. Holley, "Identification of differentiating cochlear hair cells in vitro," *Am J Otol*, vol. 21, no. 1, pp. 130–134, 2000.

[113] T. C. Badea, J. Williams, P. Smallwood, M. Shi, O. Motajo, and J. Nathans, "Combinatorial expression of Brn3 transcription factors in somatosensory neurons: genetic and morphologic analysis," *J Neurosci*, vol. 32, no. 3, pp. 995–1007, 2012.

[114] M. J. Phillips, K. A. Wallace, S. J. Dickerson, M. J. Miller, A. D. Verhoeven, J. M. Martin, L. S. Wright, W. Shen, E. E. Capowski, E. F. Percin, E. T. Perez, X. Zhong, M. V. Canto-Soler, and D. M. Gamm, "Blood-derived human iPS cells generate optic vesicle-like structures with the capacity to form retinal laminae and develop synapses," *Invest Ophthalmol Vis Sci*, vol. 53, no. 4, pp. 2007–2019, 2012.

[115] G. Keller, "Embryonic stem cell differentiation: emergence of a new era in biology and medicine," *Genes Dev*, vol. 19, no. 10, pp. 1129–1155, 2005.

[116] M. F. Pera and A. O. Trounson, "Human embryonic stem cells: prospects for development," *Development*, vol. 131, no. 22, pp. 5515–5525, 2004.

[117] K. J. Brennand, A. Simone, N. Tran, and F. H. Gage, "Modeling psychiatric disorders at the cellular and network levels," *Mol Psychiatry*, vol. 17, no. 12, pp. 1239–1253, 2012.

[118] V. B. Mattis, C. Tom, S. Akimov, J. Saeedian, M. E. Ostergaard, A. L. Southwell, C. N. Doty, L. Ornelas, A. Sahabian, L. Lenaeus, B. Mandefro, D. Sareen, J. Arjomand, M. R. Hayden, C. A. Ross, and C. N. Svendsen, "HD iPSC-derived neural progenitors accumulate in culture and are susceptible to BDNF withdrawal due to glutamate toxicity," *Hum Mol Genet*, vol. 24, no. 11, pp. 3257–3271, 2015.

[119] T. Yoshida, Y. Ozawa, K. Suzuki, K. Yuki, M. Ohyama, W. Akamatsu, Y. Matsuzaki, S. Shimmura, K. Mitani, K. Tsubota, and H. Okano, "The use of induced pluripotent stem cells to reveal pathogenic gene mutations and explore treatments for retinitis pigmentosa," *Mol Brain*, vol. 7, p. 45, 2014.

[120] Z. B. Jin, S. Okamoto, F. Osakada, K. Homma, J. Assawachananont, Y. Hirami, T. Iwata, and M. Takahashi, "Modeling retinal degeneration using patient-specific induced pluripotent stem cells," *PLoS One*, vol. 6, no. 2, p. e17084, 2011.

[121] N. Schwarz, A. J. Carr, A. Lane, F. Moeller, L. L. Chen, M. Aguila, B. Nommiste, M. N. Muthiah, N. Kanuga, U. Wolfrum, K. Nagel-Wolfrum, L. da Cruz, P. J. Coffey, M. E. Cheetham, and A. J. Hardcastle, "Translational read-through of the RP2 Arg120stop mutation in patient iPSC-derived retinal pigment epithelium cells," *Hum Mol Genet*, vol. 24, no. 4, pp. 972–986, 2015.

[122] E. R. Burnight, L. A. Wiley, A. V. Drack, T. A. Braun, K. R. Anfinson, E. E. Kaalberg, J. A. Halder, L. M. Affatigato, R. F. Mullins, E. M. Stone, and B. A. Tucker, "CEP290 gene transfer rescues Leber congenital amaurosis cellular phenotype," *Gene Ther*, vol. 21, no. 7, pp. 662–672, 2014.

[123] C. B. Mellough, E. Sernagor, I. Moreno-Gimeno, D. H. Steel, and M. Lako, "Efficient stage-specific differentiation of human pluripotent stem cells toward retinal photoreceptor cells," *Stem Cells*, vol. 30, no. 4, pp. 673–686, 2012.

[124] C. Boucherie, S. Mukherjee, E. Henckaerts, A. J. Thrasher, J. C. Sowden, and R. R. Ali, "Brief report: self-organizing neuroepithelium from human pluripotent stem cells facilitates derivation of photoreceptors," *Stem Cells*, vol. 31, no. 2, pp. 408–414, 2013.

[125] C. Cedrone, R. Mancino, A. Cerulli, M. Cesareo, and C. Nucci, "Epidemiology of primary glaucoma: prevalence, incidence, and blinding effects," *Prog Brain Res*, vol. 173, pp. 3–14, 2008.

[126] G. Y. Wang, G. Ratto, S. Bisti, and L. M. Chalupa, "Functional development of intrinsic properties in ganglion cells of the mammalian retina," *J Neurophysiol*, vol. 78, no. 6, pp. 2895–2903, 1997.

[127] R. R. Allingham, Y. Liu, and D. J. Rhee, "The genetics of primary open-angle glaucoma: a review," *Exp Eye Res*, vol. 88, no. 4, pp. 837–844, 2009.

[128] J. H. Fingert, "Primary open-angle glaucoma genes," *Eye (Lond)*, vol. 25, no. 5, pp. 587–595, 2011.

[129] M. Sarfarazi, I. Stoilov, and J. B. Schenkman, "Genetics and biochemistry of primary congenital glaucoma," *Ophthalmol Clin North Am*, vol. 16, no. 4, pp. 543–554, vi, 2003.

[130] M. Sarfarazi and T. Rezaie, "Optineurin in primary open angle glaucoma," *Ophthalmol Clin North Am*, vol. 16, no. 4, pp. 529–541, 2003.

[131] T. Rezaie, A. Child, R. Hitchings, G. Brice, L. Miller, M. Coca-Prados, E. Heon, T. Krupin, R. Ritch, D. Kreutzer, R. P. Crick, and M. Sarfarazi, "Adult-onset primary open-angle glaucoma caused by mutations in optineurin," *Science*, vol. 295, no. 5557, pp. 1077–1079, 2002.

[132] Y. Minegishi, D. Iejima, H. Kobayashi, Z. L. Chi, K. Kawase, T. Yamamoto, T. Seki, S. Yuasa, K. Fukuda, and T. Iwata, "Enhanced optineurin E50K-TBK1 interaction evokes protein insolubility and initiates familial primary open-angle glaucoma," *Hum Mol Genet*, vol. 22, no. 17, pp. 3559–3567, 2013.

[133] H. Ying, X. Shen, B. Park, and B. Y. Yue, "Posttranslational modifications, localization, and protein interactions of optineurin, the product of a glaucoma gene," *PLoS One*, vol. 5, no. 2, p. e9168, 2010.

[134] L. Warren, P. D. Manos, T. Ahfeldt, Y. H. Loh, H. Li, F. Lau, W. Ebina, P. K. Mandal, Z. D. Smith, A. Meissner, G. Q. Daley, A. S. Brack, J. J. Collins, C. Cowan, T. M. Schlaeger, and D. J. Rossi, "Highly efficient reprogramming to pluripotency and directed differentiation of human cells with synthetic modified mRNA," *Cell Stem Cell*, vol. 7, no. 5, pp. 618–630, 2010.

[135] B. C. Park, X. Shen, M. Samaraweera, and B. Y. Yue, "Studies of optineurin, a glaucoma gene: Golgi fragmentation and cell death from overexpression of wild-type and mutant optineurin in two ocular cell types," *Am J Pathol*, vol. 169, no. 6, pp. 1976–1989, 2006.

[136] S. Turturro, X. Shen, R. Shyam, B. Y. Yue, and H. Ying, "Effects of mutations and deletions in the human optineurin gene," *Springerplus*, vol. 3, p. 99, 2014.

[137] B. L. Finlay, "The developing and evolving retina: using time to organize form," *Brain Res*, vol. 1192, pp. 5–16, 2008.

[138] M. D. Rollag, D. M. Berson, and I. Provencio, "Melanopsin, ganglion-cell photoreceptors, and mammalian photoentrainment," *J Biol Rhythms*, vol. 18, no. 3, pp. 227–234, 2003.

[139] R. J. Lucas, S. N. Peirson, D. M. Berson, T. M. Brown, H. M. Cooper, C. A. Czeisler, M. G. Figueiro, P. D. Gamlin, S. W. Lockley, J. B. O'Hagan, L. L. Price, I. Provencio, D. J. Skene, and G. C. Brainard, "Measuring and using light in the melanopsin age," *Trends Neurosci*, vol. 37, no. 1, pp. 1–9, 2014.

[140] A. Sand, T. M. Schmidt, and P. Kofuji, "Diverse types of ganglion cell photoreceptors in the mammalian retina," *Prog Retin Eye Res*, vol. 31, no. 4, pp. 287–302, 2012.

[141] L. Erskine and E. Herrera, "Connecting the retina to the brain," *ASN Neuro*, vol. 6, no. 6, 2014.

[142] N. Egawa, S. Kitaoka, K. Tsukita, M. Naitoh, K. Takahashi, T. Yamamoto, F. Adachi, T. Kondo, K. Okita, I. Asaka, T. Aoi, A. Watanabe, Y. Yamada, A. Morizane, J. Takahashi, T. Ayaki, H. Ito, K. Yoshikawa, S. Yamawaki, S. Suzuki, D. Watanabe, H. Hioki, T. Kaneko, K. Makioka, K. Okamoto, H. Takuma, A. Tamaoka, K. Hasegawa, T. Nonaka, M. Hasegawa, A. Kawata, M. Yoshida, T. Nakahata, R. Takahashi, M. C. Marchetto, F. H. Gage, S. Yamanaka, and H. Inoue, "Drug screening for ALS using patient-specific induced pluripotent stem cells," *Sci Transl Med*, vol. 4, no. 145, p. 145ra104, 2012.

[143] S. Corti, I. Faravelli, M. Cardano, and L. Conti, "Human pluripotent stem cells as tools for neurodegenerative and neurodevelopmental disease modeling and drug discovery," *Expert Opin Drug Discov*, vol. 10, no. 6, pp. 615–629, 2015.

[144] H. C. Ko and B. D. Gelb, "Concise review: drug discovery in the age of the induced pluripotent stem cell," *Stem Cells Transl Med*, vol. 3, no. 4, pp. 500–509, 2014.

[145] R. D. Almeida, B. J. Manadas, C. V. Melo, J. R. Gomes, C. S. Mendes, M. M. Graos, R. F. Carvalho, A. P. Carvalho, and C. B. Duarte, "Neuroprotection by BDNF against glutamate-induced apoptotic cell death is mediated by ERK and PI3-kinase pathways," *Cell Death Differ*, vol. 12, no. 10, pp. 1329–1343, 2005.

[146] V. Vigneswara, M. Berry, A. Logan, and Z. Ahmed, "Pigment epithelium-derived factor is retinal ganglion cell neuroprotective and axogenic after optic nerve crush injury," *Invest Ophthalmol Vis Sci*, vol. 54, no. 4, pp. 2624–2633, 2013.

[147] B. Alsina, T. Vu, and S. Cohen-Cory, "Visualizing synapse formation in arborizing optic axons in vivo: dynamics and modulation by BDNF," *Nat Neurosci*, vol. 4, no. 11, pp. 1093–1101, 2001.

[148] Y. Hu, S. Cho, and J. L. Goldberg, "Neurotrophic effect of a novel TrkB agonist on retinal ganglion cells," *Invest Ophthalmol Vis Sci*, vol. 51, no. 3, pp. 1747–1754, 2010.

[149] I. H. Pang, H. Zeng, D. L. Fleenor, and A. F. Clark, "Pigment epithelium-derived factor protects retinal ganglion cells," *BMC Neurosci*, vol. 8, p. 11, 2007.

[150] J. Tombran-Tink and C. J. Barnstable, "Therapeutic prospects for PEDF: more than a promising angiogenesis inhibitor," *Trends Mol Med*, vol. 9, no. 6, pp. 244–250, 2003.

[151] F. M. Nadal-Nicolas, M. Jimenez-Lopez, M. Salinas-Navarro, P. Sobrado-Calvo, J. J. Alburquerque-Bejar, M. Vidal-Sanz, and M. Agudo-Barriuso, "Whole number, distribution and co-expression of brn3 transcription factors in retinal ganglion cells of adult albino and pigmented rats," *PLoS One*, vol. 7, no. 11, p. e49830, 2012.

[152] N. Hirokawa, T. Funakoshi, R. Sato-Harada, and Y. Kanai, "Selective stabilization of tau in axons and microtubule-associated protein 2C in cell bodies and dendrites contributes to polarized localization of cytoskeletal proteins in mature neurons," *J Cell Biol*, vol. 132, no. 4, pp. 667–679, 1996.

[153] J. Qu, D. Wang, and C. L. Grosskreutz, "Mechanisms of retinal ganglion cell injury and defense in glaucoma," *Exp Eye Res*, vol. 91, no. 1, pp. 48–53, 2010.

[154] H. Bagga, J. H. Liu, and R. N. Weinreb, "Intraocular pressure measurements throughout the 24 h," *Curr Opin Ophthalmol*, vol. 20, no. 2, pp. 79–83, 2009.

[155] Z. L. Chi, M. Akahori, M. Obazawa, M. Minami, T. Noda, N. Nakaya, S. Tomarev, K. Kawase, T. Yamamoto, S. Noda, M. Sasaoka, A. Shimazaki, Y. Takada, and T. Iwata, "Overexpression of optineurin E50K disrupts Rab8 interaction and leads to a progressive retinal degeneration in mice," *Hum Mol Genet*, vol. 19, no. 13, pp. 2606–2615, 2010.

[156] H. C. Tseng, T. T. Riday, C. McKee, C. E. Braine, H. Bomze, I. Barak, C. Marean-Reardon, S. W. John, B. D. Philpot, and M. D. Ehlers, "Visual impairment in an optineurin mouse model of primary open-angle glaucoma," *Neurobiol Aging*, vol. 36, no. 6, pp. 2201–2212, 2015.

[157] W. Eichler, H. Savkovic-Cvijic, S. Burger, M. Beck, M. Schmidt, P. Wiedemann, A. Reichenbach, and J. D. Unterlauft, "Muller Cell-Derived PEDF Mediates Neuroprotection via STAT3 Activation," *Cell Physiol Biochem*, vol. 44, no. 4, pp. 1411–1424, 2017.

[158] J. D. Unterlauft, W. Eichler, K. Kuhne, X. M. Yang, Y. Yafai, P. Wiedemann, A. Reichenbach, and T. Claudepierre, "Pigment epithelium-derived factor released by Muller glial cells exerts neuroprotective effects on retinal ganglion cells," *Neurochem Res*, vol. 37, no. 7, pp. 1524–1533, 2012.

[159] L. A. Levin, M. E. Crowe, and H. A. Quigley, "Neuroprotection for glaucoma: Requirements for clinical translation," *Exp Eye Res*, vol. 157, pp. 34–37, 2017.

[160] K. R. Martin, H. A. Quigley, D. J. Zack, H. Levkovitch-Verbin, J. Kielczewski, D. Valenta, L. Baumrind, M. E. Pease, R. L. Klein, and W. W. Hauswirth, "Gene therapy with brain-derived neurotrophic factor as a protection: retinal ganglion cells in a rat glaucoma model," *Invest Ophthalmol Vis Sci*, vol. 44, no. 10, pp. 4357–4365, 2003.

[161] M. E. Pease, S. J. McKinnon, H. A. Quigley, L. A. Kerrigan-Baumrind, and D. J. Zack, "Obstructed axonal transport of BDNF and its receptor TrkB in experimental glaucoma," *Invest Ophthalmol Vis Sci*, vol. 41, no. 3, pp. 764–774, 2000.

[162] E. J. Huang and L. F. Reichardt, "Neurotrophins: roles in neuronal development and function," *Annu Rev Neurosci*, vol. 24, pp. 677–736, 2001.

[163] A. J. Weber, C. D. Harman, and S. Viswanathan, "Effects of optic nerve injury, glaucoma, and neuroprotection on the survival, structure, and function of ganglion cells in the mammalian retina," *J Physiol*, vol. 586, no. 18, pp. 4393–4400, 2008.

[164] S. Isenmann, A. Kretz, and A. Cellerino, "Molecular determinants of retinal ganglion cell development, survival, and regeneration," *Prog Retin Eye Res*, vol. 22, no. 4, pp. 483–543, 2003.

[165] K. H. Herzog, K. Bailey, and Y. A. Barde, "Expression of the BDNF gene in the developing visual system of the chick," *Development*, vol. 120, no. 6, pp. 1643–1649, 1994.

[166] H. A. Quigley, "Glaucoma," *Lancet*, vol. 377, no. 9774, pp. 1367–1377, 2011.

[167] A. Sridhar, S. K. Ohlemacher, K. B. Langer, and J. S. Meyer, "Robust Differentiation of mRNA-Reprogrammed Human Induced Pluripotent Stem Cells Toward a Retinal Lineage," *Stem Cells Transl Med*, 2016.

[168] K. P. Gill, S. S. Hung, A. Sharov, C. Y. Lo, K. Needham, G. E. Lidgerwood, S. Jackson, D. E. Crombie, B. A. Nayagam, A. L. Cook, A. W. Hewitt, A. Pebay, and R. C. Wong, "Enriched retinal ganglion cells derived from human embryonic stem cells," *Sci Rep*, vol. 6, p. 30552, 2016.

[169] E. Guenther, S. Schmid, D. Reiff, and E. Zrenner, "Maturation of intrinsic membrane properties in rat retinal ganglion cells," *Vision Res*, vol. 39, no. 15, pp. 2477–2484, 1999.

[170] E. Sernagor, S. J. Eglen, and R. O. Wong, "Development of retinal ganglion cell structure and function," *Prog Retin Eye Res*, vol. 20, no. 2, pp. 139–174, 2001.

[171] L. M. Chalupa, I. Skaliora, and R. P. Scobey, "Responses of isolated cat retinal ganglion cells to injected currents during development," *Prog Brain Res*, vol. 95, pp. 25–31, 1993.

[172] E. A. Rossi, C. E. Granger, R. Sharma, Q. Yang, K. Saito, C. Schwarz, S. Walters, K. Nozato, J. Zhang, T. Kawakami, W. Fischer, L. R. Latchney, J. J. Hunter, M. M. Chung, and D. R. Williams, "Imaging individual neurons in the retinal ganglion cell layer of the living eye," *Proc Natl Acad Sci U S A*, vol. 114, no. 3, pp. 586–591, 2017.

[173] F. Valtorta and C. Leoni, "Molecular mechanisms of neurite extension," *Philos Trans R Soc Lond B Biol Sci*, vol. 354, no. 1381, pp. 387–394, 1999.

[174] J. Stiles and T. L. Jernigan, "The basics of brain development," *Neuropsychol Rev*, vol. 20, no. 4, pp. 327–348, 2010.

[175] T. E. Ogden, "Nerve fiber layer astrocytes of the primate retina: morphology, distribution, and density," *Invest Ophthalmol Vis Sci*, vol. 17, no. 6, pp. 499–510, 1978.

[176] H. Bussow, "The astrocytes in the retina and optic nerve head of mammals: a special glia for the ganglion cell axons," *Cell Tissue Res*, vol. 206, no. 3, pp. 367–378, 1980.

[177] L. Pellerin and P. J. Magistretti, "Glutamate uptake into astrocytes stimulates aerobic glycolysis: a mechanism coupling neuronal activity to glucose utilization," *Proc Natl Acad Sci U S A*, vol. 91, no. 22, pp. 10 625–10 629, 1994.

[178] R. C. Janzer and M. C. Raff, "Astrocytes induce blood-brain barrier properties in endothelial cells," *Nature*, vol. 325, no. 6101, pp. 253–257, 1987.

[179] E. Vecino and N. Osborne, *Expression of Neurotrophins and their Receptors Within the Glial Cells of Retina and Optic Nerve*. Springer, 1998.

[180] B. A. Barres, "New roles for glia," *J Neurosci*, vol. 11, no. 12, pp. 3685–3694, 1991.

[181] E. M. Ullian, K. S. Christopherson, and B. A. Barres, "Role for glia in synaptogenesis," *Glia*, vol. 47, no. 3, pp. 209–216, 2004.

[182] R. Krencik and S. C. Zhang, "Directed differentiation of functional astroglial subtypes from human pluripotent stem cells," *Nat Protoc*, vol. 6, no. 11, pp. 1710–1717, 2011.

[183] R. Krencik, J. P. Weick, Y. Liu, Z. J. Zhang, and S. C. Zhang, "Specification of transplantable astroglial subtypes from human pluripotent stem cells," *Nat Biotechnol*, vol. 29, no. 6, pp. 528–534, 2011.

[184] F. W. Pfrieger and B. A. Barres, "Synaptic efficacy enhanced by glial cells in vitro," *Science*, vol. 277, no. 5332, pp. 1684–1687, 1997.

[185] M. A. Johnson, J. P. Weick, R. A. Pearce, and S. C. Zhang, "Functional neural development from human embryonic stem cells: accelerated synaptic activity via astrocyte coculture," *J Neurosci*, vol. 27, no. 12, pp. 3069–3077, 2007.

[186] E. M. Ullian, S. K. Sapperstein, K. S. Christopherson, and B. A. Barres, "Control of synapse number by glia," *Science*, vol. 291, no. 5504, pp. 657–661, 2001.

[187] R. H. Masland, "The neuronal organization of the retina," *Neuron*, vol. 76, no. 2, pp. 266–280, 2012.

[188] M. Meister, R. O. Wong, D. A. Baylor, and C. J. Shatz, "Synchronous bursts of action potentials in ganglion cells of the developing mammalian retina," *Science*, vol. 252, no. 5008, pp. 939–943, 1991.

[189] J. L. Goldberg, J. S. Espinosa, Y. Xu, N. Davidson, G. T. Kovacs, and B. A. Barres, "Retinal ganglion cells do not extend axons by default: promotion by neurotrophic signaling and electrical activity," *Neuron*, vol. 33, no. 5, pp. 689–702, 2002.

[190] N. C. Spitzer, "Electrical activity in early neuronal development," *Nature*, vol. 444, no. 7120, pp. 707–712, 2006.

[191] H. A. Quigley and W. R. Green, "The histology of human glaucoma cupping and optic nerve damage: clinicopathologic correlation in 21 eyes," *Ophthalmology*, vol. 86, no. 10, pp. 1803–1830, 1979.

[192] T. Boiko, A. Van Wart, J. H. Caldwell, S. R. Levinson, J. S. Trimmer, and G. Matthews, "Functional specialization of the axon initial segment by isoform-specific sodium channel targeting," *J Neurosci*, vol. 23, no. 6, pp. 2306–2313, 2003.

[193] J. Xi, Y. Liu, H. Liu, H. Chen, M. E. Emborg, and S. C. Zhang, "Specification of midbrain dopamine neurons from primate pluripotent stem cells," *Stem Cells*, vol. 30, no. 8, pp. 1655–1663, 2012.

[194] Y. Liu, H. Liu, C. Sauvey, L. Yao, E. D. Zarnowska, and S. C. Zhang, "Directed differentiation of forebrain GABA interneurons from human pluripotent stem cells," *Nat Protoc*, vol. 8, no. 9, pp. 1670–1679, 2013.

[195] D. Pre, M. W. Nestor, A. A. Sproul, S. Jacob, P. Koppensteiner, V. Chinchalongporn, M. Zimmer, A. Yamamoto, S. A. Noggle, and O. Arancio, "A time course analysis of the electrophysiological properties of neurons differentiated from human induced pluripotent stem cells (iPSCs)," *PLoS One*, vol. 9, no. 7, p. e103418, 2014.

[196] A. Fraichard, O. Chassande, G. Bilbaut, C. Dehay, P. Savatier, and J. Samarut, "In vitro differentiation of embryonic stem cells into glial cells and functional neurons," *J Cell Sci*, vol. 108 (Pt 10), pp. 3181–3188, 1995.

[197] F. Perez-Cerda, M. V. Sanchez-Gomez, and C. Matute, "Pio del Rio Hortega and the discovery of the oligodendrocytes," *Front Neuroanat*, vol. 9, p. 92, 2015.

[198] R. K. Small, P. Riddle, and M. Noble, "Evidence for migration of oligodendrocyte–type-2 astrocyte progenitor cells into the developing rat optic nerve," *Nature*, vol. 328, no. 6126, pp. 155–157, 1987.

[199] T. A. Watkins, B. Emery, S. Mulinyawe, and B. A. Barres, "Distinct stages of myelination regulated by gamma-secretase and astrocytes in a rapidly myelinating CNS coculture system," *Neuron*, vol. 60, no. 4, pp. 555–569, 2008.

[200] N. J. Allen and B. A. Barres, "Neuroscience: Glia - more than just brain glue," *Nature*, vol. 457, no. 7230, pp. 675–677, 2009.

[201] C. Eroglu and B. A. Barres, "Regulation of synaptic connectivity by glia," *Nature*, vol. 468, no. 7321, pp. 223–231, 2010.

[202] E. Vecino, F. D. Rodriguez, N. Ruzafa, X. Pereiro, and S. C. Sharma, "Glia-neuron interactions in the mammalian retina," *Prog Retin Eye Res*, vol. 51, pp. 1–40, 2016.

[203] M. M. Halassa, T. Fellin, and P. G. Haydon, "The tripartite synapse: roles for gliotransmission in health and disease," *Trends Mol Med*, vol. 13, no. 2, pp. 54–63, 2007.

[204] M. M. Halassa, T. Fellin, H. Takano, J. H. Dong, and P. G. Haydon, "Synaptic islands defined by the territory of a single astrocyte," *J Neurosci*, vol. 27, no. 24, pp. 6473–6477, 2007.

[205] M. Lohner, N. Babai, T. Muller, K. Gierke, J. Atorf, A. Joachimsthaler, A. Peukert, H. Martens, A. Feigenspan, J. Kremers, S. Schoch, J. H. Brandstatter, and H. Regus-Leidig, "Analysis of RIM Expression and Function at Mouse Photoreceptor Ribbon Synapses," *J Neurosci*, vol. 37, no. 33, pp. 7848–7863, 2017.

[206] L. E. Clarke and B. A. Barres, "Emerging roles of astrocytes in neural circuit development," *Nat Rev Neurosci*, vol. 14, no. 5, pp. 311–321, 2013.

[207] E. A. Bushong, M. E. Martone, Y. Z. Jones, and M. H. Ellisman, "Protoplasmic astrocytes in CA1 stratum radiatum occupy separate anatomical domains," *J Neurosci*, vol. 22, no. 1, pp. 183–192, 2002.

[208] A. J. Barker, S. M. Koch, J. Reed, B. A. Barres, and E. M. Ullian, "Developmental control of synaptic receptivity," *J Neurosci*, vol. 28, no. 33, pp. 8150–8160, 2008.

[209] D. H. Mauch, K. Nagler, S. Schumacher, C. Goritz, E. C. Muller, A. Otto, and F. W. Pfrieger, "CNS synaptogenesis promoted by glia-derived cholesterol," *Science*, vol. 294, no. 5545, pp. 1354–1357, 2001.

[210] N. J. Allen, M. L. Bennett, L. C. Foo, G. X. Wang, C. Chakraborty, S. J. Smith, and B. A. Barres, "Astrocyte glypicans 4 and 6 promote formation of excitatory synapses via GluA1 AMPA receptors," *Nature*, vol. 486, no. 7403, pp. 410–414, 2012.

[211] J. B. Zuchero and B. A. Barres, "Glia in mammalian development and disease," *Development*, vol. 142, no. 22, pp. 3805–3809, 2015.

[212] A. V. Molofsky, R. Krencik, E. M. Ullian, H. H. Tsai, B. Deneen, W. D. Richardson, B. A. Barres, and D. H. Rowitch, "Astrocytes and disease: a neurodevelopmental perspective," *Genes Dev*, vol. 26, no. 9, pp. 891–907, 2012.

[213] A. M. Haidet-Phillips, M. E. Hester, C. J. Miranda, K. Meyer, L. Braun, A. Frakes, S. Song, S. Likhite, M. J. Murtha, K. D. Foust, M. Rao, A. Eagle, A. Kammesheidt, A. Christensen, J. R. Mendell, A. H. Burghes, and B. K. Kaspar, "Astrocytes from familial and sporadic ALS patients are toxic to motor neurons," *Nat Biotechnol*, vol. 29, no. 9, pp. 824–828, 2011.

[214] S. A. Liddelow, K. A. Guttenplan, L. E. Clarke, F. C. Bennett, C. J. Bohlen, L. Schirmer, M. L. Bennett, A. E. Munch, W. S. Chung, T. C. Peterson, D. K. Wilton, A. Frouin, B. A. Napier, N. Panicker, M. Kumar, M. S. Buckwalter, D. H. Rowitch, V. L. Dawson, T. M. Dawson, B. Stevens, and B. A. Barres, "Neurotoxic reactive astrocytes are induced by activated microglia," *Nature*, vol. 541, no. 7638, pp. 481–487, 2017.

[215] F. P. Di Giorgio, G. L. Boulting, S. Bobrowicz, and K. C. Eggan, "Human embryonic stem cell-derived motor neurons are sensitive to the toxic effect of glial cells carrying an ALS-causing mutation," *Cell Stem Cell*, vol. 3, no. 6, pp. 637–648, 2008.

[216] J. Lasiene and K. Yamanaka, "Glial cells in amyotrophic lateral sclerosis," *Neurol Res Int*, vol. 2011, p. 718987, 2011.

[217] K. Yamanaka, S. J. Chun, S. Boillee, N. Fujimori-Tonou, H. Yamashita, D. H. Gutmann, R. Takahashi, H. Misawa, and D. W. Cleveland, "Astrocytes as determinants of disease progression in inherited amyotrophic lateral sclerosis," *Nat Neurosci*, vol. 11, no. 3, pp. 251–253, 2008.

[218] L. Wang, D. H. Gutmann, and R. P. Roos, "Astrocyte loss of mutant SOD1 delays ALS disease onset and progression in G85R transgenic mice," *Hum Mol Genet*, vol. 20, no. 2, pp. 286–293, 2011.

[219] L. Chalupa and J. Werner, "The Visual Neurosciences." MIT Press, 2004.

[220] D. Y. Yu, S. J. Cringle, C. Balaratnasingam, W. H. Morgan, P. K. Yu, and E. N. Su, "Retinal ganglion cells: Energetics, compartmentation, axonal transport, cytoskeletons and vulnerability," *Prog Retin Eye Res*, vol. 36, pp. 217–246, 2013.

[221] F. Osakada, Z. B. Jin, Y. Hirami, H. Ikeda, T. Danjyo, K. Watanabe, Y. Sasai, and M. Takahashi, "In vitro differentiation of retinal cells from human pluripotent stem cells by small-molecule induction," *J Cell Sci*, vol. 122, no. Pt 17, pp. 3169–3179, 2009.

[222] I. Munoz-Sanjuan and A. H. Brivanlou, "Neural induction, the default model and embryonic stem cells," *Nat Rev Neurosci*, vol. 3, no. 4, pp. 271–280, 2002.

[223] A. Gonzalez-Cordero, E. L. West, R. A. Pearson, Y. Duran, L. S. Carvalho, C. J. Chu, A. Naeem, S. J. Blackford, A. Georgiadis, J. Lakowski, M. Hubank, A. J. Smith, J. W. Bainbridge, J. C. Sowden, and R. R. Ali, "Photoreceptor precursors derived from three-dimensional embryonic stem cell cultures integrate and mature within adult degenerate retina," *Nat Biotechnol*, vol. 31, no. 8, pp. 741–747, 2013.

[224] N. Arimura and K. Kaibuchi, "Neuronal polarity: from extracellular signals to intracellular mechanisms," *Nat Rev Neurosci*, vol. 8, no. 3, pp. 194–205, 2007.

[225] P. J. Foster, R. Buhrmann, H. A. Quigley, and G. J. Johnson, "The definition and classification of glaucoma in prevalence surveys," *Br J Ophthalmol*, vol. 86, no. 2, pp. 238–242, 2002.

[226] E. E. Chang and J. L. Goldberg, "Glaucoma 2.0: neuroprotection, neuroregeneration, neuroenhancement," *Ophthalmology*, vol. 119, no. 5, pp. 979–986, 2012.

[227] R. Lisboa, Y. S. Chun, L. M. Zangwill, R. N. Weinreb, P. N. Rosen, J. M. Liebmann, C. A. Girkin, and F. A. Medeiros, "Association between rates of binocular visual field loss and vision-related quality of life in patients with glaucoma," *JAMA Ophthalmol*, vol. 131, no. 4, pp. 486–494, 2013.

[228] M. Almasieh, A. M. Wilson, B. Morquette, J. L. Cueva Vargas, and A. Di Polo, "The molecular basis of retinal ganglion cell death in glaucoma," *Prog Retin Eye Res*, vol. 31, no. 2, pp. 152–181, 2012.

[229] N. Walsh, K. Valter, and J. Stone, "Cellular and subcellular patterns of expression of bFGF and CNTF in the normal and light stressed adult rat retina," *Exp Eye Res*, vol. 72, no. 5, pp. 495–501, 2001.

[230] H. A. Quigley, "Ganglion cell death in glaucoma: pathology recapitulates ontogeny," *Aust N Z J Ophthalmol*, vol. 23, no. 2, pp. 85–91, 1995.

[231] H. A. Quigley, S. J. McKinnon, D. J. Zack, M. E. Pease, L. A. Kerrigan-Baumrind, D. F. Kerrigan, and R. S. Mitchell, "Retrograde axonal transport of BDNF in retinal ganglion cells is blocked by acute IOP elevation in rats," *Invest Ophthalmol Vis Sci*, vol. 41, no. 11, pp. 3460–3466, 2000.

[232] J. P. Vrabec and L. A. Levin, "The neurobiology of cell death in glaucoma," *Eye (Lond)*, vol. 21 Suppl 1, pp. S11–4, 2007.

[233] M. E. Pease, D. J. Zack, C. Berlinicke, K. Bloom, F. Cone, Y. Wang, R. L. Klein, W. W. Hauswirth, and H. A. Quigley, "Effect of CNTF on retinal ganglion cell survival in experimental glaucoma," *Invest Ophthalmol Vis Sci*, vol. 50, no. 5, pp. 2194–2200, 2009.

[234] W. M. Cowan, J. W. Fawcett, D. D. O'Leary, and B. B. Stanfield, "Regressive events in neurogenesis," *Science*, vol. 225, no. 4668, pp. 1258–1265, 1984.

[235] P. Rakic and K. P. Riley, "Overproduction and elimination of retinal axons in the fetal rhesus monkey," *Science*, vol. 219, no. 4591, pp. 1441–1444, 1983.

[236] T. Aung, T. Rezaie, K. Okada, A. C. Viswanathan, A. H. Child, G. Brice, S. S. Bhattacharya, O. J. Lehmann, M. Sarfarazi, and R. A. Hitchings, "Clinical features and course of patients with glaucoma with the E50K mutation in the optineurin gene," *Invest Ophthalmol Vis Sci*, vol. 46, no. 8, pp. 2816–2822, 2005.

[237] W. L. Alward, Y. H. Kwon, K. Kawase, J. E. Craig, S. S. Hayreh, A. T. Johnson, C. L. Khanna, T. Yamamoto, D. A. Mackey, B. R. Roos, L. M. Affatigato, V. C. Sheffield, and E. M. Stone, "Evaluation of optineurin sequence variations in 1,048 patients with open-angle glaucoma," *Am J Ophthalmol*, vol. 136, no. 5, pp. 904–910, 2003.

[238] T. Osawa, Y. Mizuno, Y. Fujita, M. Takatama, Y. Nakazato, and K. Okamoto, "Optineurin in neurodegenerative diseases," *Neuropathology*, vol. 31, no. 6, pp. 569–574, 2011.

[239] H. Ying and B. Y. Yue, "Cellular and molecular biology of optineurin," *Int Rev Cell Mol Biol*, vol. 294, pp. 223–258, 2012.

[240] I. Khalin, R. Alyautdin, G. Kocherga, and M. A. Bakar, "Targeted delivery of brain-derived neurotrophic factor for the treatment of blindness and deafness," *Int J Nanomedicine*, vol. 10, pp. 3245–3267, 2015.

[241] E. M. Del Amo, A. K. Rimpela, E. Heikkinen, O. K. Kari, E. Ramsay, T. Lajunen, M. Schmitt, L. Pelkonen, M. Bhattacharya, D. Richardson, A. Subrizi, T. Turunen, M. Reinisalo, J. Itkonen, E. Toropainen, M. Casteleijn, H. Kidron, M. Antopolsky, K. S. Vellonen, M. Ruponen, and A. Urtti, "Pharmacokinetic aspects of retinal drug delivery," *Prog Retin Eye Res*, vol. 57, pp. 134–185, 2017.

[242] B. Castillo Jr., M. del Cerro, X. O. Breakefield, D. M. Frim, C. J. Barnstable, D. O. Dean, and M. C. Bohn, "Retinal ganglion cell survival is promoted by genetically modified astrocytes designed to secrete brain-derived neurotrophic factor (BDNF)," *Brain Res*, vol. 647, no. 1, pp. 30–36, 1994.

[243] L. A. Cunningham, J. T. Hansen, M. P. Short, and M. C. Bohn, "The use of genetically altered astrocytes to provide nerve growth factor to adrenal chromaffin cells grafted into the striatum," *Brain Res*, vol. 561, no. 2, pp. 192–202, 1991.

[244] M. Suzuki, J. McHugh, C. Tork, B. Shelley, A. Hayes, I. Bellantuono, P. Aebischer, and C. N. Svendsen, "Direct muscle delivery of GDNF with human mesenchymal stem cells improves motor neuron survival and function in a rat model of familial ALS," *Mol Ther*, vol. 16, no. 12, pp. 2002–2010, 2008.

[245] A. Di Polo, L. J. Aigner, R. J. Dunn, G. M. Bray, and A. J. Aguayo, "Prolonged delivery of brain-derived neurotrophic factor by adenovirus-infected Muller cells temporarily rescues injured retinal ganglion cells," *Proc Natl Acad Sci U S A*, vol. 95, no. 7, pp. 3978–3983, 1998.

[246] X. Mo, A. Yokoyama, T. Oshitari, H. Negishi, M. Dezawa, A. Mizota, and E. Adachi-Usami, "Rescue of axotomized retinal ganglion cells by BDNF gene electroporation in adult rats," *Invest Ophthalmol Vis Sci*, vol. 43, no. 7, pp. 2401–2405, 2002.

[247] R. Ren, Y. Li, Z. Liu, K. Liu, and S. He, "Long-term rescue of rat retinal ganglion cells and visual function by AAV-mediated BDNF expression after acute elevation of intraocular pressure," *Invest Ophthalmol Vis Sci*, vol. 53, no. 2, pp. 1003–1011, 2012.

[248] H. A. Quigley, E. M. Addicks, W. R. Green, and A. E. Maumenee, "Optic nerve damage in human glaucoma. II. The site of injury and susceptibility to damage," *Arch Ophthalmol*, vol. 99, no. 4, pp. 635–649, 1981.

[249] S. Wu, K. C. Chang, M. Nahmou, and J. L. Goldberg, "Induced Pluripotent Stem Cells Promote Retinal Ganglion Cell Survival After Transplant," *Invest Ophthalmol Vis Sci*, vol. 59, no. 3, pp. 1571–1576, 2018.

[250] C. Anasetti, D. Amos, P. G. Beatty, F. R. Appelbaum, W. Bensinger, C. D. Buckner, R. Clift, K. Doney, P. J. Martin, E. Mickelson, and E. al., "Effect of HLA compatibility on engraftment of bone marrow transplants in patients with leukemia or lymphoma," *N Engl J Med*, vol. 320, no. 4, pp. 197–204, 1989.

[251] P. J. Morris, S. V. Fuggle, A. Ting, and K. J. Wood, "HLA and organ transplantation," *Br Med Bull*, vol. 43, no. 1, pp. 184–202, 1987.

[252] C. J. Taylor, E. M. Bolton, S. Pocock, L. D. Sharples, R. A. Pedersen, and J. A. Bradley, "Banking on human embryonic stem cells: estimating the number of donor cell lines needed for HLA matching," *Lancet*, vol. 366, no. 9502, pp. 2019–2025, 2005.

[253] J. Y. Niederkorn, "Corneal transplantation and immune privilege," *Int Rev Immunol*, vol. 32, no. 1, pp. 57–67, 2013.

[254] A. W. Taylor, "Ocular Immune Privilege and Transplantation," *Front Immunol*, vol. 7, p. 37, 2016.

[255] L. Q. Jiang and J. W. Streilein, "Immune responses elicited by transplantation and tissue-restricted antigens expressed on retinal tissues implanted subconjunctivally," *Transplantation*, vol. 52, no. 3, pp. 513–519, 1991.

VITA

VITA

Education

Purdue University- Indianapolis	PhD Biology	May 2013-2018
University of Texas at Dallas	B.S. Neuroscience	August 2007-May 2011

Research Experience

Purdue University-Indianapolis	PhD Candidate	May 2013-2018

- Differentiating and optimizing protocols leading to generation of physiologically active retinal organoids from human pluripotent stem cells (hPSCs)
- Reprograming mutated patient fibroblasts to investigate cell and non-cell autonomous mechanisms of glaucoma in hPSC-derived retinal ganglion cells (RGCs)
- Producing hPSC-derived astrocytes to elucidate their contributions to RGC maturation and function
- Independently designing and executing experiments focused on differentiation of multiple neural and retinal populations for multidisciplinary research endeavors

Publications

1. Fligor CM, Edler MC, Sridhar A, Ren Y, Shields PK, Langer KB, Ohlemacher SK, Sluch VM, Zack DJ, Suter DM, Zhang C, Meyer JS (2017) Extensive Neurite Outgrowth and Pathfinding from Retinal Ganglion Cells Derived from Human Pluripotent Stem Cells. Scientific Reports, under review.
2. Ohlemacher SK, Edler MC, Fligor CF, Langer KB, Feder EM, Meyer JS (2018) Advances in Differentiation and Engineering of Human Pluripotent Stem Cell-Derived Retinal Ganglion Cells. Frontiers in Cell and Developmental Biology. Submitted
3. Langer KB, Ohlemacher SK, Phillips JM, Fligor CM, Jiang P, Gamm DM, Meyer JS (2017) Investigation of Retinal Ganglion Cell Diversity and Subtype Specification From Human Pluripotent Stem Cells. Stem Cell Reports, 6711(18) 30101-2.

4. Sridhar A, Langer KB, Fligor CM, Steinhart M, Miller CA, Ho-A-Lim KT, Ohlemacher SK, Meyer JS (2017) Human Pluripotent Stem Cells As In Vitro Models for Retinal Development and Disease. Regenerative Medicine and Stem Cell Therapy for the Eye, under review.

5. Ohlemacher SK, Sridhar A, XiaoY, HochstetlerAE, Sarfarazi M, CumminsTR, Meyer JS (2016) Stepwise Differentiation of Retinal Ganglion Cells from Human Pluripotent Stem Cells Enables Analysis of Glaucomatous Neurodegeneration, Stem Cells 34(6):1553-62.

6. Sridhar A, Ohlemacher SK, Meyer JS (2016) Robust Differentiation of mRNA-Reprogrammed Human Induced Pluripotent Stem Cells Toward a Retinal Lineage, Stem Cells Translational Medicine 5(4):417-26.

7. Ohlemacher SK, Iglesias CL, Sridhar A, Gamm DM, & Meyer JS (2015) Generation of highly enriched populations of optic vesicle-like retinal cells from human pluripotent stem cells, Current protocols in stem cell biology 32:1h.8.1-1h.8.20.

Patents

- Ohlemacher, SK and Meyer JS. Method for Producing Retinal Ganglion Cells from Pluripotent Cells. International Patent Number PCT/US2015/029321, filed 15 May 2015.

- Ohlemacher, SK and Meyer JS. Method for Producing Retinal Ganglion Cells from Pluripotent Cells. International Patent Number PCT/US2015/029321, filed 15 May 2015.

Selected Honors Awarded

Outstanding Graduate (PhD) Research Award	2018
Eli Lilly/Stark Neurosciences Predoctoral Research Fellowship	2017-2018
IUPUI Graduate Professional Student Government Elite 50 Award	2017
1st Place Oral Presentation- Midwest Eye Research Symposium	2017
1st Place Oral Presentation- Sigma Xi Scientific Research Society	2016
1st Place Oral Presentation- Women in Science Regional Conference	2016
Elizabeth Steele Creveling Memorial Scholarship	2016
Best Poster Award/$1000 Travel Grant Award CTSI Symposium	2015
Indiana Clinical/ Translational Sciences Institute Predoc Fellowship	2015-2017
ARVO Retina Research Foundation Travel Grant	2015
IUPUI 2nd year Academic Excellence Fellowship	2015

Invited Talks

- Alzheimers Disease Scientific Spring Symposium. Indianapolis, IN. May 2018. Modeling Neurodegeneration using Human Induced Pluripotent Stem Cells.
- Purdue University- Department of Cell and Molecular Biology Seminar Series. West Lafayette, IN. January 2018. Human Induced Pluripotent Stem Cells and their Application for Visual System Neurodegeneration.
- Society for Neuroscience. Washington, D.C. November 2017. Analysis of Retinal Ganglion Cell Development and Maturation from Human Pluripotent Stem Cell-Derived Organoids.
- Midwest Eye Research Symposium. Iowa City, IA. August 2017. Analysis of Retinal Ganglion Cell Development and Maturation from Human Pluripotent Stem Cell-Derived Organoids
- Sigma XI Graduate Biomedical Research Competition. Indianapolis, IN. October 2016. Human Induced Pluripotent Stem Cells and their Application for Visual System Neurodegeneration.
- Stark Neurosciences Spinal Cord and Brain Injury Symposium. Indianapolis, IN. October 2016. Human Induced Pluripotent Stem Cells and their Application for Visual System Neurodegeneration.

- Association for Women in Science. South Bend, IN. October 2016. Induced Pluripotent Stem Cells and their Application for Visual System Neurodegeneration.

Poster Presentations

International Society for Eye Research	(1 poster, 2017)
International Society for Stem Cell Research	(1 poster, 2016)
Association for Clinical and Translational Science	(1 poster, 2015)
Society for Neuroscience	(1 poster, 2015)
Cold Spring Harbor Laboratory Stem Cell Meeting	(1 poster, 2015)
Eli Lilly and Company	(2 posters,2015-2016)
CTSI Annual Meeting	(2 posters, 2015-2016)
Midwest Eye Research Symposium	(1 poster, 2015)
Midwest Motorneuron Consortium	(2 posters, 2014, 2016)
Indianapolis Society for Neuroscience	(4 posters, 2014-2017)
Glick Eye Institute	(1 poster, 2014)
Association for Research in Vision and Ophthalmology	(3 posters, 2014-2017)

Leadership/Outreach

ARVO Science Communication Training Fellowship	February 2017-2018
Central Indiana Science Outreach	September 2016- present
Starfish Initiative	August 2016- 2017
Undergraduate Research Opportunities Program	August 2015- 2017
Freshman Work Program	August 2014- 2018
Project SEED	June 2014-August 2015

Professional Memberships

International Society for Eye Research	2017-present
American Association for the Advancement of Science	2016-present
International Society for Stem Cell Research	2016-present
Association for Clinical and Translational Science	2016-present
Society for Neuroscience	2014-present
Association for Research in Vision and Ophthalmology	2014-present